



This is to certify that the

dissertation entitled

Effects of Flow and Rheology on the Functionalization of Polyolefin Melts

presented by

Robert G. Polance

has been accepted towards fulfillment of the requirements for

Ph.D. degree in Chemical Engineering

Date 6/13/94

0-12771

LIBRARY Michigan State University

PLACE IN RETURN BOX to remove this checkout from your record.

TO AVOID FINES return on or before date due.

DATE DUE	DATE DUE	DATE DUE
· · ·		

MSU is An Affirmative Action/Equal Opportunity Institution cycledeledus.pm3-p.1



EFFECTS OF FLOW AND RHEOLOGY ON THE FUNCTIONALIZATION OF POLYOLEFIN MELTS

Ву

Robert G. Polance

A DISSERTATION

Submitted to
Michigan State University
in partial fulfillment of the requirements
for the degree of

DOCTOR OF PHILOSOPHY

Department of Chemical Engineering

ABSTRACT

EFFECTS OF FLOW AND RHEOLOGY ON THE FUNCTIONALIZATION OF POLYOLEFIN MELTS

By

Robert G. Polance

Reactive extrusion of polymer melts is an area of tremendous commercial and research interest. The specific contribution of this work is that the effects of both extensional and shear components of flow and rheology on reaction progress were examined. Model reactor experiments demonstrated the importance of the extensional flow on the reaction progress. In the reaction, a peroxide stream must be dispersed into a viscous polypropylene and dibutyl maleate blend. The reaction was carried out in two distinct reactors under operating conditions which provided a range of shear and extensional strain rates in the flow where the peroxide was injected to initiate the reaction. The addition of extensional flow, which produces more efficient mixing, yielded up to a four fold increase in the extent of maleation as determined by calibrated FTIR measurements. Contrastingly, increases in the shear strain rates led to smaller increases in reaction levels, presumably due to the smaller levels of deformation provided in the flow.

Two functionalization reactions were carried out in a co-rotating, fully intermeshing, twin screw extruder. The residence time distribution of peroxide in the extruder was found adequate to predict observed trends in the level of grafting. Since the chemical reactivity of different polyolefins depends upon their chain structure, the effects of melt rheology on the flow of other polyolefins were examined by comparing their residence time distributions rather than their extents of reaction. The effects of extensional viscosity on flow in the extruder were examined

for two different low density polyethylenes, one linear and the other branched. The two have comparable shear viscosity curves, but the branched polyethylene exhibits much more resistance to extensional flow over a wide range of stretch rates. The forward and reverse axial flow generated in the extruder mixing zones, which can have significant extensional strain components, broaden the residence time distribution. The higher extensional viscosity of the branched polyethylene results in narrower, more peaked residence time distributions across a wide range of operating conditions. The net effect of this increased resistance to axial flow depends upon the configuration of the extruder screws.

ACKNOWEDGEMENTS

I take this opportunity to thank the State of Michign for its financial support of this work through REF. I am also grateful to my research committee which consists of Professors Narayan and Scranton from the Department of Chemical Engineering and Professor Giacin from the School of Packaging. I wish to thank the students and staff of the Engineering Research Complex who have helped in this research, or have simply been willing to tolerate my complaints. In particular, Craig Chmielewski and Kevin Nichols have been generous with their time, either in helping me to obtain materials or demonstrating the operation of equipment. I especially wish to thank my advisor, Professor Krishnamurthy Jayaraman for his enthusiasm, availability, and patience throughout the work.

TABLE OF CONTENTS

LIST	OF TA	BLES	vii
LIST	OF FIC	GURES	viii
	I.	BACKGROUND	1
	1.1	Tuana dinasia n	
		Introduction	1
	1.2	Mixing in Polymer Systems	3
	1.3	Functionalization Reaction	4
	1.4	Reactive Extrusion	10
	1.5	Dissertation Outline	15
II.	MALI	EATION OF POLYPROPYLENE IN MODEL REACTORS .	17
	2.1	Introduction	17
	2.2	Model Reactors	20
	2.3	Experimental Procedure	25
	2.4	Experimental Results and Discussion	29
	2.5	Model Flow Fields	32
	2.6	Flow Field Discussion	35
	2.7	Conclusions	41
III.	MIXI	NG AND REACTIVE EXTRUSION OF POLYPROPYLENE	
	IN A	CO-ROTATING TWIN SCREW EXTRUDER	43
	3.1	Introduction	43
	3.2	Experimental Procedure	45
	3.3	Effect of Barrel Valve Setting, Q, and N on Extruder Flow	54
	3.4	Effect of Extruder Operating Conditions on Extent of	<i>5</i> 7
	J. T	Maleation	63
	3.5	Effect of Degradation on Extruder Flow	64
	3.6	Discussion	66
	J. U		,,,

	3.7	Conclusions	• • • • • • • • • • • • • • • • • • • •
IV.	EFFI	ECT OF RHEOLO	OGY ON MIXING
	IN R	EACTIVE EXTR	USION
	4.1	Introduction	
	4.2	Rheology of Po	olyethylene
	4.3	Experimental	
	4.4	Results on Mix	ing of Unreacted Melts
	4.5	Results on Mix	ing of Reacted Melts
	4.6		Conclusions
	5.1	Introduction	
	5.2	Experimental	
	5.3		
		Results	
	5.4	Results Discussion	
	5.4 5.5	2302000	
VI.	5.5	Discussion	
VI.	5.5	Discussion Conclusions CLUSIONS	
VI.	5.5 CON	Discussion Conclusions CLUSIONS Functionalization	

LIST OF TABLES

2-1	Relative extents of maleation from simple s	hear batch reactor	29
2-2	Relative extents of maleation from continou		30
3-1	Mean residence time		56
3-2	Degree of fill		57
3-3	Spread of residence time distribution		57
3-4	Relative level of axial dispersion		61
3-5	Level of maleation with closed barrel valve		63
3-6	Level of peroxide dissociation		68
4-1	Residence time distribution and mixing for	polyethylene melts	91
4-2			101
4-3	Maleation levels for LLDPE		101
4-4	Residence time distribution and mixing for		
	polyethylene melts		105
5-1	Summary of micelle core measurements		119

LIST OF FIGURES

1-1	Simplified reaction scheme for functionalization of polypropylene	6
1-2	Simplified reaction scheme for functionalization of polyethylene	8
2-1	Cross-sectional view of continuous flow model reactor	21
2-2	Continuous flow model reactor assembly	23
2-3	Cross-sectional view of Couette batch reactor	24
2-4	FTIR absorbance spectra of maleated polypropylene	28
2-5	Residence time distribution of peroxide in model flow reactor for two sets of operating conditions	31
2-6	Computed two-dimensional flow pattern, showing three regions of	<i>J</i> 1
	recirculating flow	36
2-7	Computed flow patterns in the forwarding gap for each set of	50
	operating conditions	37
2-8	Profiles of shear strain rates across forwarding gap for each set of	<i>3</i> ,
20	operating conditions	38
2-9	Profile of extensional strain rates along center of forwarding gap for	50
_ ,	each set of operating conditions	39
2-10	Deformation of fluid element in forwarding gap over 2.5 seconds	40
3-1	Effect of dibutyl maleate on the shear viscosity of polypropylene	
	melt	46
3-2	Twin screw extruder configuration showing feed inputs and screw arrangement	47
3-3	Extruder screw configuration	49
3-4	Barrel valve assembly, showing variation of clearance with setting	51
3-5	Calibration of FTIR measured extent of maleation with weight	-
	change measurements	54
3-6	Effect of barrel valve setting on residence time distribution of	
	polypropylene and dibutyl maleate in extruder	55
3-7	Dependence of degree of fill on the ratio of throughput rate to	
	screw rotation rate	58
3-8	Effect of screw rotation rate on the residence time distribution of	
-	polypropylene and dibutyl maleate in extruder	60
	1 71 17	

3-9	Effect of throughput rate on the residence time distribution of	
	polypropylene and dibutyl maleate in extruder	62
3-10	Effect of degradation on the shear viscosity of polypropylene	64
3-11	Effect of degradation on residence time distribution of	
	polypropylene and dibutyl maleate in extruder	65
3-12	Dependence of the level of grafting on the mean residence time	67
3-13	Dependence of the level of grafting on the hold-up volume	67
3-14	Dependence of the level of grafting on the calculated level	
	of peroxide dissociation	69
4-1	Circumferential pressure profile in mixing zone of twin screw extruder	75
4-2	Shear viscosity of polyethylene melts at 180°C	77
4-3	Zero length die schematic	79
4-4	Extensional viscosity index of polyethylene melts at 180°C	80
4-5	Ratio of extensional index to shear viscosity of polyethylene melts	81
4-6	Co-rotating twin screw extruder configuration	83
4-7	FTIR spectra of maleated LDPE	86
4-8	Calibration of extent of maleation with carbonyl index	87
4-9	Cross-section of partially starved mixing zone	89
4-10	Effect of operating conditions on the degree of fill	90
4-11	Residence time distribution for LDPE and LLDPE	92
4-12	Effect of throughput rate on residence time distribution of LDPE	96
4-13	Effect of throughput rate on residence time distribution of LLDPE	97
4-14	Effect of screw rotation rate on residence time distribution of LDPE.	98
4-15	Effect of screw rotation rate on residence time distribution of LLDPE	99
4-16	Effect of cross-linking on the shear viscosity of LLDPE melt at 180°C	103
4-17	Effect of throughput rate on RTD of LLDPE in extruder	104
5-1	Ultra-microtome procedure for sectioning of TEM specimens	115
5-2	Oriented morphology of extruded blend as extruded	117
5-3	Morphology of blend after annealing 5 minutes at 180°C	119
5-4	Growth of micelle cores upon annealing at elevated temperatures	120
5-5	Distributions of micelle core radii after annealing at 180°C	121
5-6	Distributions of micelle core radii after annealing at 200°C	122
5-7	Morphology of blend after annealing at elevated temperatures	124
5-8	Distributions distances between nearest neighbors	125
5-9	Median nearest neighbor distance plotted against square root of	
	annealing times	126

CHAPTER I

BACKGROUND

1.1 Introduction

Mixing is performed in alloying, compounding and carrying out reactions on polymer melts. The form and magnitude of strain applied in the flow of the melt is a critical factor in each of these operations. The strain must be sufficient to provide homogeneity of the melt at the desired scale. If the strain in the flow field is insufficient, the resulting product will not have the required uniformity of properties. If the strain in the flow field is excessive, undesirable consequences such as shear induced degradation can result.

The peroxide catalyzed melt functionalization reaction of polyolefin melts is an important processing application which requires the mixing of a polymer melt. The chemical modification of a polymer to improve its utility towards a specific application is of considerable commercial interest. It is generally more economically feasible to modify an existing polymer than to engineer an entirely new polymer.

The reaction is most often carried out in standard polymer processing equipment such as extruders. Extruders are well suited for melting the polymer and blending the viscous melt with an initiator and functionalizing agent. Extruders provide flow fields which may be extremely complex and difficult to characterize without the use of gross

simplifications. Key aspects of the flow can be overlooked in the model when such simplifications are made. The chemistry of the free radical reaction is also complex because the high reactivity and low selectivity of free radicals can lead to several different side reactions. The rheology of the melt, which itself may also be quite complex, affects the mixing characteristics and residence time of the reactants within the reactor. The melt rheology and flow may be dynamic factors in the reacting system since side reactions which occur along with the functionalization also affect the rheology of the melt which in turn affects its flow and mixing characteristics.

Mixing is also a critical factor in the compounding of immiscible polymer blends.

The thermal and mechanical processing history as well as the chemistry of the system determine the final blend morphology. The morphology of the polymer blend is of primary significance since it is a determining factor for the final mechanical properties.

This work is an investigation of flow and mixing in the reactive processing of polymer melts. The effects of flow and melt rheology on the progress of functionalization reactions are first examined. The significance of the details of the flow field are investigated for a miscible reacting system. The observations of the effects of extension and shear strain on the reaction progress are applied in interpreting the effects of flow conditions on the reaction progress within an extruder. Similar reactions of immiscible systems are also carried out in the extruder. The melts were carefully chosen to facilitate the investigation of the effects of melt rheology on the extruder flow and reaction progress. Finally, an investigation of the effects of thermal processing history on the morphology of an immiscible polymer blend is presented.

1.2 Mixing in Polymer Systems

Effective mixing is an essential feature in the processing of all polymer systems. Even in the processing of a pure polymer, mixing in the form of thermal homogenization must occur in order to prevent warping and to avoid residual stresses in the final molded part (1). Blends of polymers and other polymers or blends of polymers and additives can be either miscible or immiscible. Most polymer-polymer blends are largely immiscible (2). For such systems, mixing is required in order to provide homogeneity at some scale. Reacting systems may be either miscible or immiscible. In reactive systems, mixing is required to allow the constituents to come into contact and react. If inadequate mixing is provided in complex reacting systems, undesired side reactions may predominate or the level of reaction achieved may not be uniform throughout the product (3).

Effective laminar mixing requires large strain, frequent reorientation of the flow front, and the randomization of interfacial area elements (4). The mixing may be divided into its distributive and dispersive components. These aspects of mixing may be differentiated by their order and the scale at which they occur in the formation of a two component blend (1). The distribution of drops or material threads of one component throughout the other occurs in the laminar flow of a polymer melt as adjacent material elements experience different levels of strain. This may be followed by the breakup of these threads or drops which produces a homogenization of the blend on a finer spatial scale. The processing conditions as well as the thermodynamic properties of the blend constituents determine the levels of mixing attained.

1.3 Functionalization Reaction

A functionalization reaction is simply a chemical reaction carried out on a polymer to improve its utility for a selected application. The enhanced utility of the polymer may be achieved either through an improvement in a key set of material properties or by preparing the polymer to undergo a subsequent procedure which then improves some set of key material properties. The particular set of functionalization reactions examined in this work is the maleation of polyolefins. In the reaction, polar molecules are grafted to the polyolefin macromolecules. The reaction may be performed to increase the compatibility of the grafted melt with dyes or with other polymers in blends such as nylons which already contain polar sites. Often, the maleation is carried out to improve the adhesion of the polymer to reinforcing agents such as chopped wood or glass fiber with suitable sizing. Large changes in physical properties have been measured in cases with only a modest level of maleation. Merely one weight percent grafting of maleic anhydride onto polypropylene results in better adhesion to glass fiber. This improved adhesion results in significantly better mechanical properties of the composite (5). A similarly modest level of grafting significantly reduces the size of its dispersed functionalized polypropylene particles when melt blended into a Nylon 6 matrix **(6)**.

The maleation reaction may be performed on the polymer melt (or solution) through the use of an active free radical initiator such as an organic peroxide. The exact mechanism of the reaction is not fully known since the identity and concentration of all intermediate species has not yet been determined (7). A most probable mechanism has

been suggested by a number of researchers (7 - 13). Initially, a homolytic cleavage of the oxygen-oxygen bond in dicumyl peroxide is thermally induced. This results in the formation of 2 alkoxy radicals. Each alkoxy radical may then abstract a hydrogen from a polyolefin chain to form a macro-radical. The macro-radical may then attack the unsaturated bond of a maleating agent. The reaction is propagated as the grafted radical abstracts a hydrogen from another polyolefin chain segment. The initiating and intermediate free radicals are highly reactive and thus not very selective. Therefore, side reactions involving the macro-radicals can occur either in series or in parallel with the grafting reaction. At sufficiently high temperatures or strain rates, oxygen can also function as an initiator (8). For these conditions, the reactions would progress without the addition of peroxide.

Instead of grafting to the maleating agent, the polyolefin macro-radicals can either combine in a cross-linking reaction or disproportionate which results in chain scission. The predominance of particular side reactions depends upon the molecular structure of the polyolefin. Tertiary radicals are prone to disproportionate which results in a degradation through β chain scission. A reaction mechanism for the dicumyl peroxide initiated grafting of dibutyl maleate onto polypropylene is shown in Figure 1-1. Additional intermediate species as well as products can also be formed. The homopolymerization of dibutyl maleate can occur at high radical concentrations.

Secondary radicals do not undergo chain scission to an appreciable extent (8). Polyethylene macro-radicals are therefore more likely to combine in a cross-linking reaction than to degrade. Borsig and coworkers (9) found that in a 1 to 1 blend of

Figure 1-1 Simplified reaction scheme for functionalization of polypropylene

polyethylene and polypropylene with 2.5 weight percent dicumyl peroxide added, only the polyethylene cross-linked appreciably at 160°C. Unlike the degradation reaction, the cross-linking reaction is a termination step in the grafting reaction mechanism. Although less probable, some degradation can still occur since polyethylene does contains tertiary carbons at its branch sites. A reaction mechanism for the grafting of maleic anhydride onto polyethylene is shown in Figure 1-2. Additional intermediates and final products have been suggested by Gaylord et al. (10-11). These can involve the homopolymerization of maleic anhydride or the formation of complexes.

Selectivity is the degree to which one reaction predominates over a competing reaction. The selectivity of these reactions depends upon the reactant and initiator concentrations and the reactor operating conditions. An apparent disagreement exists over whether the presence of a maleating agent reduces the probability for side reactions to occur. Hogt (3) has noted that for a concentration of 2 parts maleic anhydride per hundred parts polypropylene by weight, both the degradation and maleation levels increase proportionally with an increase in the initial concentration of peroxide. With the same peroxide concentration and a higher concentration of maleic anhydride (5 parts per hundred), more grafting and less degradation occur. Conversely, Gaylord and coworkers found that at a fixed peroxide concentration, the presence of maleic anhydride increases the level of cross-linking of ethylene-propylene rubber (10) and also increases the level of degradation in polypropylene melt (11). Both (3,9) have pointed out that maleic anhydride and the polyolefins are immiscible in melts where the maleic anhydride fraction exceeds about 5%. Dibutyl maleate and ethylene-propylene rubber may be

Figure 1-2 Simplified reaction scheme for functionalization of polyethylene

miscible at dibutyl maleate concentrations up to 10%. For this more homogeneous system, the side reactions are suppressed by the presence of the maleate (11).

Still other side reactions may occur through the free radical process in addition to cross-linking and degradation. One such potential side reaction is the oligomerization of the maleating agent such as maleic anhydride. The product from this reaction is a polyolefin with grafts of maleate chains. A radical could abstract a hydrogen from a free maleate unit to initiate this reaction. The free radical maleate could then attack the unsaturated bond of another maleate to form a linkage. This process could be repeated to form chains of the maleate units. The resulting poly (maleic anhydride) could then be grafted onto the polyolefin through a chain transfer mechanism. Aglietto *et al.* (12) have investigated the structure of diethyl maleate grafted to low molecular weight polyethylene in solution. They were able to conclude through the use of NMR (nuclear magnetic resonance) that primarily single units rather than chains of diethyl succinate were grafted to the polyethylene at the reaction conditions they selected.

Temperature and mixing can also affect reaction selectivity. Shiah and Chen (14) investigated the dicumyl peroxide initiated grafting of maleic anhydride onto a triblock copolymer (polystyrene end blocks with poly (ethylene-butylene) mid block) melt within a single screw extruder. The concentrations of peroxide in their study were very high, ranging 10 to 30 parts per hundred of the copolymer. They found that the polymerization of maleic anhydride was favored at extruder temperatures exceeding 200°C. They also noted that the level of cross-linking increased when the screw rotation rate was increased from 20 to 60 rpm. This observation is remarkable since one would

expect the corresponding reduction in residence time to reduce the level of reaction. They attribute the increased cross-linking to an increase in the production of macro-radicals through mechanical degradation of the copolymer. A consideration of the mixing characteristics of the reaction constituents inside the extruder suggests an alternative explanation for the observed increase in cross-linking. Low screw rotation rates may provide inadequate mixing to allow the peroxy free radicals to efficiently attack the copolymer chains. If the peroxide and maleic anhydride are phase separated from the polymer, the peroxy radicals may polymerize the maleic anhydride rather than form radical sites on the copolymer.

1.4 Reactive Extrusion

1.4a Flow Field and Mixing in Extruder

Extruders when designed and operated properly serve as ideal reactors for the functionalization of polymer melts. Complex flow fields are required to adequately perform the necessary melting and mixing of viscous fluids. The flow within the extruder is determined in part by the geometry and action of the mixing elements. Greco et al. (13) performed the maleation reaction as a batch process in a Brabender mixer. This gave them direct control of the residence time. More commonly, extruders are used to carry out the reaction in continuous mode. The geometry and screw action determine the flow field which affects the reaction progress. Single screw extruders are sometimes used as reactors. In general, these extruders are more sensitive to fluctuations in the feed rate and provide less efficient mixing than twin screw extruders (15). Suwanda and

Balke (16) concluded that the single screw extruder provided for insufficient dispersive mixing of the peroxide into a polyethylene melt. This can be partially ascribed to the relative lack of extensional strain imparted to the fluid processed in a typical single screw extruder as compared to a twin screw extruder under similar operating conditions. However, some single screw machines are now designed with self wiping action and do provide enhanced mixing capability (17). Fully intermeshing co-rotating and counterrotating twin screw extruders may also be compared in very general terms. Counterrotating screws impart higher stresses than do co-rotating screws operated at the same rotation rates (18). Therefore, the counter-rotating extruders are typically operated at lower screw revolution rates. Rauwendaal (19) found that counter-rotating extruders therefore provided better distributive mixing of small particles. For the same screw rotation rates, the counter-rotating extruder also tends to provide a narrower residence time distribution than that provided from a co-rotating extruder (20). The kneading disc sections which may be present in either extruder provide for open channels which allow for more axial mixing.

The modular co-rotating screw elements may be configured to affect the level of mixing and the residence time distribution. The screw geometry of the kneading disc or paddle region has been described by Booy (21). The analysis is complicated because the orientation of the intermeshing paddles changes as the screws rotate. The axial arrangement of the discs determines the degree of forwarding or reversing action and affects the level of mixing. Kalyon and Sangani (22) studied the effect of co-rotating extruder screw configurations on the level of mixing achieved for a polymer melt. They

conclude that the interfacial area between dyed and undyed polymer increases the most when passing through the nip region between the paddles. They further note that forwarding paddles promote faster axial mixing than neutral or reversing paddles.

The pressure driven flow through the paddle geometry can lead to significant extensional as well as shear strain rates for the melt. A number of investigators have attempted to model the complex flow within an extruder more rigorously. Generally, these modelling efforts rely upon simplifying assumptions which limit the applicability of the resulting model. Szydlowski and White (23) modelled the flow of a power law fluid in the three lobed kneading disc section. They neglect the curvature of the kneading discs and the barrel wall in their analysis and assumed fully flooded conditions. Xiaozheng et al. (24) also predict axial pressure profiles relying on these assumptions. Wang and coworkers (25) model the flow in the kneading disc region and the rest of the screw relying on the same assumptions. McCullough and coworkers (26) present predicted pressure profiles when the expansion - compression cycle is accounted for in the flow modeling. They do not account for recirculating flows. Bigio and Wigginton (27) observed experimentally that the three dimensional flow generated in the nip region between counter-rotating kneading discs promotes reorientation of interfacial areas that enhances mixing. Gotsis et al. (28) present a fully three dimensional model for flow in the kneading disc region of a co-rotating extruder. Their model assumes fully filled screw regions. They determine that for arbitrary chosen axial pressure drops, the axial flow is proportional to the pressure drop. Bigio and coworkers (29) note that a degree of fill greater than 40% in a co-rotating twin screw extruder results in more fluid contact with the barrel surface and better mixing.

The residence time distribution can be used to characterize the distributive or macro-mixing in a continuous flow. Eise and coworkers (30) varied throughput and rotation rate in a fully intermeshing co-rotating twin screw extruder. They determined residence times of a metallic tracer through conductivity measurements and concluded that higher screw rotation rates and a smaller degree of fill resulted in greater axial mixing. Nichols (31) used radioactive tracer to determine the residence time distribution in each modular section of a co-rotating twin screw extruder. He notes that tracer materials which are chemically different from the bulk material could produce artifacts in the residence time measurements. Todd (32) points out that after the dye injection, additional dye should not be allowed to gradually bleed into the flow or the tail of the residence time distribution will not be measured accurately.

1.4b Effect of Operating Conditions on Reaction Progress

Because of the complex flow field, the effects of reactor conditions on the products of a graft maleation reaction have often been interpreted in terms of mechanical energy input rather than attempting to characterize the flow field in any detail. Ganzeveld and Janssen (7) investigated the grafting of maleic anhydride on high density polyethylene (HDPE) in a counter-rotating twin screw extruder. They concluded that the reaction was diffusion limited and difficult to find optimal conditions. As an example, they found that increasing the screw rpm led to better mixing but shorter residence times. Grenci et al. (32) premixed a peroxide with maleic anhydride and then added this

mixture to molten polyethylene in a single screw extruder. They observed that higher screw rotation rates led to higher levels of maleation as well as increased levels of crosslinking. They also report that lower throughput rates or longer residence times had the same effect. Sakai (20) also observed that greater inputs of mechanical yielded higher extents of maleation of ethylene-vinyl acetate copolymer. Sakai preblended all reactants (ethylene vinyl acetate copolymer, maleic anhydride and benzoyl peroxide) before carrying out the reaction in a two stage extrusion process. However, the details of the flow field govern the extent of deformation and mixing obtained for a given level of mechanical energy input or stress level (33). For example, the critical stress required for drop breakup and dispersive mixing is lower in extensional flows than in shear (34). When the viscosity ratio between the dispersed phase and the continuous phase is greater than four, extensional strain results in a smaller ultimate dispersed particle size than does simple shear (35).

When carrying out the maleation reaction in an extruder, the order of introduction of reactants is an important consideration. White (36) noted that when adding the peroxide, polymer and maleic anhydride to the extruder at the same time, the co-rotating extruder yielded higher levels of grafting and less cross-linking than did the counter rotating extruder. He attributes this to the added viscous dissipation in the counter rotating extruder resulting decomposition of the peroxide before the reactants are sufficiently dispersed.

1.4c Effect of Rheology on Extruder Flow

Changes in the molecular weight distribution of the polymer during processing also may affect its residence time distribution. Tzoganakis *et al.* (37) found that the peroxide promoted degradation of polypropylene resulted in a broadening of its residence time distribution in a single screw extruder. They attributed this change to a relative increase of pressure driven back flow to shear driven forwarding flow in the melt due to the reduced shear viscosity. The viscosity in shear and the viscosity in extension each depend differently upon the molecular weight distribution. The shear viscosity depends strongly upon the average molecular weight while the extensional viscosity depends more heavily upon the high molecular weight tail end of the molecular weight distribution. Since the controlled degradation reaction primarily affects the high molecular weight tail of the polypropylene molecular weight distribution, the reduction in extensional viscosity could be much more significant than the decrease in shear viscosity.

1.5 Dissertation Outline

The three following chapters of the thesis are each self contained studies which examine specific issues relating to the effects of rheology and flow on the functionalization of polymer melts. A study of the effects of flow on the maleation of polypropylene in model reactors is presented in Chapter II. A model reactor design which provides estimable levels of shear and extensional strain rates is presented. The maleation reaction is carried out in the model reactor and also in a simple Couette flow batch reactor to determine the effects of extensional and shear strain on the reaction

progress. In Chapter III, the results from this analysis are applied to the investigation of the progress of the same reaction within a twin screw extruder. The effects of the extruder operating conditions on the flow in the extruder are characterized through the determination of the residence time distributions. The effects of extruder flow on the measured reaction progress discussed. In Chapter IV, a study of the maleation of low density polyethylenes in a twin screw extruder is presented. The particular polyethylenes were selected in order to determine the effects of the extensional rheology of a polymer melt on its flow and reaction progress.

The effects of thermal and mechanical processing history on a non-reacting, immiscible blend of polymers are examined in Chapter V. Here, the kinetics of micelle growth and clustering in a blend of butadiene-styrene diblock copolymer and high molecular weight polystyrene are presented. The conclusions for the work along with recommendations comprise the sixth and final chapter.

CHAPTER II

MALEATION OF POLYPROPYLENE IN MODEL REACTORS

2.1 Introduction

Polyolefins are modified with maleic anhydride in order to improve their adhesion to reinforcements such as short glass fibers or to other polymers such as nylon (5,6,38). This functionalization reaction is often carried out in the melt state in the presence of a free radical initiator (3,32,39,40). Several investigators (10,11,13,41,42) have discussed the reaction mechanism of polyethylene and polypropylene maleation. An organic peroxide initiator first promotes the formation of macro-radicals which may then combine with a maleic group in a grafting reaction. The polypropylene macro-radicals may also degrade by chain scission at the tertiary carbon while the more reactive polyethylene macro-radicals may instead cross-link to form a gel. The secondary radical resulting from chain scission may then combine with a maleic group. Together, these steps form a complex series-parallel reaction system.

The grafted anhydride readily hydrolyses and must be dried at elevated temperatures in a vacuum oven immediately before the determination of the extent of grafting. The extent of maleation has been determined quantitatively in terms of wt.

percent of the unhydrolyzed succinic adduct on the polymer using titration. The dry modified polymer is dissolved in xylene and titrated to its endpoint using potassium hydroxide in an alcohol solution with thymol blue present as an indicator. Fourier transform infrared spectroscopy on a thin film of the dry modified polymer has also been used to determine the extent of maleation (41). The ratio of the intensity of the carbonyl absorption peak to that of the methyl group peak, known as the carbonyl index indicates the relative levels of grafting. This latter method was employed in this work.

The effects of initial composition and temperature of the reaction mixture on the progress of the polypropylene maleation have been explored by Hogt (3, 41), by Gaylord and coworkers (10,11), and by Greco et al. (13). Hogt has noted that at low concentrations (2 parts per hundred resin) of maleic anhydride, the extent of maleation and the extent of degradation increase simultaneously with the level of peroxide; at higher concentrations (5 phr), the scission reaction is suppressed and the extent of maleation is higher for a given peroxide concentration (0.5 phr). Both Gaylord et al. (10) and Hogt (3) have pointed out that this reaction is heterogeneous when a higher concentration (> 5 phr) of maleic anhydride is present in the reaction mixture because excess maleic anhydride becomes segregated from the polymer phase. However, Greco et al. (13) have developed a chemically similar reaction system consisting of dibutyl maleate, dicumyl peroxide and ethylene-propylene rubber that remains homogeneous even at greater maleate concentrations (10 phr). In this work, the functionalization reaction carried out with dibutyl maleate and a polypropylene lightly copolymerized with ethylene. The presence of 3% ethylene on the polypropylene chain enables the mixture to be processed at a lower temperature while still avoiding the crosslinking reactions characteristic of polyethylene.

The effect of other processing conditions on the products of a graft maleation reaction has been interpreted in terms of mechanical energy input. Grenci et al. (32) premixed a peroxide with maleic anhydride and then added this mixture to molten polyethylene in a single screw extruder. They observed that higher screw rotation rates led to higher levels of maleation as well as increased cross-linking. They also report that lower throughput rates (longer residence times) had the same effect as the higher screw rotation rates. Sakai (40) carried out the maleation of an ethylene-vinyl acetate copolymer in a two-stage extrusion process. He reported that greater inputs of mechanical energy yielded higher extents of maleation. However, the details of the flow field govern the extent of deformation obtained for a given level of mechanical energy input or stress level (33). The efficiency of the dispersive mixing depends upon the details of the flow field. The critical stress required for droplet breakup is lower in elongational flows than in shear flows (34).

The method of reactant addition has also been found to affect the reaction progress. Greco et al. (13) point out that when the time required for mixing is greater than the time required for reaction, local concentration inhomogeneities may not be levelled before the reaction occurs. For their low temperature ethylene-propylene rubber system they were able to preblend the reactants including the peroxide at a temperature below the reaction threshold. Other investigators (32) have added the maleic anhydride and peroxide after first melting the polymer thereby reducing the amount of reactions that

occur before mixing. In this work, the polymer and dibutyl maleate are preblended before adding the initiator. The initiator added to a single phase system so that it can not be entrapped in the dibutyl maleate phase and lead to dibutyl maleate homopolymerization.

The object of this work is to examine the relation between the deformation field and the progress of a polymer melt functionalization reaction. This is done with two model reactors. The first is operated as a continuous flow reactor. The computed flow fields and deformation fields in this reactor are described for a variety of operating conditions. The second reactor is a batch reactor providing uniform residence times and a simple shear flow. Operating conditions for this reactor are selected so as to compare to those explored in the continuous flow reactor. In both reactors, the peroxide is added to a preblended single phase mixture of polymer and dibutyl maleate. Experimental results are presented on the extents of maleation obtained with each reactor. Experimentally determined residence time distributions are also presented for the continuous flow reactor. Comparison of the extents of maleation obtained with these well characterized flow fields provides insight into the importance of the details of the flow field as they relate to the progress of the polymer reaction.

2.2 Model Reactors

2.2a Continuous Flow Reactor

A design of the continuous flow model reactor was developed on the basis of the following considerations. The geometry of the fluid holdup region should be time

invariant in order to obtain a steady and well characterized flow field within the reactor. A significant extensional flow region must be produced within the reactor to obtain a wide range of deformation fields under different operating conditions. Recirculating eddies appear typically in converging or diverging flow geometries. The sizes of these eddies must be balanced against increases in extensional strain rate while selecting the taper and gap dimensions. Finite element simulations of the flow were carried out to select a reactor design according to these criteria.

A schematic of the continuous flow reactor used for maleation of polypropylene is shown in Figure 2-1. This reactor consists of a rotating cylinder with a radius of 2.2

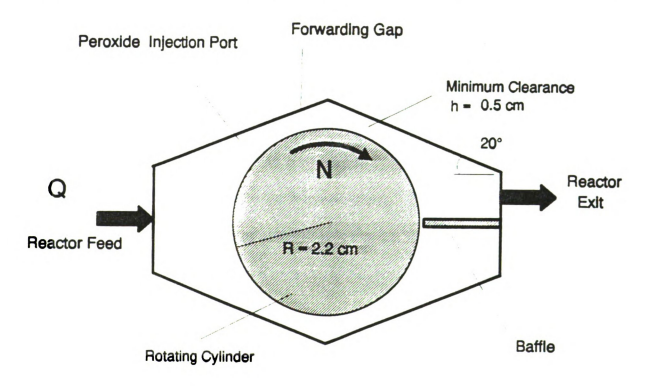


Figure 2-1 Cross-sectional view of continous flow model reactor

cm and length of 20.3 suspended in a converging and diverging enclosure with walls at 20° taper. The minimum clearance in the nip region between the rotating cylinder and the enclosure is 5 mm. Smaller clearances lead to greater pressure differences within the reactor and to much larger recirculating eddies. The nip region where cylinder rotation is along the direction of the inlet flow, is termed the forwarding gap. A baffle on the downstream end prevents flow into the exit port from the opposing gap. The baffle also serves to reduce the size of the downstream eddy. The resulting flow field resembles those encountered in roll processing devices described by Tadmor (39). Flow in the nip is dominated by shear and flow in the converging region upstream of the nip is dominated by extensional effects.

The major feed stream into the reactor is a blend of molten polypropylene and dibutyl maleated supplied in a 10 to 1 ratio by weight from a twin screw extruder. The capacity of the extruder imposes an upper limit on the feed rate Q of 100 ml/min. The peroxide initiator dissolved in xylene is injected separately into the reactor slightly upstream of the nip region into the forwarding gap. The locations of the primary feed and the exit port of the reactor are shown in Figure 2-2. They are both circular with a 1/4 inch diameter and are located near the vertical center of the reactor which is 20.3 cm in height.

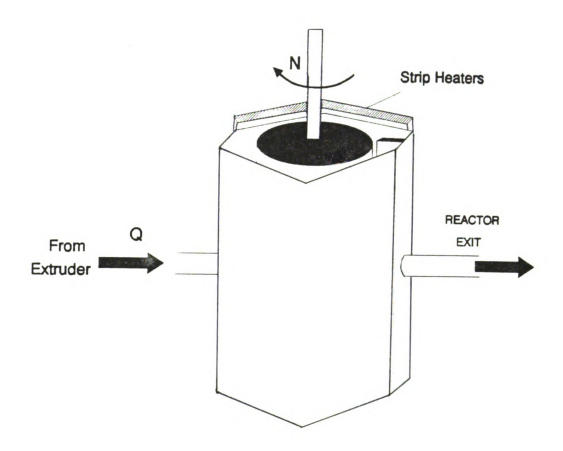


Figure 2-2 Continuous flow model reactor assembly

2.2b Batch Reactor

Maleation of polypropylene melt was also studied in a batch reactor with a simple shear flow. This was done for two reasons. First, a nearly homogeneous shear flow is obtained in the batch reactor, while a range of shear strain rates and extensional strain rates are obtained in the continuous flow reactor. Second, the residence time is uniform in the batch reactor while a distribution of residence times is associated with the flow field in the continuous flow reactor. The batch flow reactor shown in Figure 2-3 consists of a rotating circular cylinder of radius 2.54 cm positioned concentrically in a stationary outer cylinder with a clearance of 0.4 cm.

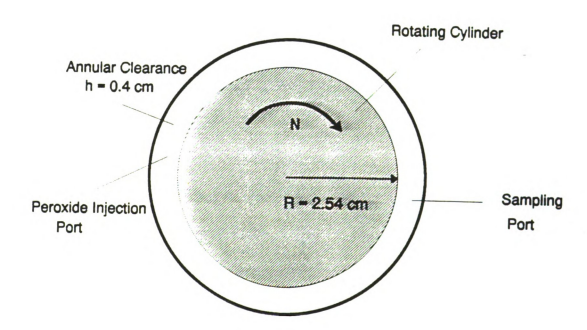


Figure 2-3 Cross-sectional view of Couette batch flow reactor

2.3 Experimental Procedure

2.3a Preblending Operation

Ten parts by weight of dibutyl maleate, a liquid at ambient temperature, was added to a hundred parts of polypropylene pellets (Himont SA-849) in the hopper of a Baker-Perkins (APV) model MPC/V-30 co-rotating, fully intermeshing twin screw extruder having an L/D ratio of 13. The feed rate was maintained at either 45 ml per minute or 90 ml per minute. The extruder was operated with screw rotation rate of 250 rpm while the melt temperature in the mixing zones and in the exit die was maintained at 180°C. Polypropylene and dibutyl maleate extruded together under these conditions form a single phase blend. The dibutyl maleate acts as a plasticizer, lowering the viscosity of the polypropylene by nearly 50%. This preblending operation reduces the amount of polypropylene degradation in the reactor (39). The extent of maleation obtained in this step is negligible (see Figure 2-4a and section 2.3c).

2.3b Reactor Operation

A short coupling was used to connect the extruder exit directly to the inlet of either the continuous flow or batch reactor. Both model reactors were maintained at 180°C by external silicone heating strips with heating output adjusted by a separate single channel controller. The temperature of the melt was measured at several locations within the reactor by inserting a thermocouple. The variation measured in either reactor did not exceed 1°C. A 0.15g/cc solution of dicumylperoxide in dry xylene was prepared for injection into the reactor. Either reactor was filled with the molten mixture in 2 minutes.

Four sets of operating conditions were investigated with the continuous flow reactor. The feed rate Q was set alternately at 45 ml/min and 90 ml/min. The rotation rate N was set alternately at 30 rpm and 100 rpm. After a steady flow of the molten polymer mixture was established, the peroxide solution was injected via a 1.75 mm diameter syringe. The tip of the syringe was located just upstream of the forwarding gap in the central plane of the reactor. The rate of injection was adjusted according to the feed rate Q in order to provide the initial 100 to 10 to 1 ratio by weight of polypropylene to dibutyl maleate to dicumyl peroxide. After injecting the peroxide steadily for 1 minute, a sample was collected at the exit port and quenched in cool water to arrest the reaction.

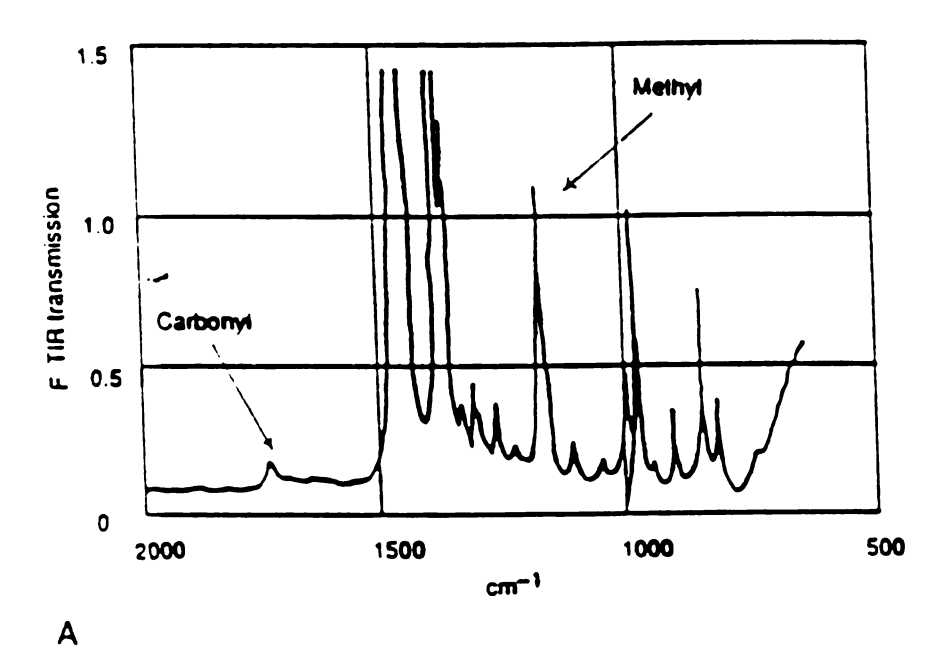
The rotation rate of the inner cylinder in the batch reactor was set alternately at 67 rpm and at 100 rpm to provide shear strain rates of 45 s⁻¹ and 67 s⁻¹ respectively. A pulse of peroxide solution was added through an injection port located on one side of the central plane of the apparatus. The peroxide solution aliquot was preweighed to provide the same 100 to 10 to 1 initial proportion of reactants. Samples were collected after 10 and 20 seconds from the other side of the cylinder directly across from the peroxide injection port and immediately quenched in water to stop the reaction. The chosen combinations of shear strain rates and sampling times provide sufficient shear strain in this reactor to make meaningful comparisons with the results of the continuous flow reactor.

2.3c Product Analysis

The collected samples in the form of thin strands were placed in an acetone bath for 12 hours in order to remove any residual dibutyl maleate or dicumylperoxide. These strands were then heated to 180°C and pressed for 1 minute at 10,000 lb, into thin (\sim .08 mm) films. These films were placed in a vacuum oven and heated to 100°C at 29" Hg of vacuum for a period of 72 hours in order to remove any moisture or residual dibutyl maleate. Upon removal from the vacuum oven, thin film FTIR absorbance spectra were obtained in a Perkin-Elmer 1800 system. The carbonyl peak associated with the maleate component occurs at 1760 cm⁻¹. The methyl group peak due to the polypropylene appears at 1060 cm⁻¹. The ratio of the area of the carbonyl peak indicating anhydride groups to that of the methyl group peaks from the polypropylene is known as the carbonyl index and provides a qualitative indication of the extent of the maleation reaction. Hogt (41) has confirmed that the carbonyl index is linearly proportional to the extent of maleation. The two absorbance spectra shown in Figure 2-4 have carbonyl indices of 0.07 and 1.4. These indices correspond to 0.2 weight percent and 3.5 weight percent (see section 3.2e2). The carbonyl index of 0.07 was measured from a specimen of the preblended extrudate without any peroxide. The carbonyl index of 1.4 was measured from a specimen processed with peroxide in the continuous flow reactor.

2.3d Tracer Tests

Residence time distributions in the continuous flow model reactor for the different sets of operating conditions. A 5 ml pulse of red tracer dye was injected instead of the



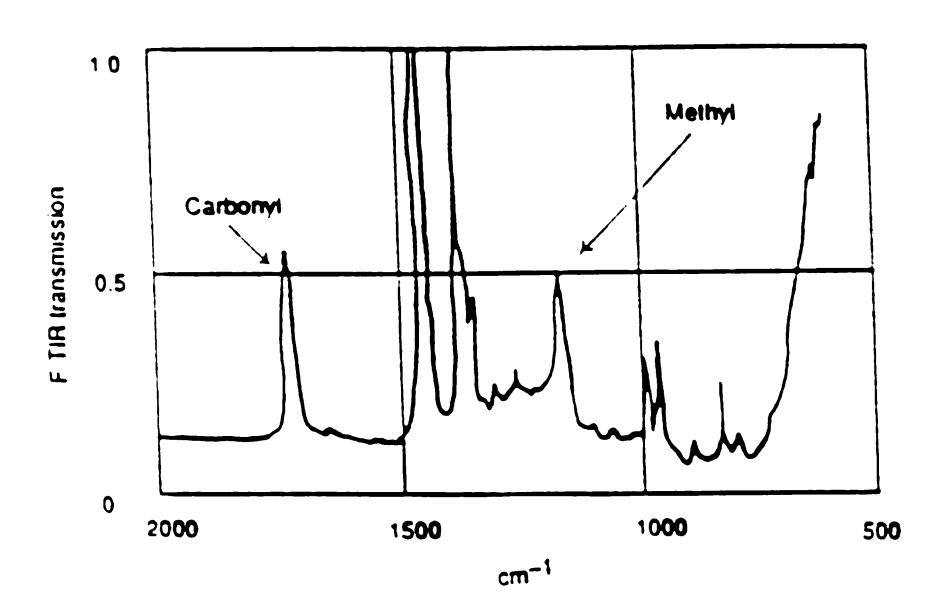


Figure 2-4 FTIR absorbance spectra of maleated polypropylene A) 0.3 % grafted B) 2.6% grafted

peroxide solution at the same location. Small samples (less than 1 gram) of the materialexiting the reactor were collected at time intervals of 5 seconds. These samples were pressed into films. The films were then tested in a spectrophotometer where a color index proportional to dye concentration was obtained.

2.4 Experimental Results and Discussion

The carbonyl indices measured from the specimens processed in the batch reactor are shown below in Table 2-1. The indices extend from 0.3 to 0.5 only, with shear strain rates from 45 s⁻¹ to 67 s⁻¹. For a residence time of 10 seconds, this increase in the shear strain rate does not lead to a noticeable increase in the extent of maleation. The relative extents of maleation obtained in the continuous flow reactor are shown in Table 2-2. The carbonyl index ranges from 0.3 to 1.4 for the continuous flow reactor, compared to a range of 0.3 to 0.5 for the batch reactor. As the rotation rate is increased from 20 to 100 rpm in the continuous flow reactor, the extent of maleation obtained with either flow rate is increased two-fold. This occurs despite the fact that the larger value of the characteristic shear strain rate in this reactor is only 46 s⁻¹.

Table 2-1 Relative Extents of Maleation From Simple Shear Batch Reactor

	20 rpm	67 rpm
20 sec	0.3	0.4
10 sec	0.1	0.3

standard deviation = ± 0.05

Table 2-2 Relative Extents of Maleation From Continuous Flow Reactor

	30 rpm	100 rpm
45 cc/min	0.7	1.4
90 cc/min	0.3	0.6

standard deviation = ± 0.05

The difference in the effectiveness of the two reactors may be attributed to differences in residence time distribution and to differences in the deformation of fluid elements in the two reactors. The significance of these two factors has been examined by studying variations in these factors with operating conditions in the continuous flow reactor. The exit age or residence time distribution has been evaluated experimentally with tracer tests. Differences in deformation of fluid elements under different operating conditions within the same reactor have been evaluated by fluid dynamics computations. These results are discussed in the following sections.

Experimentally determined residence time distributions in the fluid exiting the continuous flow reactor are presented in Figure 2-5 for two sets of operating conditions. Each set of data was fitted to a sum of two exponentials in order to estimate the mean residence time. A mean residence time of 12 seconds was calculated for the run with Q=90 ml/min and N=30 rpm while the mean residence time was determined to be 15 seconds for the run with Q=45 ml/min and N=100 rpm. These values of mean residence time may be compared with a reaction time scale estimated as follows. The controlling reaction step is the decomposition of the peroxide (13). The half-life of dicumyl

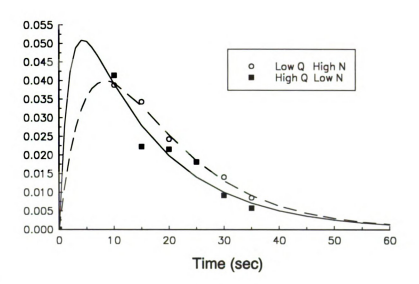


Figure 2-5 Residence time distributions of peroxide in model flow reactor for two sets of operating conditions

peroxide at 180° C is estimated from the data of Peacock (43) to be 60 seconds. The degree of axial dispersion may be characterized by the spread in exit age distribution. Although the distribution is slightly more peaked at earlier times for the case with Q=90 ml/min and N=30 rpm, the spread in exit age distribution is estimated to be close for the two cases. Hence, the difference in the residence time distributions between runs is not sufficient to explain the more than four fold enhancement in the extent of maleation. The following analysis of the flow field in the continuous flow reactor will establish that the changes in extent of deformation of a fluid element are consistent with the observed changes in the extent of maleation.

2.5 Model Flow Field

2.5a Finite Element Simulation

Finite element simulations of flow in the continuous flow model reactor were carried out with the help of FIDAP (44), a finite element flow simulation software package. The object of these simulations is to explore the differences in fluid deformation and dispersion among various runs in the model reactor. The computations were done for isothermal, two dimensional flow of a Newtonian fluid within the cross section shown in Figure 2-1. Inertial terms were neglected and no-slip boundary conditions were used in the simulations. With the feed arrangement depicted in Figure 2-2, the reactor throughput is concentrated near the vertical middle and necessarily limited near the top and bottom. In order to carry out two-dimensional flow simulations that are useful in interpreting the experimental runs, an equivalent flow rate per unit height through the reactor must be specified. The effective holdup volume in the reactor was estimated for the experimental runs from the corresponding residence time distributions within the reactor. Consistent values of the inlet velocity and inlet port width were then selected for the numerical simulations of four separate cases. The results of these simulations depict the trends in the flow field as operating conditions are changed.

A penalty approach was used to decouple the solution of the nodal velocities from the pressure values. The resulting form of the continuity equation is shown below.

$$\nabla \cdot V = -\epsilon P \tag{2-1}$$

 \underline{V} is the velocity vector, P is the pressure and λ , the penalty parameter, is a small

positive constant (10⁻⁹). The equation of motion for Stokes flow is

$$\nabla P = \eta \nabla^2 \underline{V} \tag{2-2}$$

where η is the fluid viscosity. Combining Equations 1 and 2 yields

$$-\frac{1}{\epsilon}\nabla\left(\nabla\cdot\underline{V}\right) = \eta\nabla^{2}\underline{V} \tag{2-3}$$

This equation is solved on a finite element mesh with 2,057 nine noded elements. A biquadratic interpolation scheme is used for the velocities with nine nodes per element.

Strain rates in the forwarding gap region were calculated from the nodal velocity values. The forwarding gap region is of particular importance since this is where the peroxide is injected and presumably where the reaction rates are highest. The nodal velocities along the shortest line drawn from the outer wall to the rotating cylinder were fit to low order Tschebyshev polynomials. The procedure was repeated for the nodes along a streamline in the center of the gap. The derivatives of these functions along the direction normal to the streamline, y and along the tangent to the streamline, x were used to calculate the shear and extensional strain rates respectively.

$$\gamma = \frac{dV_x}{dy} \tag{2-4}$$

$$\epsilon = \frac{dV_x}{dx} \tag{2-5}$$

2.5b Reactor Control Variables

The two significant control variables inherent in this model reactor operation are the volumetric throughput rate Q, and the cylinder rotation rate N. The ranges of these two parameters are bounded only by the limitations imposed by the experimental equipment. The maximum level of Q is determined by the capacity of the extruder which is used to melt and preblend the polypropylene and dibutylmaleate and meter them into the model reactor. N is maintained by an external electric motor and thus is limited by the maximum torque supplied by the motor. Two levels of the control parameters designated as High and Low are investigated.

Two dimensional model simulations of flow in the reactor are accomplished by neglecting flow in the axial direction. The three dimensional experimental schematic is shown in Figure 2-2. The 1/2" diameter feed and exit ports are positioned near the vertical center of the reactor which is 20.3 cm in height. The geometry suggests that the flow through the reactor is concentrated in the middle section and necessarily limited near the top and bottom. In order to model the flow in two dimensions, a satisfactory method of converting the feed rate into a flux through the cross-section (q) is required. An approximate means is provided by determining the effective reactor holdup volume V_e . This is given by Equation 2-6.

$$V_{a} = \tau \cdot Q \tag{2-6}$$

A value of τ , the mean residence time, of 20 sec for the low feed rate was estimated from the results of tracer experiments carried out in the model reactor which will be

further discussed in the experimental section. The estimated V_e of 15 cm³ was then divided by the cross-sectional area available for flow (17 cm²) to give the effective reactor height H_e (1 cm). This height is then used to determine the flux in the simulations.

$$q = \frac{Q}{H_a} \tag{2-7}$$

2.6 Flow Field Discussion

The computed streamline pattern over the entire cross section of the reactor is shown in Figure 2-6 for the high Q, low N set of operating conditions. Three eddy regions, indicated by closed streamlines, are evident. One eddy is located just upstream from the cylinder. The other two are located on the downstream side of the cylinder separated from each other by the baffle. The eddy appearing downstream of the peroxide injection port is especially important because it controls the distribution of peroxide in the melt flowing to the exit. The changing size of this eddy with changing operating conditions may be seen in Figure 2-7. As the feed rate is increased, the size of the eddy is decreased. Increasing the cylinder rotation rate leads to larger eddies. Hence the size of this eddy decreases with increasing values of the ratio Q/N. The presence of eddies reduces the effective reactor area through which the exiting material passes. A larger eddy leads to a lower effective reactor holdup area. Hence, the effective reactor holdup increases monotonically with increasing values of the ratio Q/N. This trend is confirmed by estimates of effective reactor holdup volume from experimental measurements of residence time distributions (see section 2.4).

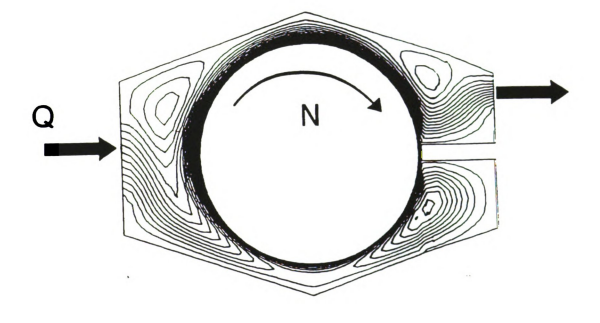


Figure 2-6 Computed two-dimensional flow pattern for continuous flow reactor showing three regions of recirculating flow

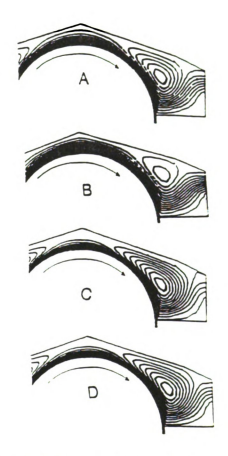


Figure 2-7 Computed flow patterns in the forwarding gap for each set of operating conditions

A) low Q, low N B) high Q, low N C) low Q, high N

D) high Q, high N

The shear strain rates across the gap are shown in Figure 2-8 for each case. The distance across the gap is measured from the outer wall to the cylinder surface. The variation of shear strain rate across the gap is most pronounced for the two higher rotation rate cases. The extensional strain rates along the centerline of the gap are shown in Figure 2-9. The distance along the gap is measured from 1.2 cm upstream of the minimum clearance point in the gap. The highest extensional strain rate is produced for the low Q high N case. For the same case, the extensional strain rate is held at the highest level for most of the distance along the gap, leading to significant stretching of fluid elements.

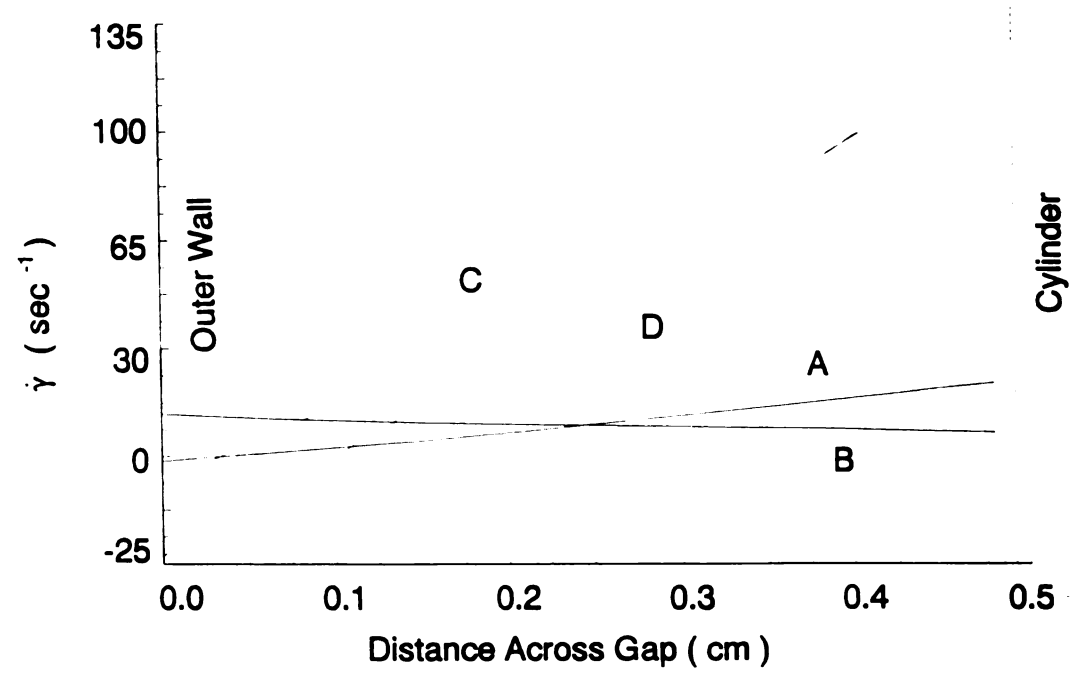


Figure 2-8 Profile of shear strain rates across forwarding gap for each set of operating conditions

A) low Q, low N B) high Q, low N C) low Q, high N

D) high Q, high N

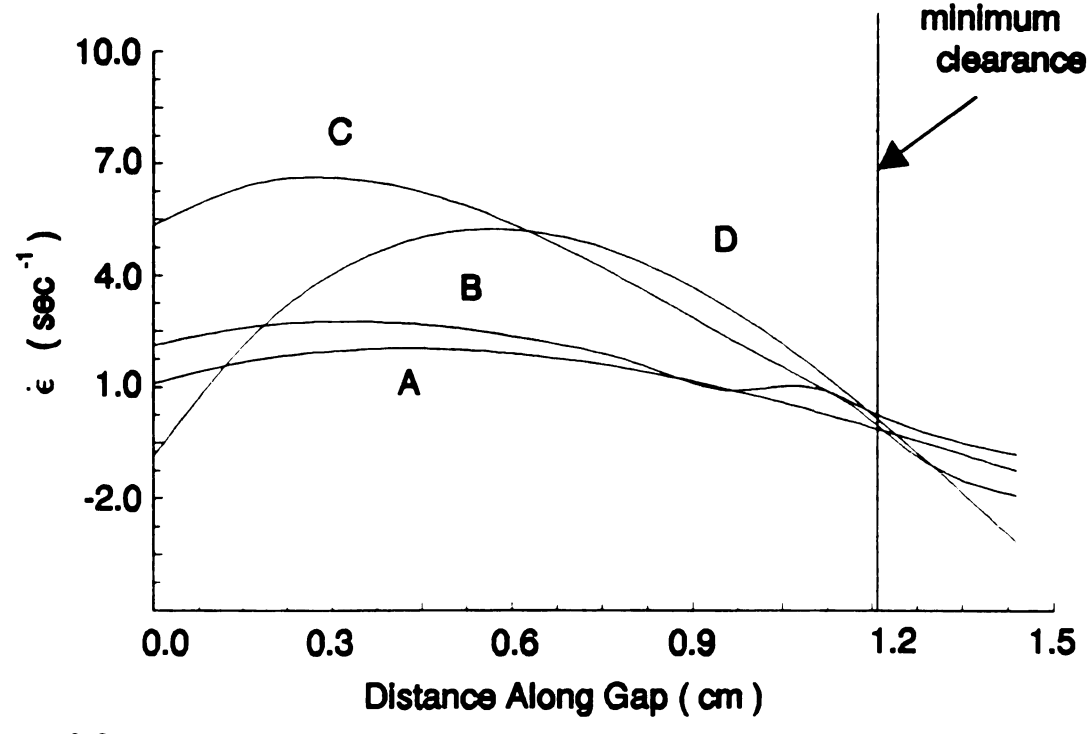
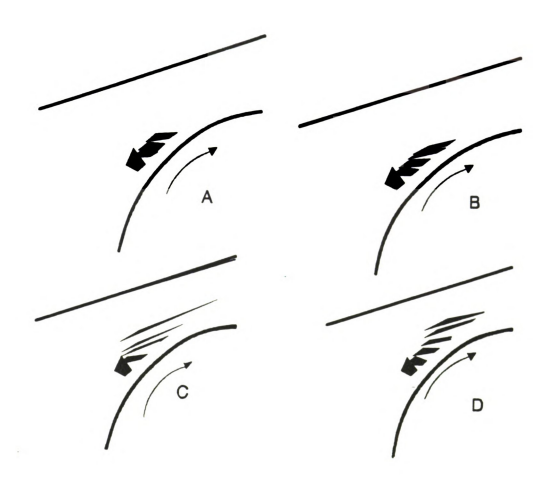


Figure 2-9 Profile of extensional strain rates along center of forwarding gap for each set of operating conditions

A) low Q, low N B) high Q, low N C) low Q, high N
D) high Q, high N

The motion and shape of a particular fluid element in the forwarding gap was followed over a time interval of 0.25 seconds in order to visualize the stretching. This was accomplished by tracking the four corner points of the fluid element at discrete time intervals. A very similar procedure is described by Hannachi and Mitsoulis (33). The material element was assumed to remain connected without the addition of new interfaces. The assumption is reasonable for a limited amount of total strain. The resulting deformation patterns are shown in Figure 2-10. These diagrams provide insight into the effects of the operating variables and resulting strain rates on the deformation



in the forwarding gap region. The stretch ratios for the diagonal of the fluid element over 0.25 seconds are 1.3, 2, 4, and 3 for cases A, B, C, and D respectively. The lowest stretch ratios are obtained in the shear dominated flows. The highest stretch ratios are obtained in the high N cases which also have the higher extensional strain rates.

The correlation between stretching and extent of maleation is supported by a comparison of the deformation diagrams illustrated in Figure 2-10 and the relative extents of maleation shown in Table 2-2. For each flow rate, an increase in the cylinder rotation rate produces much greater deformation and maleation. The reactor flow field which stretches the fluid element the most (Figure 2-12C) also produces the highest extent of maleation. The viscosity ratio between the peroxide stream and the molten polymer mixture is of the order 10⁻⁵. With this viscosity ratio, the breakup and dissolution of the peroxide in the molten polymer requires much lower strain in extension than in shear (34).

2.7 Conclusions

The details of the deformation fields are important for carrying out functionalization reactions on polymer melts. Higher extents of maleation are obtained in polypropylene melts processed with peroxide at higher extension rates. In comparison, shear alone has a limited influence on the progress of the polymer melt reaction. Experimentally determined residence time distributions in the continuous flow reactor are not sufficiently different to account for the more than four fold increase in the extent of maleation over the range of operating conditions. The extent of maleation increases

instead primarily due to the greater efficiency of extensional flows for dispersing the low viscosity peroxide stream into the viscous polymer melt. The approach of this work may be used to evaluate reactor designs for carrying out bulk functionalization reactions on polymers.

CHAPTER III

MIXING AND REACTIVE EXTRUSION OF POLYPROPYLENE IN A CO-ROTATING TWIN SCREW EXTRUDER

3.1 Introduction

Co-rotating twin screw extruders are ideal machines for mixing viscous fluids. Their superior mixing capability is employed in the blending, compounding, and reacting of polymer melts. The fully-intermeshing screws are self-wiping. This reduces the amount of fluid retained in stagnant or dead zones (46). This can be especially important when carrying out a free radical reaction for which moderate increases in residence time could lead to increases in the level of cross-linking or degradation.

The flow in a twin screw extruder may be divided into 4 distinct flow regions: the solids, melt, partially filled and pump zone (47). Modelling efforts for complex geometry have been based upon assumptions and approximations. The results from such studies may not accurately describe the actual dynamics. The most intensive mixing is provided by kneading disc sections. Three dimensional flow around the kneading discs has been modelled by Gotsis and Kalyon (28). A fully flooded flow channel was assumed for their simulations. They determined that the axial flow was proportional to pressure drop.

The extruder operating conditions determine the residence time distribution, the degree of fill, and both the level and type of the strain experienced by the reacting fluid.

The grafting reaction is diffusion limited so the levels of mixing are critical factors in the reaction progress (7). Increased degree of fill has been shown to increase the levels of shear strain produced in the conveying screw sections within a co-rotating twin screw extruder (29). The strain level in addition to the form of strain whether extensional or shear determine the efficiency of the mixing and the reaction progress as shown in Chapter 2.

Twin screw extruders provide good flow, mixing, and residence time distribution characteristics for reactive extrusion (48). The residence time distribution is of key interest in reactive extrusion in that it can allow for the prediction of the levels of reaction and its usefulness in analyzing mixing characteristics (49). The operating conditions of the extruder can then be used to control the levels of mixing and attain the desired reaction levels (50).

The object of this work is to determine how the flow field within the extruder affects the reaction progress in a polymer melt functionalization reaction. Because of the complexity of the flow fields generated in the extruder, the different flows are examined through the comparison of their residence time distributions. The reaction is carried out on polypropylene in the second mixing zone and discharge region of a fully intermeshing co-rotating twin screw extruder. The feed rate and barrel valve setting are varied while maintaining a constant screw rotation rate to produce different flow fields within the extruder reactor. The levels of maleation achieved are then determined through thin film Fourier Transform Infrared (FTIR) transmission spectroscopy. The resulting residence time distribution for each set of operating conditions is determined and then used to

calculate the degree of fill. The varying extents of maleation are examined in the light of these measurements in addition to characterizations of the flow field and reaction kinetics.

3.2 Experimental Procedure

3.2a Materials

The polypropylene (Himont USA SA-849) is a random copolymer, 3% by weight of which is polyethylene. The polyethylene units on the polymer chain reduce the crystallinity of the polypropylene and make it easier to process at lower temperatures. The dibutyl maleate is a liquid with a boiling point of 281°C. One mass unit of the maleate was used per 10 units of polymer. The reaction is initiated in the extruder with the addition of dicumyl peroxide, a powder which melts at 40°C. It is dissolved in xylene at a concentration 0.15 gm peroxide per ml of solution when fed into the extruder. One mass unit of peroxide was added per hundred mass units of polymer.

A Rheometrics RMS 800 viscometer was used to obtain dynamic shear viscosity curves. Extrudate strands were compression molded into a sheet with a thickness of between 1 and 2 mm. A one inch diameter disc was cut from the sheet and placed in the parallel plate test fixture. A time interval of not less than 5 minutes was allowed for the sample to equilibrate at the test temperature before any data was collected. Viscosity measurements indicate that dibutyl maleate acts as a plasticizer, lowering the viscosity of polypropylene by a factor of two as shown in Figure 3-1.

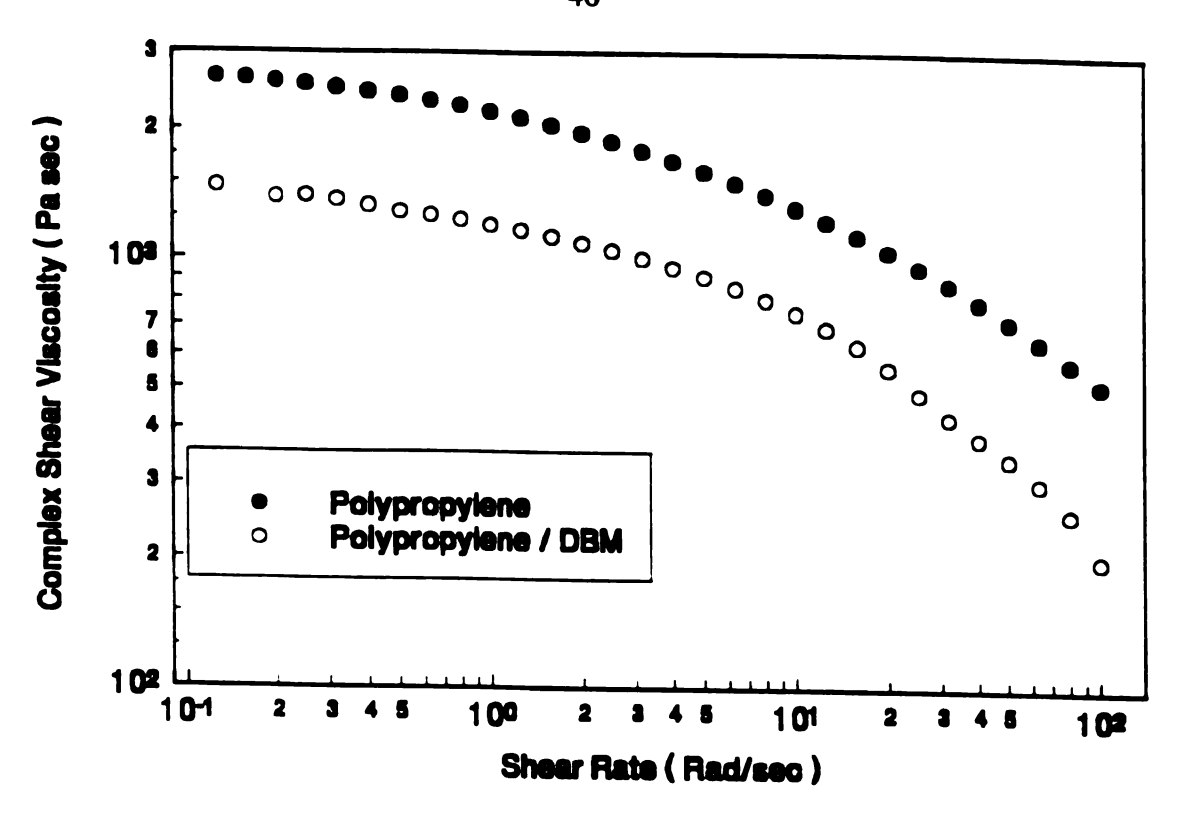


Figure 3-1 Effect of dibutyl maleate on shear viscosity of polypropylene melt

3.2b Reactive Extrusion

The maleation of polypropylene was carried out in a fully intermeshing, corotating twin screw extruder. The extruder is a Baker-Perkins (APV) MPC/V-30 model which has screws with a diameter of 30 mm and a length to diameter ratio of 13:1. The melt temperature of the mixing and discharge sections was maintained at 180°C. A diagram of the extruder is shown in Figure 3-2. For each run, from three to four pounds of polypropylene pellets were placed in the solid materials feeder in line with the feed hopper of the extruder. The feed rate control settings are in units of percent. The actual feed rate was determined by feeding the pellets into a beaker for a fixed period of time (3 to 5 minutes) and then measuring the weight increase of the beaker. This simple

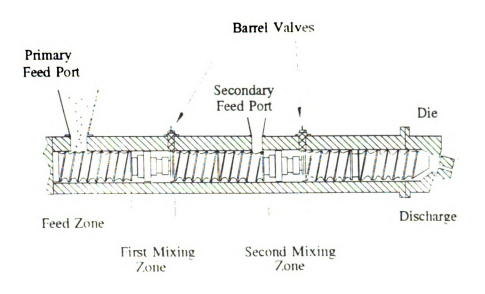


Figure 3-2 Twin screw extruder configuration showing feed inputs and screw arrangement

calibration procedure was repeated after each time the tube encasing the screw of the feeder was disassembled for cleaning. Fine adjustments in the feed rate were obtained when necessary by altering the extension of this tube. Two medical syringe type feeders were used to supply the liquid dibutyl maleate and peroxide solution to the extruder. Discrete rate settings determined these liquid feed rates. In order to maintain the constant initial concentration ratios, a combination of different diameter syringes were used. One syringe feeder was used to supply the dibutyl maleate at the main feed port in a 1:10 ratio to the polypropylene by weight. The second syringe feeder was used to supply the peroxide solution downstream at the secondary feed port at a feed rate to

provide for an initial dicumyl peroxide weight concentration of 1:100 that of the polymer. The peroxide solution was fed to the extruder only after all material from the previous extruder run was purged. A water trough at the die exit was used to quench the reaction. The extrudate produced in the first 3 minutes of the reactive extrusion process was discarded. Specimens to be used in the characterization of the reaction level were cut from the remaining extrudate in the water trough. Specimens tested from different sections exhibited no significant change in the level of grafting. An exhaust hood above the extruder was required for safety since dibutyl maleate and dicumyl peroxide are irritants.

3.2c Extruder Screw Configuration

A key advantage of twin screw extruders with a modular screw design is that the screw configuration can be tailored to suit a particular application. The screws consist of slip-on elements which each have a specific function. The screw configuration used in this work is shown in Figure 3-3. The modular elements are arranged upon the screw shafts according to their function. Feed elements are located both at the extruder entrance and between the two mixing zone sections. The initial heating of the polymer pellets is begun in the first feed section. The valve controlling the cooling water flow to this section is left fully open. Hence, the temperature of the feed section is maintained approximately 20°C below the 180°C set point. This prevents excessive heat conduction into the feed hopper which could prematurely melt the polymer pellets and cause them to clog the feed port by sticking to the sides. The polymer pellets and dibutyl maleate

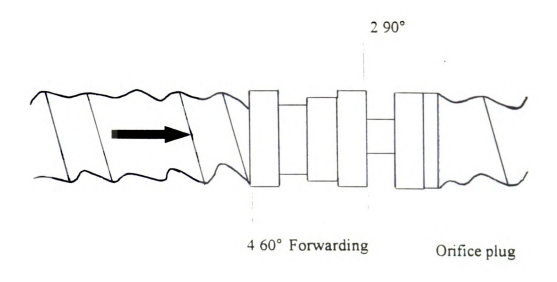


Figure 3-3 Extruder screw configuration

are forwarded to the first of the two mixing zones. The melting of the polymer and the blending with the dibutyl maleate are completed in this intensive mixing region. Each of the mixing zones consists of 6 two tipped kneading discs or paddles. Mixing is accomplished through the application of both shear and extensional stresses. Transversely neighboring paddles are perpendicular to each other. This provides for two to three separate areas to be occupied by polymer melt. As the paddles rotate, the areas of these compartments change. Polymer melt occupying a contracting compartment is effectively squeezed so that flow is created in the axial direction. This squeezing flow provides for significant extensional strain. Whether this squeezed fluid is transported primarily forward or backward along the screws is determined by the axial orientation

of the paddle elements. The first four paddles are arranged in a 60° forwarding configuration. This produces moderately strong net axial flow in the forward direction. The final two paddles of each section are configured at 90° which provides no forwarding or reversing action. Orifice plugs are positioned at the end of each mixing zone. Orifice plugs serve to restrict the area available for flow and increase the holdup and residence times in the mixing zones. The amount of flow restriction provided by the orifice plugs is determined by the positioning of the barrel valve as shown in Figure 3-4. In the closed position, the barrel valve allows for exiting flow only through the 0.5 mm clearance between the barrel and the circumference of the orifice plugs. As the barrel valve is opened, the cross-sectional area available for flow is roughly doubled. This reduces the hold-up in the mixing zone.

The second feed section forwards the polymer/dibutyl maleate blend to the second mixing zone. The peroxide injection occurs at the entrance to this zone. Here, the peroxide is dispersed into the polymer/dibutyl maleate phase and the reaction is initiated. From here, the reacting blend is forwarded to the exit die. The die exit has twin 3 mm diameter circular ports so the extrudate is in the form of twin cylindrical strands.

3.2d Residence Time Distribution Measurements

Tracer dye was substituted for the peroxide solution in the residence time measurements. No other operating conditions from the reaction experiments were changed. The dye is oil soluble and is used commercially to detect oil leaks in auto engines. The viscosity of the tracer dye used was comparable to that of the peroxide

solution. The procedure is essentially the same as that described for reactive extrusion

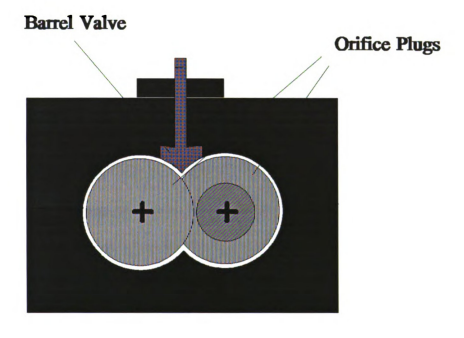


Figure 3-4 Barrel valve assembly, showing variation of clearance with valve position

except a tracer die is added instead of a peroxide solution. Three ml of red tracer dye was added as a pulse into the second feed port after residual material from the previous run had been purged from the extruder. The extrudate strands were collected from the water bath. The time from the peroxide injection to the exit of the extrudate was determined by dividing the cumulative weight of the strands collected by the extruder throughput rate. Sections of extrudate corresponding to either 5 or 10 seconds (finer increments for steeper rates of color change) were pressed into thin films. These films were tested in a Hunter Labs spectrophotometer. The meter measures the intensity of the primary colors in a 1 inch diameter circular area of a surface. The redness index from the tracer dye was measured for each film. The concentration of dye was assumed to be proportional to this index. The residence time density curves were obtained by first fitting the data to high order polynomial curves. The curves were then extended by fitting the last 3 data points to an exponential decay as suggested by Todd (46). The total area under both curves was then normalized to 1 for each run.

3.2e Characterization of Reaction Extent

3.2e1 Infra Red Spectra Analysis

The sample was washed overnight in acetone to remove unreacted dibutyl maleate and peroxide. The acetone washed extrudate strands were placed between teflon coated sheets and left for 1 minute between press platens which had been preheated to 160°C. Ten-thousand lb_f was then applied for 1 minute before the specimen was removed. This procedure produced films approximately .08 mm thick. The thin films were then placed

in a vacuum oven and heated to 100°C 72 hours under at least 29 mercury inches of vacuum to remove any residual dibutyl maleate or moisture. The thin films were then tested in a Perkin-Elmer model 1800 FTIR spectrophotometer. Quantitative transmission mode with a nominal resolution of 1.0 cm⁻¹ was used to obtain the spectra. Transmission mode was selected because it provides a higher signal to noise ratio than attenuated total reflectance (51) and was found to give results which were more reproducible. The spectra of maleated polypropylene are discussed in section 2.6c.

3.2e2 Quantification of Reaction Progress

A calibration of FTIR data with known standards is required to obtain quantitative results. Controlled batch polypropylene graft reactions were carried out to obtain specimens for this calibration. First, polypropylene was compression molded into sheets approximately 0.2 mm thick. Dibutyl maleate and dicumyl peroxide were sandwiched between a series of sections cut from these sheets. The exact weight of the approximately 1 gram of polypropylene in each specimen was measured the nearest 0.1 mg on an analytical balance. The specimens were then pressed at a minimal pressure between press platens which were preheated to 180°C. Different levels of reaction were obtained by varying the heating times. The products were then subjected to the acetone washing and vacuum oven drying treatments as described in the previous section. The increase in weight of the final product over the initial polymer weight was recorded as the level of grafting. The carbonyl indices of the specimens were determined from their FTIR spectra. A control specimen was prepared for each batch which did not contain

any peroxide. Only specimens from batches whose control exhibited less than a 0.02 % weight change were included in the calibration curve shown in Figure 3-5.

3.3 Effect of Barrel Valve Setting, Q, and N on Extruder Flow

The setting of the barrel valve which follows the second mixing zone was used to change the screw configuration. The valve position is a determining factor for the level of hold-up in the second mixing zone. The degree to which this valve, presented in Figure 3-4, is open has a tremendous affect on the extruder flow field. The extruder

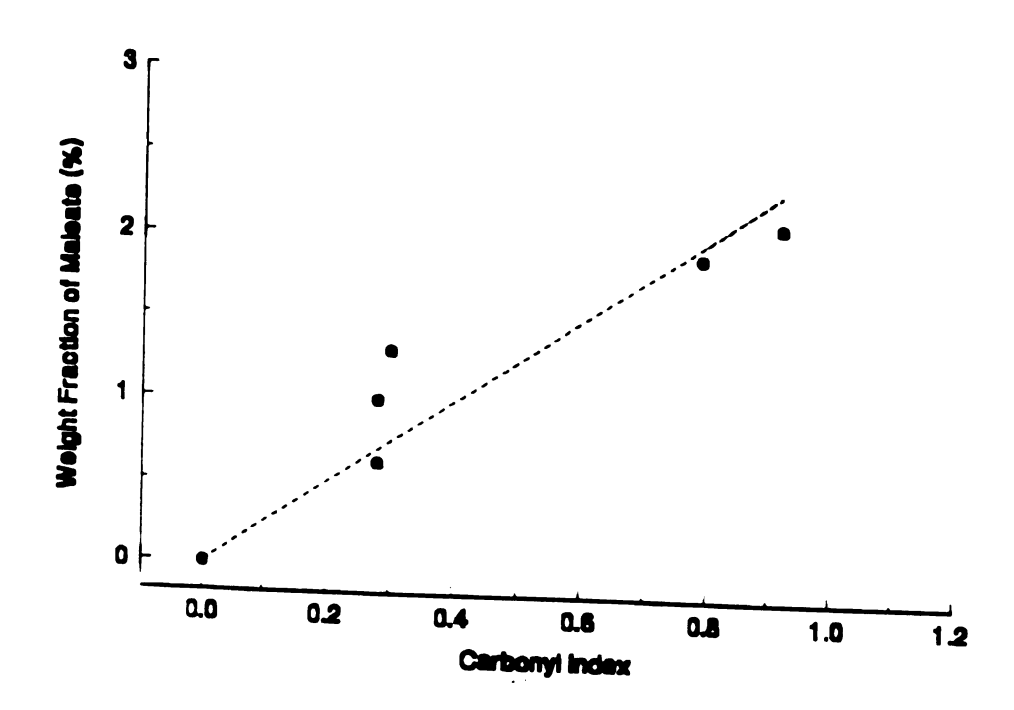


Figure 3-5 Calibration of FTIR measured extent of maleation with weight change measurements

flow with this valve fully open was compared to the flow with it closed for a throughput rate of 45 gm/min and a screw rotation rate of 250 rpm. The normalized residence time distributions of the polypropylene/dibutyl maleate blend downstream of the second feed port are shown in Figure 3-6. The spread in the residence time distribution increases from 30 to 45 seconds when the barrel valve is closed. This broadening is an indication of increased axial mixing. The mean residence time was also strongly affected by the barrel valve position. It increased from 56 seconds to 71 seconds with the valve closed. The valve position affects the amount of hold-up in the second mixing zone. The hold-up volume equals the product of the mean residence time and the volumetric throughput

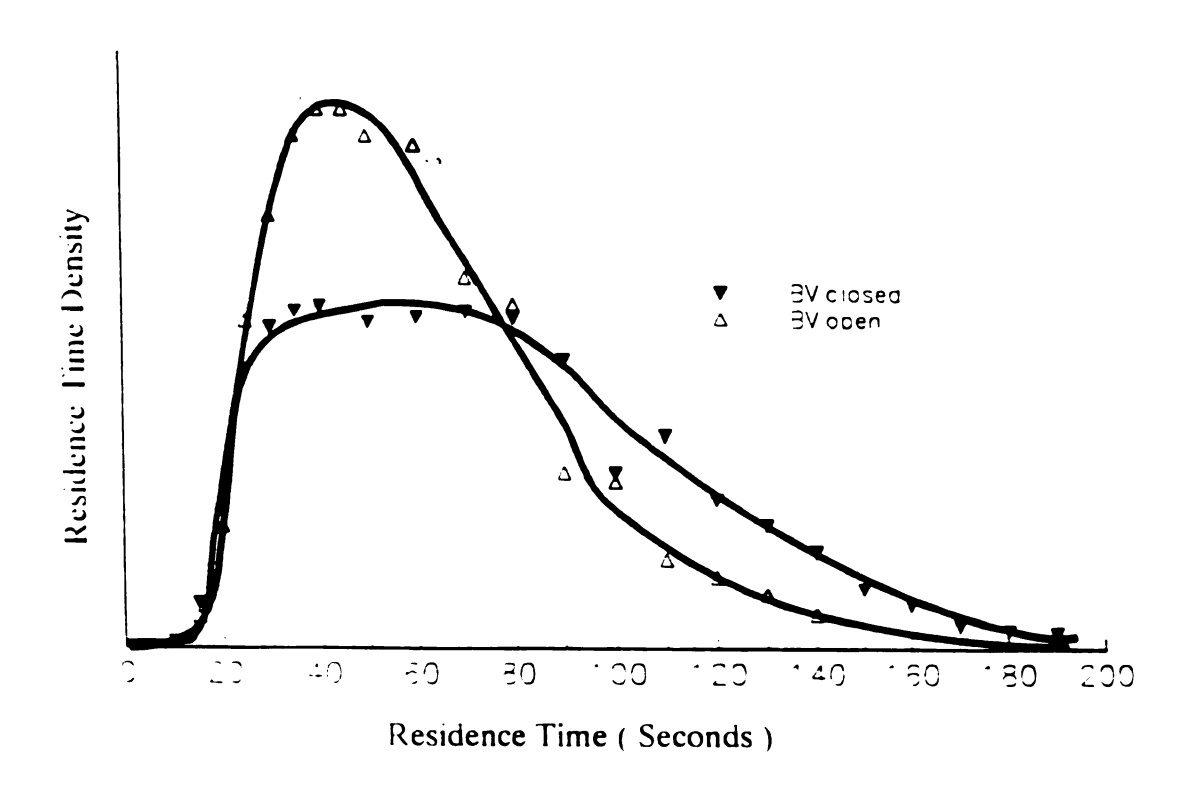


Figure 3-6 Effect of barrel valve setting on residence time distribution of polypropylene and dibutyl maleate in reaction zone of extruder

rate. The entire volume past the second available to be filled by melt is 120 ml. The open volume in the second mixing zone is 45 ml or 38% of the volume past the second feed port. The degree of fill is simply the hold-up volume divided by the volume available for flow.

The rest of the extruder runs were performed with the barrel valve closed. The rotation rate of the screws was set at 100, 250, or 450 rpm. The maximum throughput rate is limited by the selected screw rotation rate and torque capacity of the extruder motor. Throughput rates of 53, 62, and 73 grams/minute were examined to provide flow fields with different levels of hold-up within the extruder. The mean residence times, degrees of fill, and the spreads of the residence time distributions with the barrel valve closed are presented respectively in Tables 3-1, 3-2, and 3-3.

Table 3-1 Mean Residence Time

Feed Rate RPM	45 g/min	53 g/min	62 g/min	73 g/min
100			76 sec	
250	71 sec	68 sec	64 sec	56 sec
450				45 sec

^{±3} seconds

Table 3-2 Degree of Fill

Feed Rate RPM	45 g/min	53 g/min	62 g/min	73 g/min
100			0.74	
250	0.50	0.57	0.63	0.65
450				0.52

 ± 0.04

Table 3-3 Spread of Residence Time Distributions

Feed Rate RPM	45 g/min	53 g/min	62 g/min	73 g/min
100			39	
250	45	37	33	25
450				28

±3 seconds

The various sets of operating conditions provide for a degree of fill between 0.5 and 0.74. The degree of fill is frequently correlated to the ratio of volumetric throughput rate to screw rotation rate. For a fixed screw configuration, these factors correspond strongly as shown in Figure 3-7. Similar trends of changes in hold-up with extruder flow considerations were also observed by Nichols (31) for two other melts with the same extruder configuration.

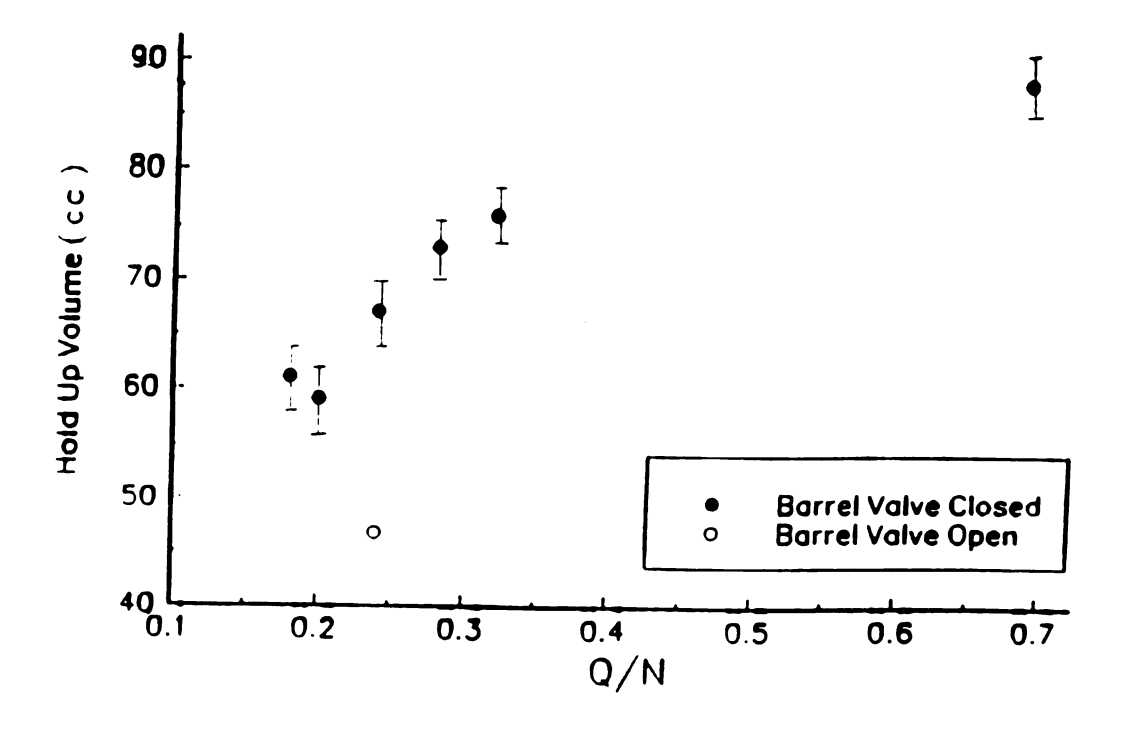


Figure 3-7 Dependence of degree of fill on ratio of throughput rate to screw rotation rate

The relative importance of the two control parameters, feed rate and screw rotation rate, is indicated by the slope of the curve. At low degrees of fill, the hold-up volume, the product of the mean residence time and feed rate, is strongly dependent upon the ratio of feed rate to screw rotation rate. This suggests that the mean residence time is more dependant upon the throughput rate at higher degrees of fill. Conversely, fluctuations in the feed rate at higher screw rotation rates, with lower degrees of fill, will more strongly affect the mean residence time.

The case with an open barrel valve (indicated in the figure by an open circle) provides an example of a separate screw configuration. The hold-up volume obtained

provides an example of a separate screw configuration. The hold-up volume obtained with an open barrel valve does not conform the closed barrel valve data. Clearly, even a relatively subtle change in the screw configuration can have significant effects on the extruder flow.

The effects of the screw rotation rate on the residence time distributions are shown in Figure 3-8. As the screw rotation rate is increased, as expected, the mean residence time is reduced. The degree of fill is also reduced at higher screw rotation rates since hold-up increases with 1/N. The effect of the screw rotation rate on the spread of the residence time distribution depends upon the other operating conditions. For operating conditions producing higher degrees of fill, (high Q/N), the residence time distribution appears to become slightly narrower when the screw rotation rate is increased. When the extruder is predominantly in the starved state, the residence time distribution broadens with increasing screw rotation rates. Because of the orifice plugs and closed barrel valve restrictions, the degree of fill in the mixing zones is greater than that the average for the entire screw length. When the extruder becomes more flooded with melt, the channel volume around the feed screws immediately preceding the second mixing zone will also begin to fill with melt and its local pressure increases. This should result in a decrease in the pressure gradient between the start of the mixing zone and the end of the feed section which would reduce the driving force for reverse flow.

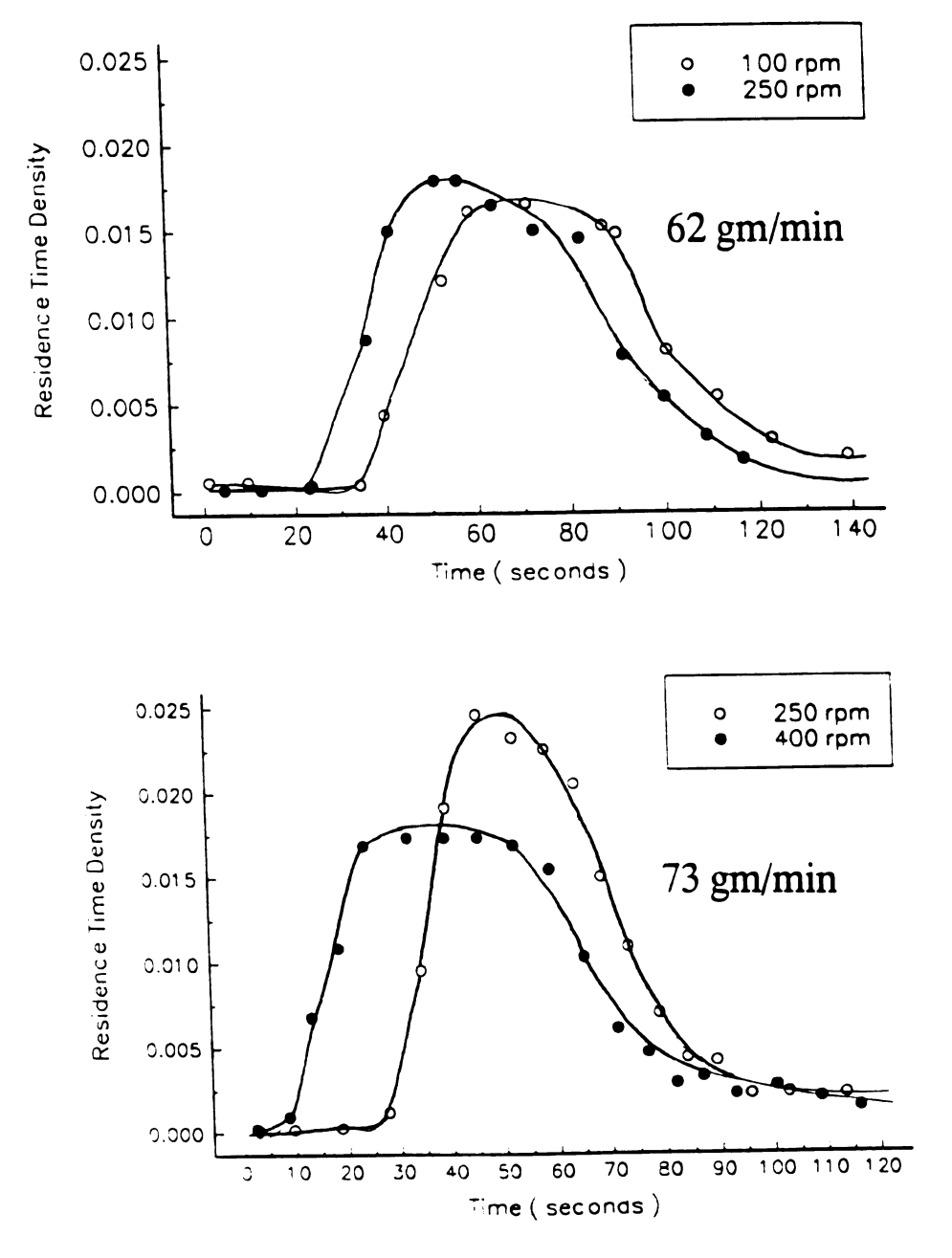


Figure 3-8 Effect of screw rotation rate on residence time distribution of polypropylene and dibutyl maleate in reaction zone of extruder

The ratio of the spread of the residence time distribution to the mean is an indicating parameter of the level of axial mixing in a flow. This ratio of the spread of the residence time distribution divided by its mean is shown in Table 3-4. The larger

Table 3-4 Relative Level of Axial Dispersion

Feed Rate RPM	45 g/min	53 g/min	62 g/min	73 g/min
100			.51	
250	.63	.54	.52	.45
450				.62

this parameter, the greater the axial mixing. The level of axial mixing of the blend increases significantly when the screw rotation rate is increased only when the degree of fill is low.

The effect of the throughput rate on the residence time distribution in the extruder is shown in Figure 3-9. Both the mean residence time and the breadth of the residence time distribution decrease markedly with an increase in throughput rate. The level of axial dispersion also decreases as the throughput rate increases. As expected, the degree of fill increases with the throughput rate.

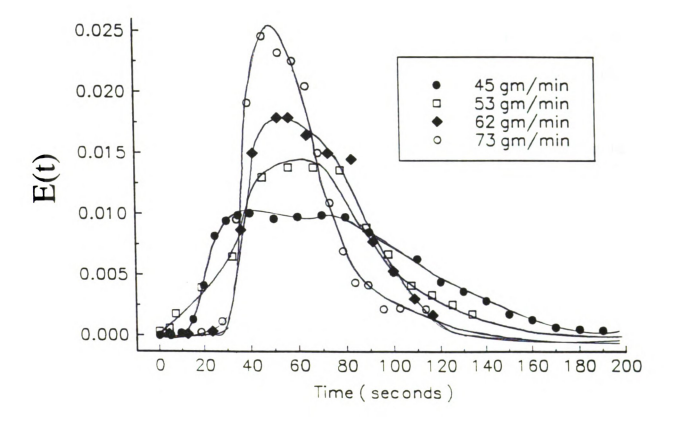


Figure 3-9 Effect of throughput rate on the residence time distribution of polypropylene and dibutyl maleate in the reaction zone of extruder

3.4 Effect of Extruder Operating Conditions on Extent of Maleation

For a screw rotation rate of 250 rpm and a throughput rate of 45 grams per minute, the level of maleation with the barrel valve open is 1.6 %. With the valve closed, the level of maleation is 2.0%. An increase in reaction level should be expected since the mean residence time increases from 56 to 71 seconds and also broadens significantly with the closure of the valve. The relatively large change in the extruder flow is accomplished with only a minor adjustment of the flow geometry.

Even larger differences in the level of maleation can be attained by varying the operating conditions as shown in Table 3-5. Unlike mean residence time and degree of fill, the level of maleation does not vary monotonically with screw rotation rate and throughput rate. The level of maleation does decrease with increasing screw rotation rate. However, with increasing throughput rate, the level of grafting reaches a maximum at an intermediate rate.

Table 3-5 Level of Maleation with Closed Barrel Valve

Feed Rate RPM	45 g/min	53 g/min	62 g/min	73 g/min
100			2.5	
250	2.0	1.6	1.9	1.5
450				1.2

 $\pm 0.1\%$

3.5 Effect of Degradation on Extruder Flow

The degradation side reaction which occurs in parallel with the maleation reaction affects the rheology of the melt. The shear viscosity decreases by more than an order of magnitude as shown in Figure 3-10. The viscosity above the entanglement molecular weight is proportional to the weight average molecular weight to the 3.4 power. The measured decrease in viscosity by a factor of 25 indicates a decrease in molecular weight by a factor of 2.6 with a grafting level of 1.2 percent.

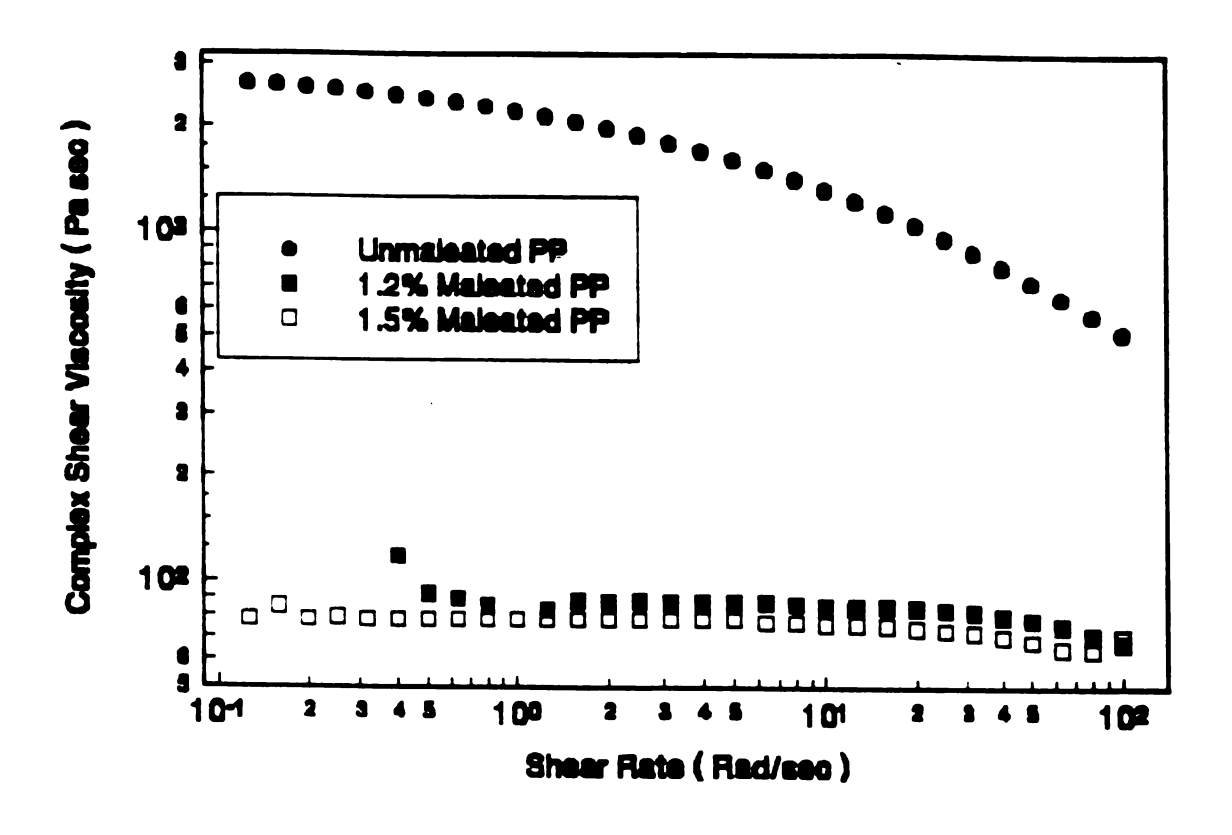


Figure 3-10 Effect of degradation on the shear viscosity of polypropylene (after removal of ungrafted dibutyl maleate)

The measurement of the residence time distribution is more difficult when the peroxide is present in the melt. The reduction in melt viscosity causes a decrease in melt strength. The continuity of the extrudate strands is difficult to maintain. The residence time distribution with peroxide was measured successfully for one set of operating conditions. In Figure 3-11, this residence time distribution is compared to the distribution associated with the same operating conditions obtained without peroxide addition. The change is minimal.

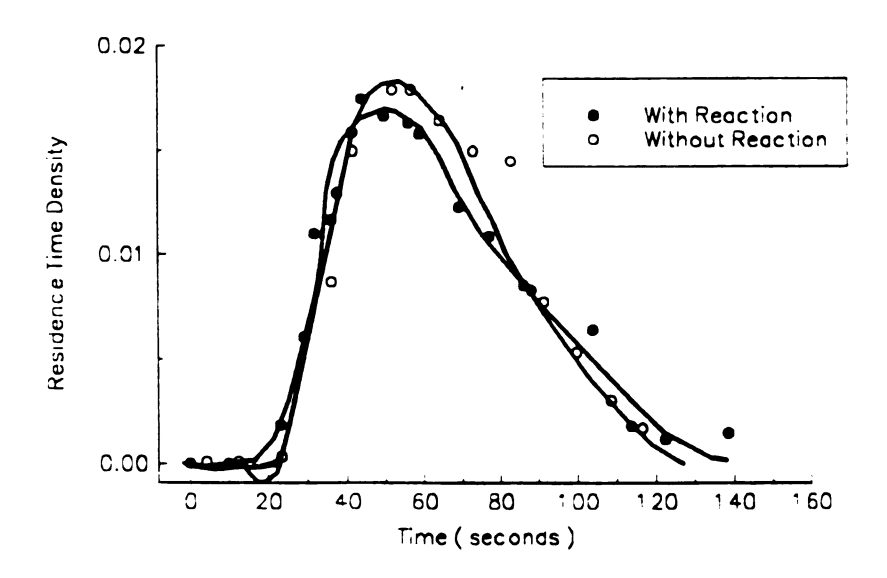


Figure 3-11 Effect of degradation on residence time distribution of polypropylene and dibutyl maleate in the reactive zone of extruder (250 rpm, 73 gpm)

This observation appears to conflict with that of Tzoganakis *et al.* (37). They measured broadened residence time distributions in a single screw extruder with reductions in the molecular weight of polypropylene. They conclude that the broadened residence time distributions were due to relative increases in the levels of pressure driven reverse flow as compared to the levels of the forwarding shear flow. They attribute this to the reduction in melt viscosity which occurs with the degradation. The different flow geometry may account for the conflicting observation. The effect of flow in the mixing zones can have a large influence on the residence time distribution in the twin screw extruder. The single screw extruder has no comparable screw section.

3.6 Discussion

The level of maleation was correlated with flow parameters in order to determine their dependance. The level of grafting *versus* the mean residence time is shown in Figure 3-12. The open point is the run with the open barrel valve. Not surprisingly, the general trend observed is an increase in extent of reaction with an increase in the mean residence time. However, this trend is not entirely uniform. A 0.3% increase was obtained when the throughput rate was increased from 53 to 62 grams per minute although the mean residence time was reduced by 4 seconds. A second parameter which can be used to characterize the flow is the hold-up volume. The level of grafting *versus* the hold-up volume is shown in Figure 3-13. This correlation is poorer than former. These two parameters alone are insufficient to predict the level of reaction. Another parameter which takes into account the breadth of the residence time distribution is

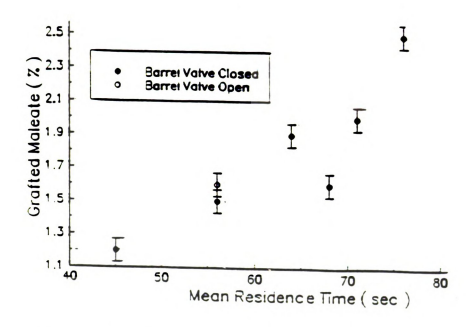


Figure 3-12 Dependence of the level of grafting on the mean residence time in the reaction zone

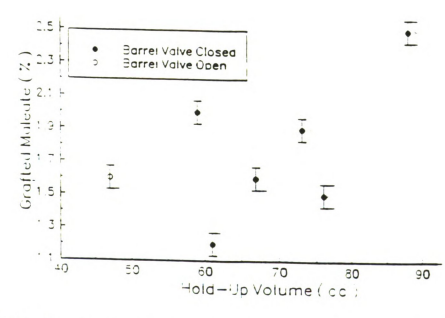


Figure 3-13 Dependence of the level of grafting on the hold-up volume in the reaction zone of the extruder

required.

The entire residence time distribution can be used to determine the amount of peroxide that is dissociated. The rate of $t_{1/2}$ of dicumyl peroxide at 180°C is 1 minute

$$\frac{I_0 - I_t}{I_0} = 1 - \int_0^t W_t *0.01155 *e^{-0.01155 *t} dt$$
 (3-1)

(44). By integrating the product of the dissociation rate and the residence time density, W_t, from time zero to the mean residence time as shown in Equation 3-1, the fraction of dissociated peroxide in the extrudate can be determined. The fraction of dissociated peroxide at different extruder operating conditions is shown in Table 3-4. The level of grafting obtain *versus* the fraction of peroxide dissociated is shown in Figure 3-14.

Table 3-6 Level of Peroxide Dissociation

Feed Rate RPM	45 g/min	53 g/min	62 g/min	73 g/min
100			0.60	
250	0.56	0.51	0.54	0.48
450				0.42

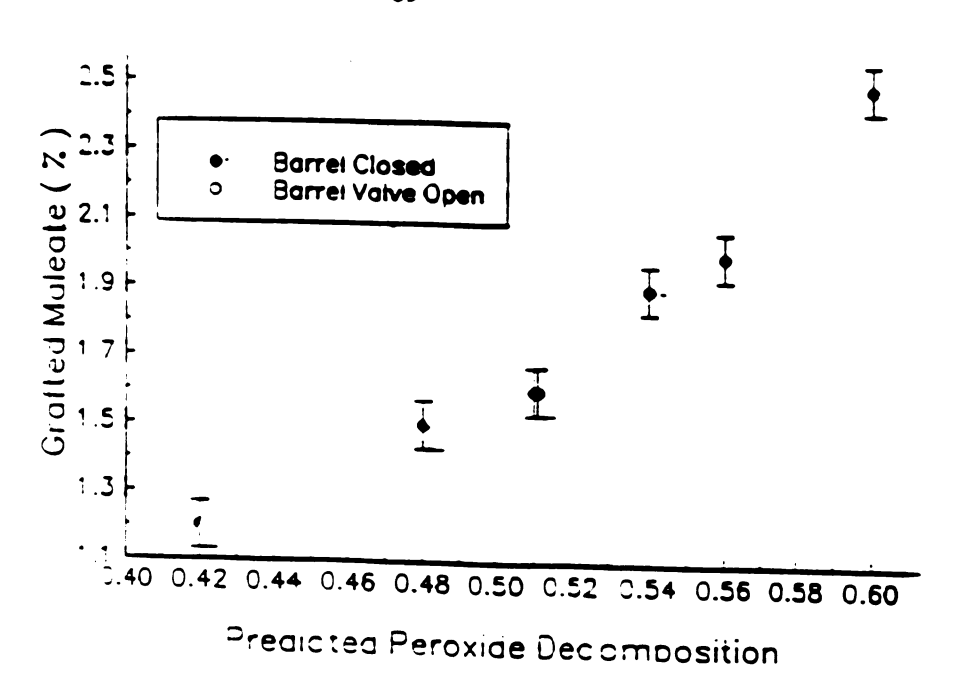


Figure 3-14 Dependence of the level of grafting on the calculated fraction of peroxide dissociation

3.7 Conclusions

The extruder flow geometry must be accounted for in the characterization of extruder flow. The barrel valve setting is a powerful control factor for the extruder flow. This relatively small change in the screw configuration caused large changes in the residence time distribution of the melt. Closing the barrel valve results in longer mean residence times and broader residence time distributions. Each of these changes results in higher levels of reaction.

The extruder flow of a blend of polypropylene and dibutyl maleate was examined for a range of operating conditions which provided various levels of extruder hold-up volume. For a constant screw configuration, the hold-up volume correlated with the ratio

of throughput rate to screw rotation rate. The mean residence time decreases with increasing screw rotation rate. The spread of the residence time distribution depends strongly on the throughput rate. As the throughput rate increases, the distribution becomes narrower and more peaked.

For a constant screw rotation rate, an increase in throughput rate reduced both the mean residence time and the spread of the residence time distribution. The effects of the screw rotation rate on the flow depended upon the operating conditions. With the extruder nearly flooded, an increase in the screw rotation rate led to a small decrease in the spread of the residence time distribution along with a decrease in the mean residence time. When the extruder was relatively starved, the residence time distribution broadened when the screw rotation rate was increased. This indicates an increase in the level of axial mixing.

The levels of grafting were correlated with parameters determined from the residence time distributions obtained in the absence of reaction. The hold-up volume is a poor predictor of the level of reaction. The mean residence time is only somewhat better. The predicted level of peroxide decomposition is determined from a combination of the peroxide dissociation kinetics and the entire residence time distribution. The level of maleation was found to correlate strongly with this parameter. Therefore, the residence time distribution is sufficient to describe the complex extruder flow in the context of a melt functionalization reaction.

CHAPTER IV

EFFECT OF RHEOLOGY ON MIXING IN REACTIVE EXTRUSION

4.1 Introduction

The utility of polyolefins can be greatly enhanced through functionalization reactions carried out on the polymer melt. The polymer melt functionalization reaction studied in this work is the maleation of polyethylene. Polyethylene is modified with maleic anhydride in order to improve its adhesion to reinforcements such as short glass fibers, to other polymers such as nylon, or to dyes. An organic peroxide initiator first dissociates to form peroxy radicals which abstract hydrogens from polyethylene chains. These macro-radicals may combine with a maleic group at the unsaturated carbon in a grafting reaction. With the selection of a proper initiator and reaction temperature to avoid the homopolymerization of maleic anhydride, the reaction results in the grafting of individual succinic anhydride units to the polymer chain. Instead of undergoing the desired grafting reaction, two polyethylene macro-radicals may combine in a crosslinking reaction. In this work, the polymer and maleating agent are premixed before the introduction of the peroxide initiator. This reduces the likelihood of cross-linking or oligomerization of the maleate that can occur when the peroxide dissociates and the polymer and maleate are not well mixed. The cross-linking reactions significantly change the rheology of the polymer melt which can affect the further mixing of the reactants.

Polymer melt reactions are commonly carried out in extruders. Since these reactions are commercially important, the effects of both extruder operating conditions (7,32,36) and reactant concentrations (3,7,52) have been investigated in some detail. The conclusions derived from these studies are sometimes limited to the environments in which the reactions were carried out. The results for different studies may even appear to conflict if the effects due to different flow geometry are not taken into account. For example, in a single screw extruder (32), the extent of reaction increases with increasing screw rotation rates while in a counter-rotating twin screw extruder, the extent of reaction does not vary monotonically with screw rotation rates (7). Clearly the effects of changes in operating conditions on the flow of the reacting melt must be accounted for to understand such observations.

A practical advantage of the twin screw extruder over the single screw extruder is that the modular twin screw sections may be configured to optimize the reactor flow. The screw configuration has been found to be more important than the operating conditions in determining the mixing characteristics (53). By changing the stagger of the kneading disc or paddle elements, the axial pressure profile is altered to produce more flow in either the forward or reverse direction. Typically, the volume available for flow in a twin screw extruder is only partially filled with the polymer. The degree of fill is affected by the stagger angle of the kneading discs. Wang *et al.*(25) have analyzed the flow of a power law fluid in a co-rotating twin screw extruder. They were able to approximately predict the filled and open regions along the screws as well as the proportion of forward and reverse axial flow for different screw configurations. The

screw configuration and extruder operating conditions may also have a pronounced effect on the residence time distribution of the melt. This residence time distribution can be determined experimentally. Differences among the flow fields and mixing levels obtained in the extruder under different operating conditions may then be inferred from through a comparison of these measured residence time distributions.

The complex rheology of the polymer melt and complex extruder flow geometry provide flows for which the strain rates are difficult to determine. The levels of mixing and therefore the reaction progress depend not only upon the strain rates themselves but also upon the type of strain. Extensional strain is more efficient at mixing since the critical stress required for droplet breakup and dispersive mixing is lower in extension than in shear (18). One study carried out in a model reactor where the flow could be better characterized showed that higher levels of reaction corresponded to the operating conditions which provided the greatest levels of fluid deformation (34). Often, a twin screw extruder is the preferred reactor because it provides for better mixing at lower shear rates than does a single screw extruder (18).

Melt rheology is a dynamic factor in free radical initiated reactions. Side reactions resulting in polymer degradation or crosslinking may occur which can themselves significantly affect the rheology of the melt and therefore the flow within the reactor. Different types of flow may predominate in an extruder depending upon both the operating conditions and melt rheology. Tzoganakis and coworkers (37) have investigated the free radical initiated degradation of polypropylene in a single screw extruder. They determined the residence time distribution experimentally as well as

theoretically (with a power law model for the melt viscosity) from the feed hopper to the die exit. The degraded polymer melt had a broader, less peaked residence time distribution indicating better mixing. They attribute this increase in axial mixing to the increase in pressure driven back flow relative to forwarding drag flow.

The viscosity of the melt is strongly dependent upon the type of strain as well as the levels of strain. The pressure generated in an extruder is related to the shear viscosity of the melt. In a co-rotating twin screw extruder, the rotation of the paddles leads to a circumferential pressure profile as shown in Figure 4-1 (30) which depends upon the degree of fill for the melt. The stagger of the paddles in the mixing zone creates pressure gradients along the axial direction, as well as a non-uniform geometry for the axial flow. Thus, a pressure driven axial flow with extensional components is produced. The extensional as well as the shear viscosity of the melt may have an important bearing on the flow in a twin screw extruder.

Different low density polyethylene melts can exhibit markedly different flow behavior because of different extensional rheology. Their extensional rheology depends upon both the concentration and length of branching. Munstedt and Laun (54) compared the steady-state elongational viscosities for low density polyethylenes with different levels of branching but with the same zero shear viscosities. They were able to quantify the increases in extensional viscosity at low stretch rates associated with increases in the levels of branching. The differences in the rheology of polyethylene melts are reflected in their flow patterns. Tremblay (55) observed the flow of linear low density polyethylene (LLDPE) and branched or low density polyethylene (LDPE) through a

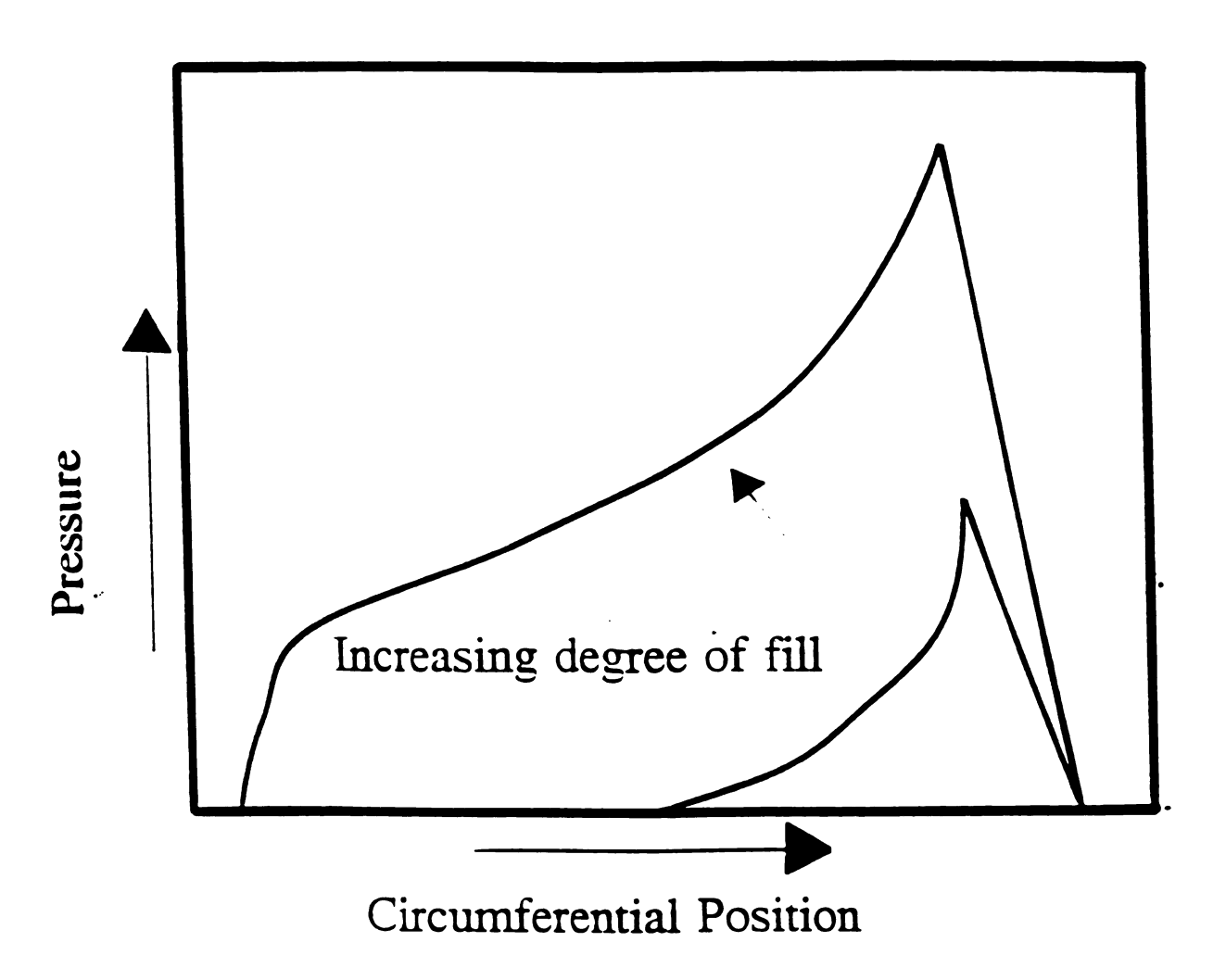


Figure 4-1 Circumferential pressure profile in twin screw extruder (from Eise and coworkers (3-4))

sudden contraction and found that the branched LDPE showed a much greater tendency to form vortices in the upstream corner. He attributes this behavior to the stretch thickening seen only for LDPE.

The object of this work is to investigate the effect of melt rheology on flow and mixing in an extruder and the resulting progress of a melt functionalization reaction. This is done by comparing the flow of two distinct polyethylenes, a LDPE and a LLDPE, which have similar shear viscosities but markedly different viscosities in extension. A co-rotating, fully intermeshing twin screw extruder was used as the reactor. Since the strain rates of the melts in the extruder could not be obtained, it is important that the extensional rheology of the LDPE and LLDPE differ over a wide range of stretch rates. Residence time distributions of the melt were obtained from the extruder at different operating conditions so that various flow fields could be studied. These flows were characterized primarily in the absence of the maleation and crosslinking reactions. A few residence time distributions were obtained from reacting melts for comparison. The conclusions drawn from this study will assist in the selection of extruder configuration and operating conditions for this and similar polymer melt reactions.

4.2 Rheology of Polyethylenes

4.2a Shear Viscosity

The polyethylenes used in this study are a LLDPE (NCX-013) and a LDPE (LGA-105) produced by Mobil. Fifty pounds each of these commercial resins was provided with some level of stabilizer already added. Their shear viscosity curves at

180°C are shown in Figure 4-2. They are very closely matched, especially at low shear rates. The LLDPE has a wider plateau which results in a viscosity slightly greater than that of LDPE at higher shear rates. It is also slightly more shear thinning with a power

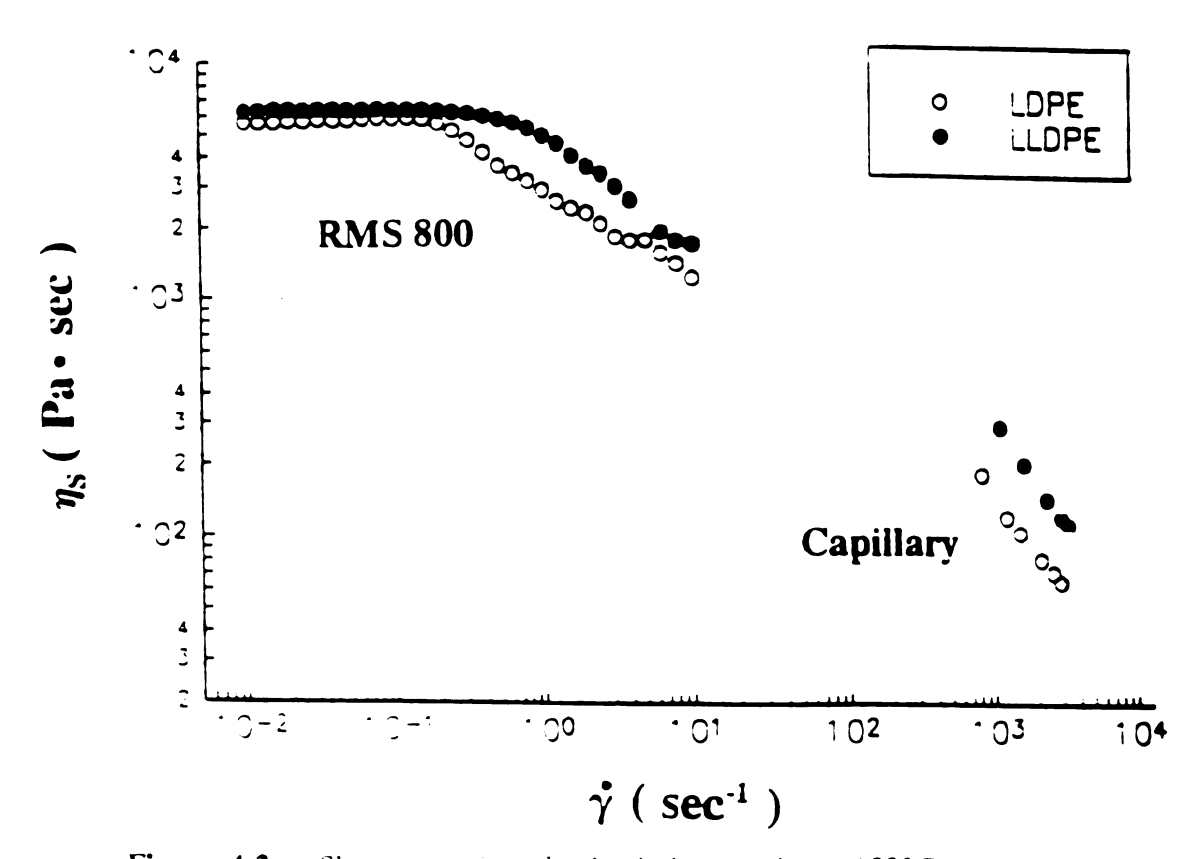


Figure 4-2 Shear viscosity of polyethylene melts at 180°C

law index of 0.25 as compared to 0.30 for the LDPE. The lower shear rate viscosities were measured using a Rheometrics RMS 800 rheogoniometer. Steady shear tests were performed with one inch diameter disposable parallel plate test fixtures. The higher shear rate viscosities were obtained through capillary rheometry. A Brabender single

screw extruder was used to pump the melts through one of three separate capillary dies. Each die had a 1 mm diameter. The lengths of the dies were 10, 15 or 30 mm. The pressure drop through each capillary was measured for each of 10 different flow rates. The Bagley correction for end effects was employed in determining the shear viscosity.

4.2b Extensional Viscosity

To obtain estimates of the extensional viscosities, the same single screw extruder was fitted with a special die whose design is shown in Figure 4-3. The 30° die taper angle is required to prevent the melt extrudate from contacting the die wall while still providing enough structural support to prevent the die itself from deforming. The result is effectively a zero length die. The contraction ratio is 9:1 with a die diameter of 1 mm. The analysis proposed by Cogswell (56) was then used to estimate the extensional viscosities from the measured pressure drop and flow rate data. The Cogswell analysis was developed based upon a shear power law fluid upstream to a sudden contraction.

The analysis is for a power law fluid in shear and the angle of convergence of the fluid is determined through the minimization of the pressure drop. The relevant equations relating pressure drop and flow rate to averaged extensional flow properties as given by Shroff and coworkers (57) follow.

$$\sigma = \frac{3}{8}(n+1)\Delta P_0 \tag{4-1}$$

$$\epsilon = \frac{4\tau\gamma}{3(n+1)\Delta P_0} \tag{4-2}$$

$$\eta_E = \sigma/\epsilon$$
 (4-3)

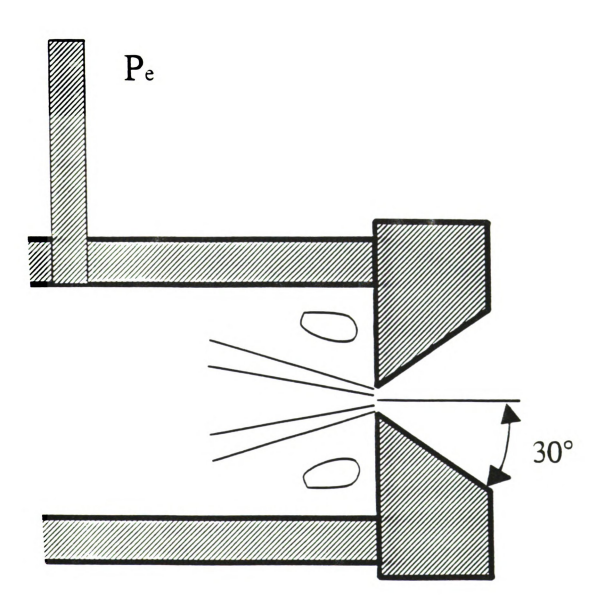


Figure 4-3 Zero length die schematic

A pressure transducer with a range of 10,000 psi was used so measurements at high strain rates such as those encountered during extrusion could be performed. The data presented with a stretch rate below 100 s⁻¹ were obtained with a piston rheometer and zero length capillary die. The extensional viscosities calculated are only apparent values since the polymer melt undergoes a non-constant stretch history. These values serve as a comparative index of the response of the melt to extensional stresses.

The LDPE exhibits much more resistance to stretching than does the LLDPE.

Indices representing the resistance of the melts to stretching are shown in Figure 4-4.

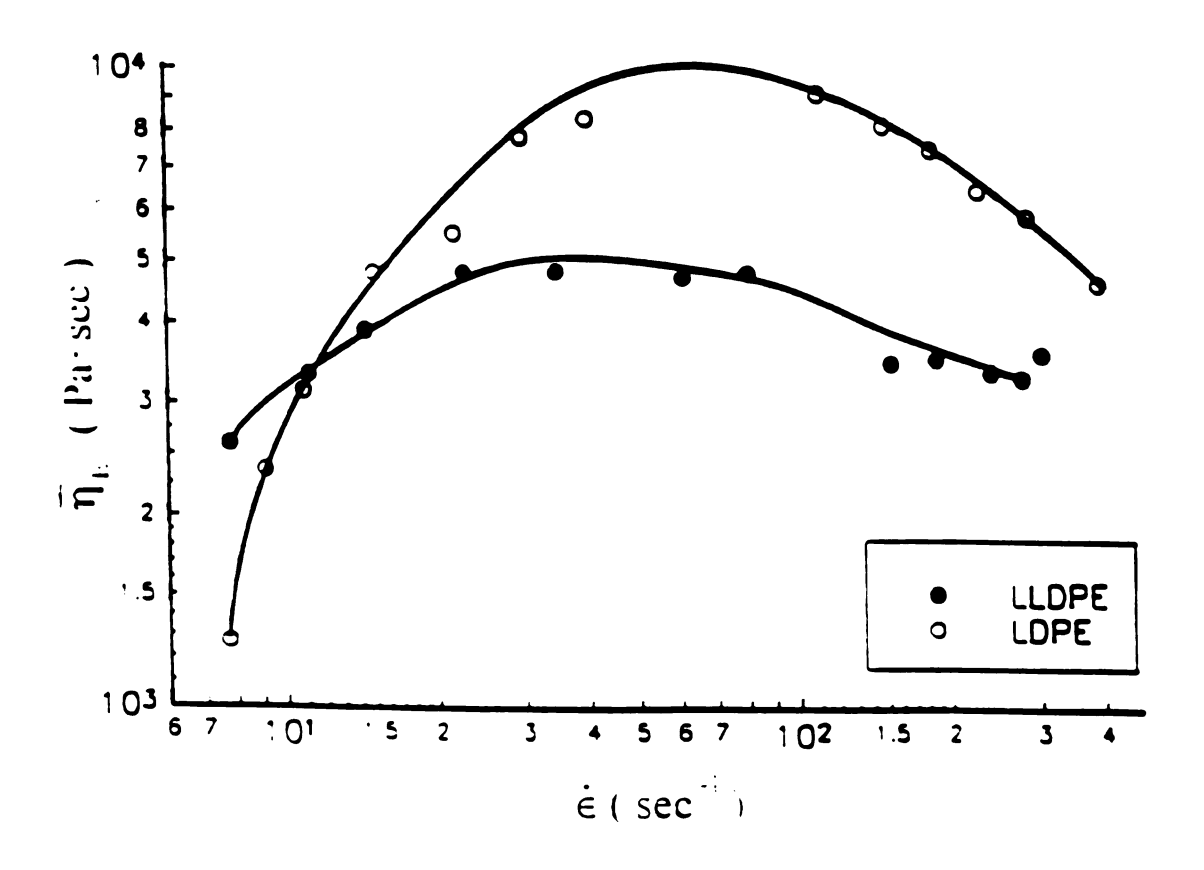


Figure 4-4 Extensional viscosity index of polyethylene melts

Unlike the shear viscosity curves which are quite similar, the extensional viscosities are markedly different. The LDPE shows more stretch thickening behavior at lower stretch rates as well as a sharper rate of decrease in extensional viscosity at higher stretch rates as compared to the LLDPE. The LLDPE extensional viscosity is less dependant upon the stretch rate over a larger range and only reaches about half the viscosity of the LDPE at its maximum. The differences in rheology between the two melts is best illustrated in Figure 4-5 where the ratio of extensional to shear viscosity is shown.

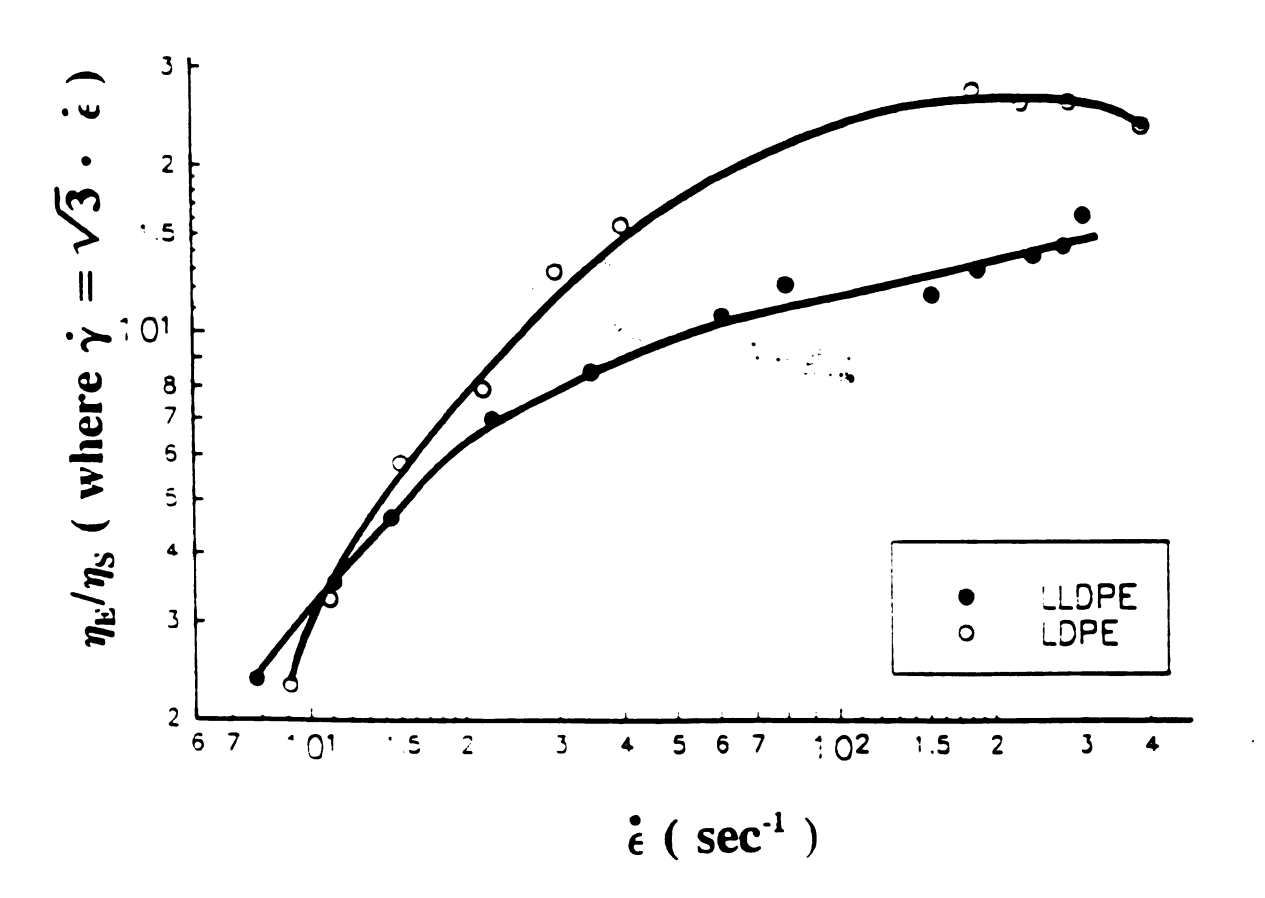


Figure 4-5 Ratio of extensional index to shear viscosity of polyethylene melts

4.3 Experimental

4.3a Extruder Operation

A Baker-Perkins (APV) model MPC/V-30 co-rotating fully-intermeshing twin screw extruder with a barrel L/D of 13/1 was used to process the melts. The extruder configuration is illustrated in Figure 4-6. The modular screws are assembled to provide two separate kneading disc regions for more intensive mixing than provided for in the other screw sections. For this study, each mixing zone consisted of 6 paddles. The first four were configured as 60° forwarding and the final two of each were in the 90° neutral arrangement. This produces moderate forwarding flow with the region of the final two paddles being nearly flooded with polymer under all operating conditions. The barrel valves following these sections were both maintained in the closed position. increases the holdup in the mixing zones allowing for better mixing. The secondary feed port is located just upstream from the second kneading disc mixing zone. A two strand 3 mm diameter die was attached to the extruder exit. The melt temperatures of the mixing zones and exit die were maintained at 180±1°C. During the extrusion, the throughput rate was maintained within 3 % of 34, 44, or 59 cc/min. The screw rotation rate selected was 100, 250 or 450 rpm. A water trough was used to collect and solidify the extrudate strands.

4.3b Residence Time Measurements

The residence times between the second feed port and the exit were obtained for the polyethylene melts through tracer dye measurements. After a period of from 3 to 5

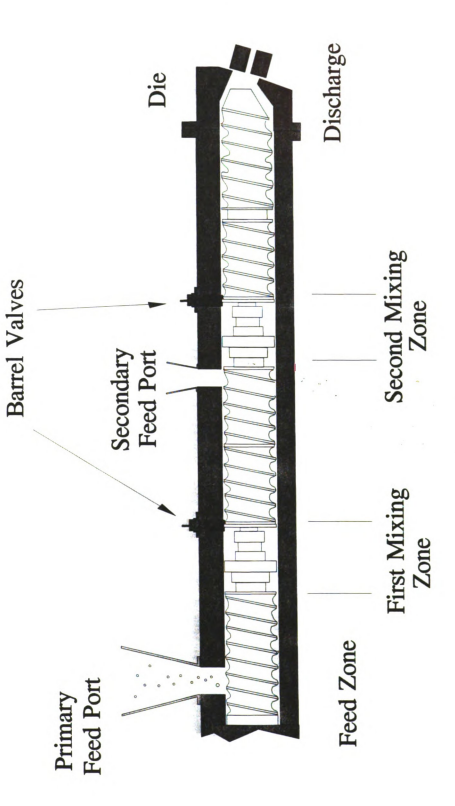


Figure 4-6 Co-rotating twin screw extruder configuration

minutes to allow for the system to reach steady state, 3 ml of oil based soluble red dye was input as a pulse at time zero into the second feed port and the extrudate was collected over time in the water trough. The extrudate strands were cut into different length segments. The strands were cut shortest where the color gradation was the steepest. These segments were each then weighed to the nearest 0.1 gram and the exit time was determined. Each strand section was then pressed into a film of thickness of 0.2 mm and a color index was obtained from a Hunterlab Colorquest Spectrophotometer. The final 3 data points of the experimental residence time distributions were fit to an exponential model to obtain the long time residence tails as described by Todd (46). The areas under the extrapolated parts of the curves generally constituted less than 10% of the area under the entire curve.

4.3c Maleation of Polyethylenes

The polymer pellets and maleic anhydride powder in a 10/1 ratio by weight were hand mixed and fed to the extruder through the main feed hopper. This produces a heterogeneous system since the melted maleic anhydride is insoluble in the polyethylene melt (58). The melted anhydride acts as a plasticizer in the extruder, lowering the viscosity of the blend. The reaction was initiated after this second feed port with the addition of 0.25 part per hundred polyethylene resin dicumyl peroxide in a xylene solution. A medical type syringe feeder was used to supply the peroxide solution (.15 gm dicumyl peroxide/ ml dry xylene) at controlled rates. The polymer melt was extruded into the water trough to quench the reaction. The reacted samples were

collected after allowing for a period of 3 minutes to come to steady state. Since the structure of the two polyethylenes is different, their reactivity is also different. The levels of grafting measured for each polymer are therefore not compared to the those of the other polymer but instead with respect to the operating conditions and resulting residence time distributions.

4.3d Characterization of Reaction Levels

These reacted specimens were rinsed in acetone 12 hours and then treated in a vacuum oven (3 days @ 100 C and > 29" vacuum) as described by Hogt (3). The specimens were then pressed into 0.08 mm thin films and Fourier-transform infrared spectroscopy (FTIR) transmission spectra were obtained from a Perkin-Elmer 1800 spectrophotometer. For both polymers, the carbonyl peak due to the anhydride was found at 1785 cm⁻¹ and the reference methyl peak due to -(CH₂)_n- rocking bands (where n>4) (51) was found at 730 cm⁻¹. The effects of the grafting reaction on the FTIR spectra of LDPE are shown in Figure 4-7. The area of the carbonyl peak divided by that of the reference peak is the carbonyl index. This index was used as a qualitative indication of the level of grafting. In order to determine quantitatively the levels of grafting obtained, the carbonyl index was calibrated against weight increase for separate batch reactions. In these reactions, films of LDPE were weighed to the nearest 0.1 mg. The area of the carbonyl peak divided by that of the reference peak is the carbonyl index. This index is directly proportional to the level of grafting.

In order to determine quantitatively the levels of grafting obtained, the carbonyl

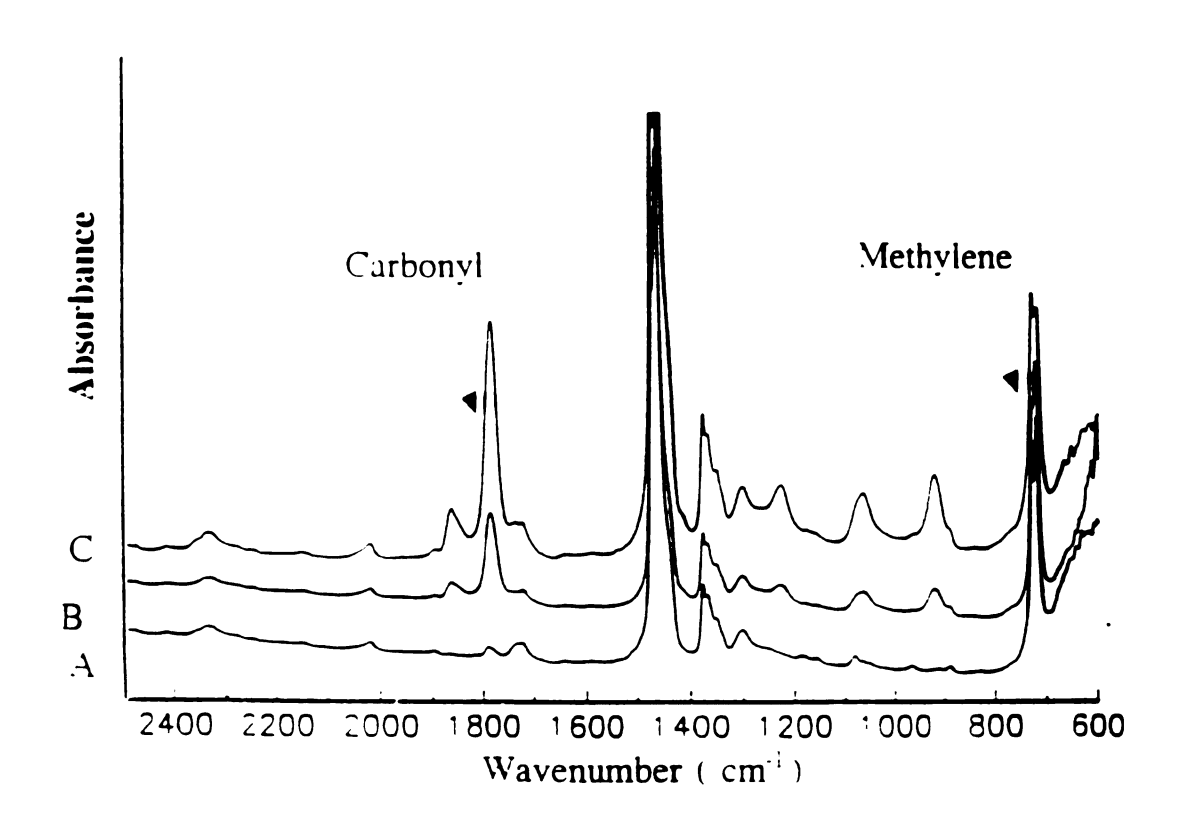


Figure 4-7 FTIR spectra of maleated LDPE

index was calibrated against weight increase for separate batch reactions to obtain the calibration curve shown in Figure 4-8. To obtain the curve, films of LDPE were

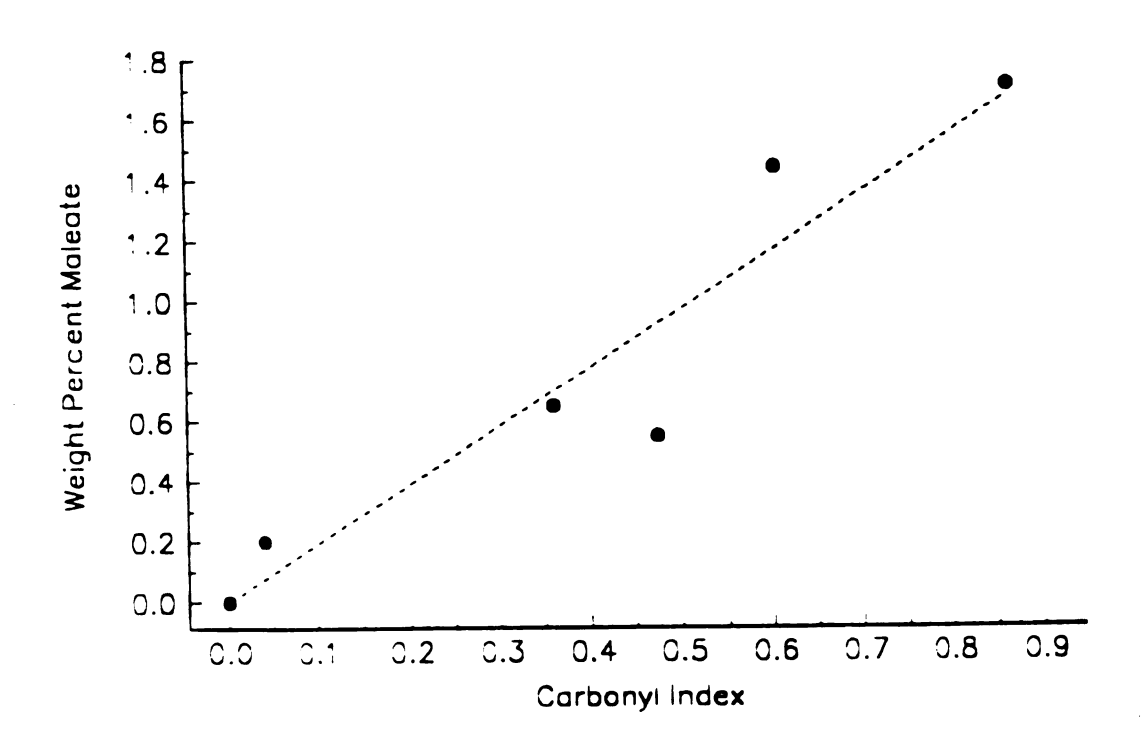


Figure 4-8 Calibration of extent of maleation with carbonyl index

weighed to the nearest 0.1 mg. They were then sandwiched with maleic anhydride powder and dicumyl peroxide powder. Approximately one gram of LDPE was used along with the same weight fractions of peroxide and maleate used in the extruder experiments. These sandwiches were then compression molded at 180°C. The heat was maintained in the mold for from 30 seconds to 3 minutes in order to obtain different levels of reaction. The reacted films were then washed in acetone for 12 hours and vacuum dried in an oven at 100°C and 29" Hg of vacuum to remove any residual unreacted maleate. These treated films were then reweighed to determine the amount of grafted anhydride. A standard was prepared with each batch to ensure that no systematic error was introduced. These standards were prepared in the same way except no peroxide was added to initiate the reaction. Only data collected on specimens from batches whose standard indicated no carbonyl peak in their FTIR spectra and had a zero weight change were used for the calibration curve.

4.4 Results on Mixing of Unreacted Melts

4.4a Degree of Fill

The twin screw extruder operates partially starved. Some screw regions are only partially filled by polymer while others such as the two kneading disc sections may, depending upon the operating conditions, be nearly flooded with polymer. The forwarding ability of the screws is greater for higher degrees of fill (53). A schematic of the paddle cross-section is shown in Figure 4-9 illustrating the partially filled or starved operating conditions. The degree of fill of the extruder from the second feed

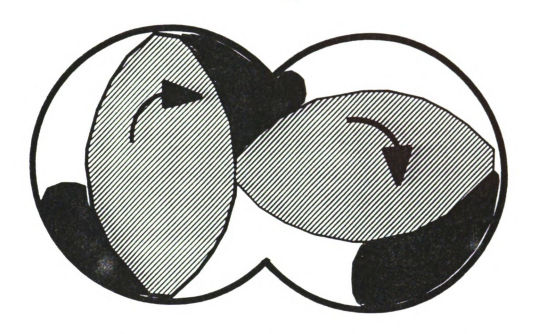


Figure 4-9 Cross-section of partially starved mixing zone

port to the exit has been determined experimentally. The product of the mean residence time and the volumetric throughput rate is the effective hold-up volume. This value is the volume of polymer contained in the extruder after the secondary feed port. Dividing this quantity by the volume past the second feed port available for flow gives the degree of fill. This degree of fill measured is the weighted average of the degrees of fill in the kneading disc and discharge screw sections.

A comparison of the degree of fill of the two polyethylenes at different operating conditions is shown in Figure 4-10. The left side of the diagram indicates starved operating conditions while the right edge of the diagram indicates nearly flooded operating conditions. The degree of fill increases with decreasing screw rotation rates

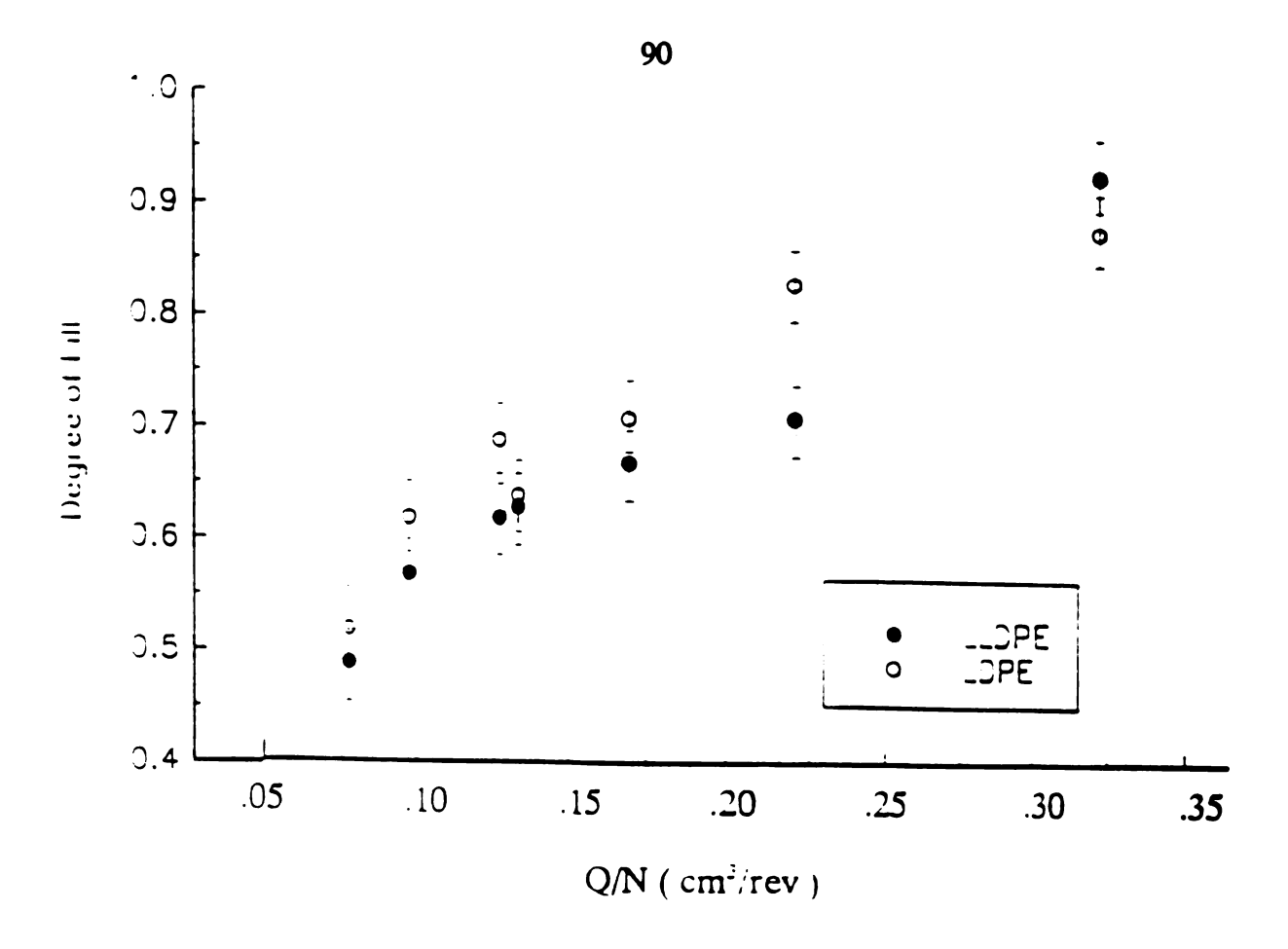


Figure 4-10 Effect of operating conditions on degree of fill

and with increasing throughput rates as seen in similar experiments performed with the same extruder screw configuration for other melts by Nichols (31). The branched polyethylene provides a higher degree of fill than the linear polyethylene from the starved region of the curves until the flooded portion. The increased extensional viscosity of the LDPE accounts for this difference. Since the mixing section is arranged to provide a slight forwarding action, greater resistance to stretching flow reduces the amount of forwarding flow and leads to greater hold up.

4.4b Effect of Extensional Rheology on Flow

The mean residence times and spread of residence times are given respectively in Tables 4-1a and 4-1b. The spread is evaluated as the square root of the variance. The

Table 4-1a Mean Residence Times For Polyethylene Melts

	LLDPE			LDPE		
	100 rpm	250 rpm	450 rpm	100 rpm	250 rpm	450 rpm
34cc/min	142	96	75	133	97	78
44cc/min		80	68		84	73
59cc/min		63	55		73	61

Time in seconds ± 3 seconds

Table 4-1b Spreads of Residence Times For Polyethylene Melts

	LLDPE			LDPE		
	100 rpm 250 rpm 450 rpm		100 rpm	250 rpm	450 rpm	
34cc/min	59	67	40	53	55	42
44cc/min		50	37		33	27
59cc/min		41	30		28	32

Time in seconds ± 3 seconds

mean residence times in the screw sections past the second feed port range from 55 to 42 seconds. The mean residence times of the branched polyethylene are greater than those of the linear polyethylene for each set of operating conditions with one exceptional. This exception occurs for the nearly flooded conditions produced for a screw rotation rate

of 100 rpm. The branched polyethylene also exhibits a narrower residence time distribution than does the linear polyethylene under the same extruder operating conditions. This is evident in the comparison of representative residence time distributions plotted for three sets of operating conditions Figure 4-11. The broader

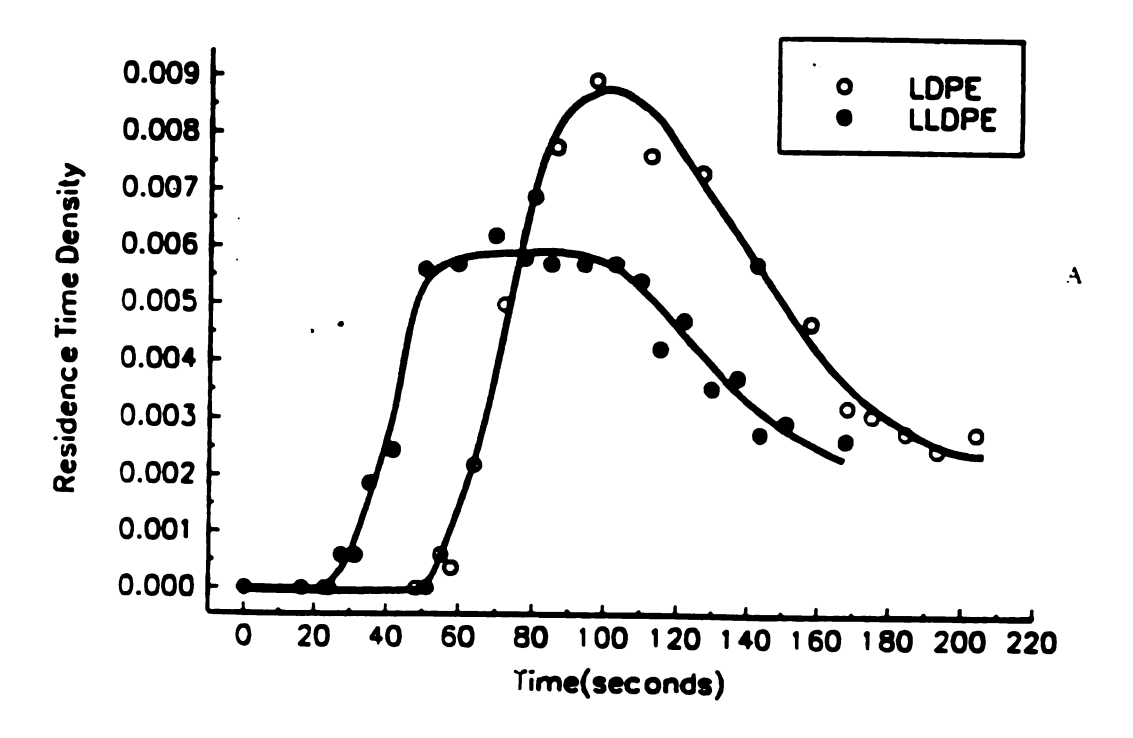
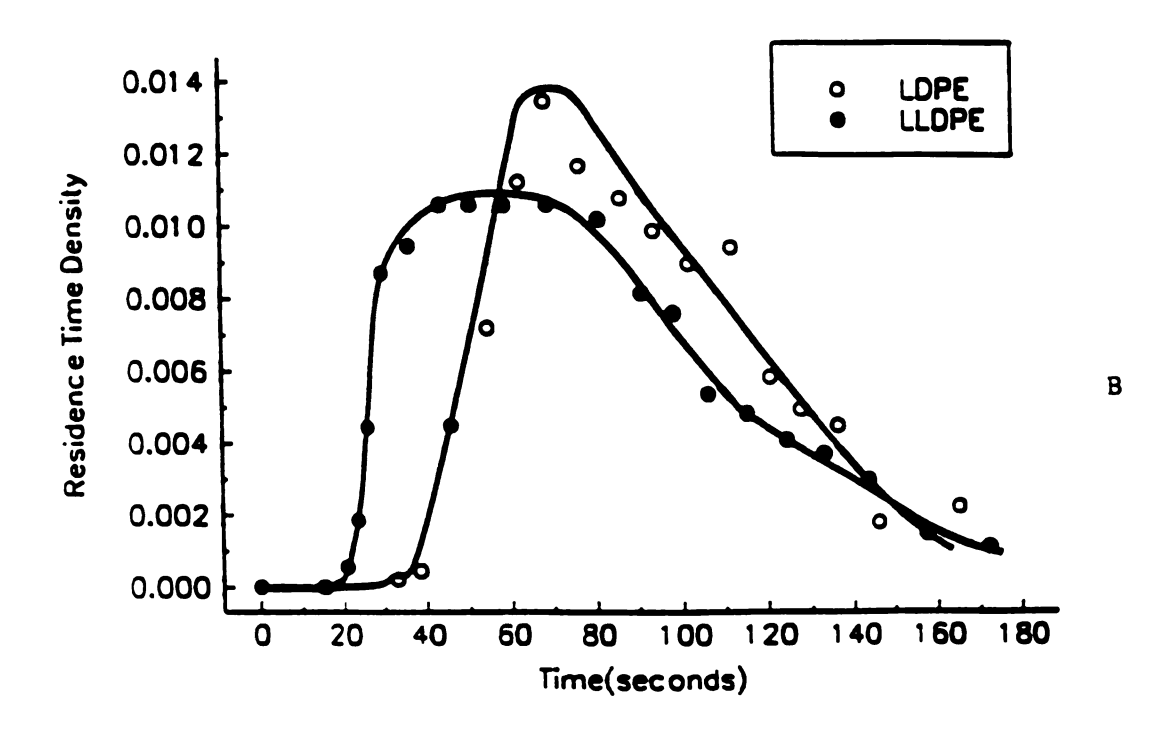


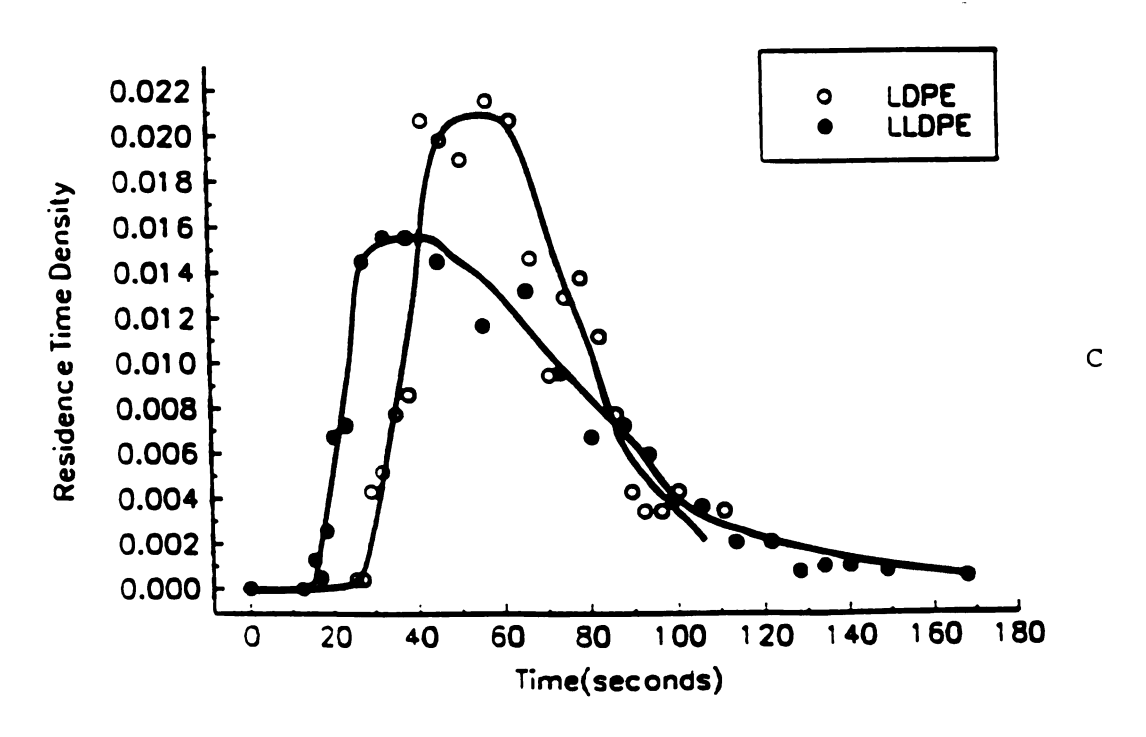
Figure 4-11 Residence distributions for LDPE and LLDPE

(a) 34 cm²/min 250 rpm

(b) 34 cm²/min 450 rpm

(c) 59 cm²/min 450 rpm





residence time distributions found for LLDPE as compared to those of LDPE are an indication of greater levels of axial mixing. The ratio of the spread of the residence time distribution to the mean is shown in Table 4-1c. This parameter provides an indication of the relative level of axial mixing or dispersion. The levels of axial dispersion indicated for the LLDPE are significantly higher, especially for the operating conditions providing a higher degree of fill.

Table 4-1c Relative Levels of Axial Dispersion of Polyethylene Melts

	LLDPE			LDPE		
	100 rpm	250 rpm	450 rpm	100 rpm	250 rpm	450 rpm
34cc/min	0.42	0.70	0.53	0.40	0.57	0.54
44cc/min		0.63	0.55		0.39	0.37
59cc/min		0.65	0.55		0.38	0.52

Time in seconds ± 3 seconds

The differences in rheology between the two melts account for the different residence time distribution features. The similar shear viscosities of the melts result in similar pressure profiles when processed at the same conditions. The differences in flow behavior arise from their differences in extensional rheology, which is relevant to the pressure driven axial flow in the mixing zones of the extruder. The branched polyethylene exhibits increased resistance to extensional or stretching flows so that the levels of axial mixing for the LDPE are less than those for the LLDPE. This reduction in axial flow results in the observed narrower residence time distributions. The net axial flow in the mixing zone of the extruder is in the forwarding direction. Hence, the LDPE

has a larger mean residence time and correspondingly greater hold up volume in the reactor.

4.4c Effect of Operating Conditions on Flow

The two polyethylenes each responded similarly to changes in extruder operating conditions. Increasing the throughput rates from 34 to 44 to 59 cm³/min results in shorter mean residence times as expected. Increasing the throughput also results in progressively narrower residence time distributions as shown in Figures 4-12 and 4-13. This indicates a greater resistance to axial mixing as the degree of fill in the extruder increases. The configuration of the six sets of paddles in the second mixing zone may be responsible for this effect. The final two paddles are at 90° which provides for equal levels of forwarding and reverse flow. These two paddles are nearly always flooded. As the degree of fill increases, the four upstream paddles arranged with a 60° forwarding configuration become more flooded. This increases the resistance to reverse flow and leads to the observed narrower residence time distributions.

Increasing the extruder rpm reduced the mean residence times as expected. It also reduced the breadths of the distributions (see Figures 4-14 and 4-15). The degree of fill decreases with increasing screw rotation rates. Therefore, the resistance to reverse flow in the paddle sections should decrease resulting in a broader residence time distribution. Instead, a narrower residence time distribution is observed. The effect of the increase in strain rates due to the faster screw rotation rates on the melt rheology may account for the observation. The ratio of extensional to shear viscosity generally



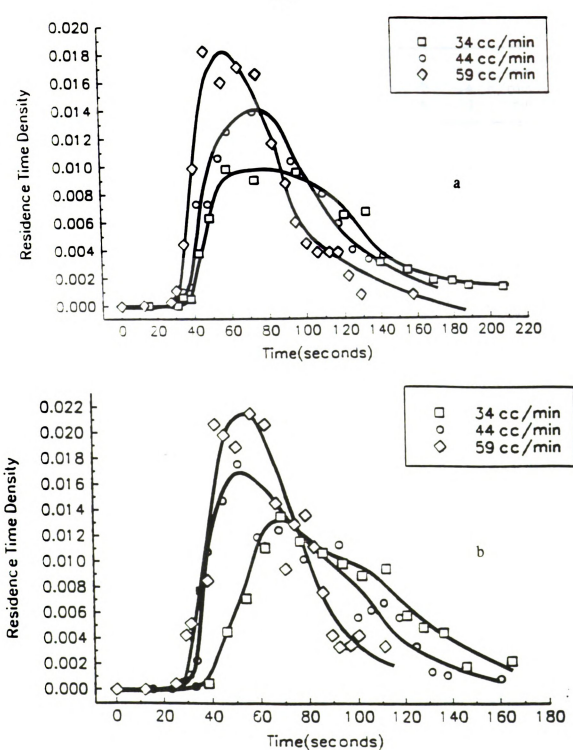


Figure 4-12 Effect of increasing throughput rate on the residence time distribution for LDPE at (a) 250 rpm (b) 450 rpm

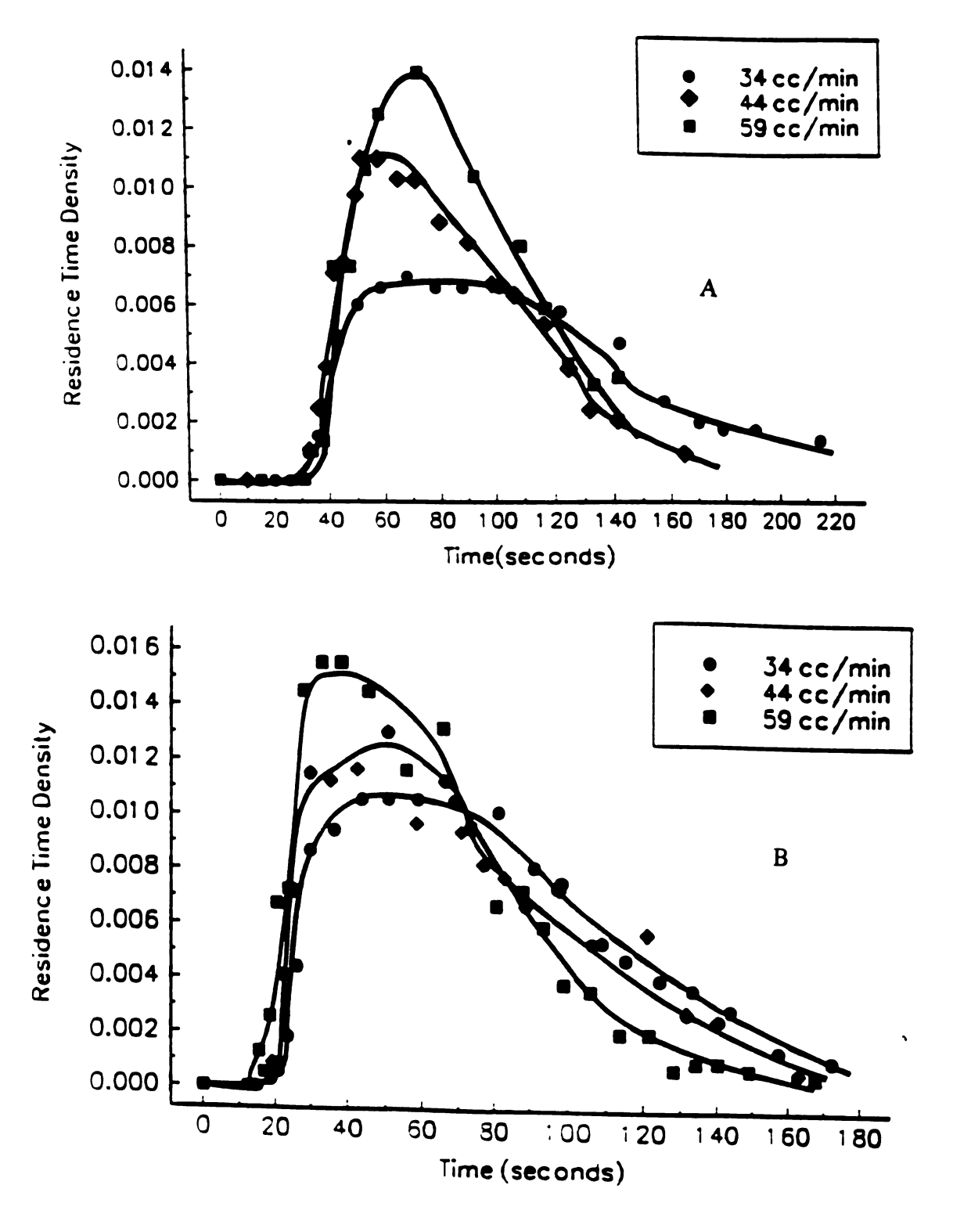


Figure 4-13 Effect of increasing throughput rate on the residence time distribution for LLDPE at (a) 250 rpm (b) 450 rpm

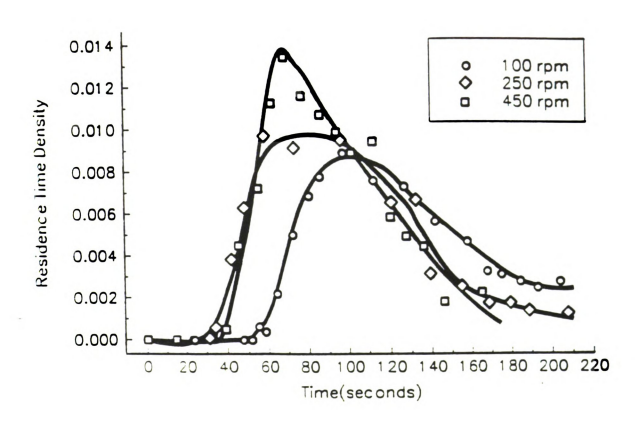


Figure 4-14 Effect of increasing extruder screw rotation rate on the residence time distribution for LDPE for 34 cm²/min throughput rate

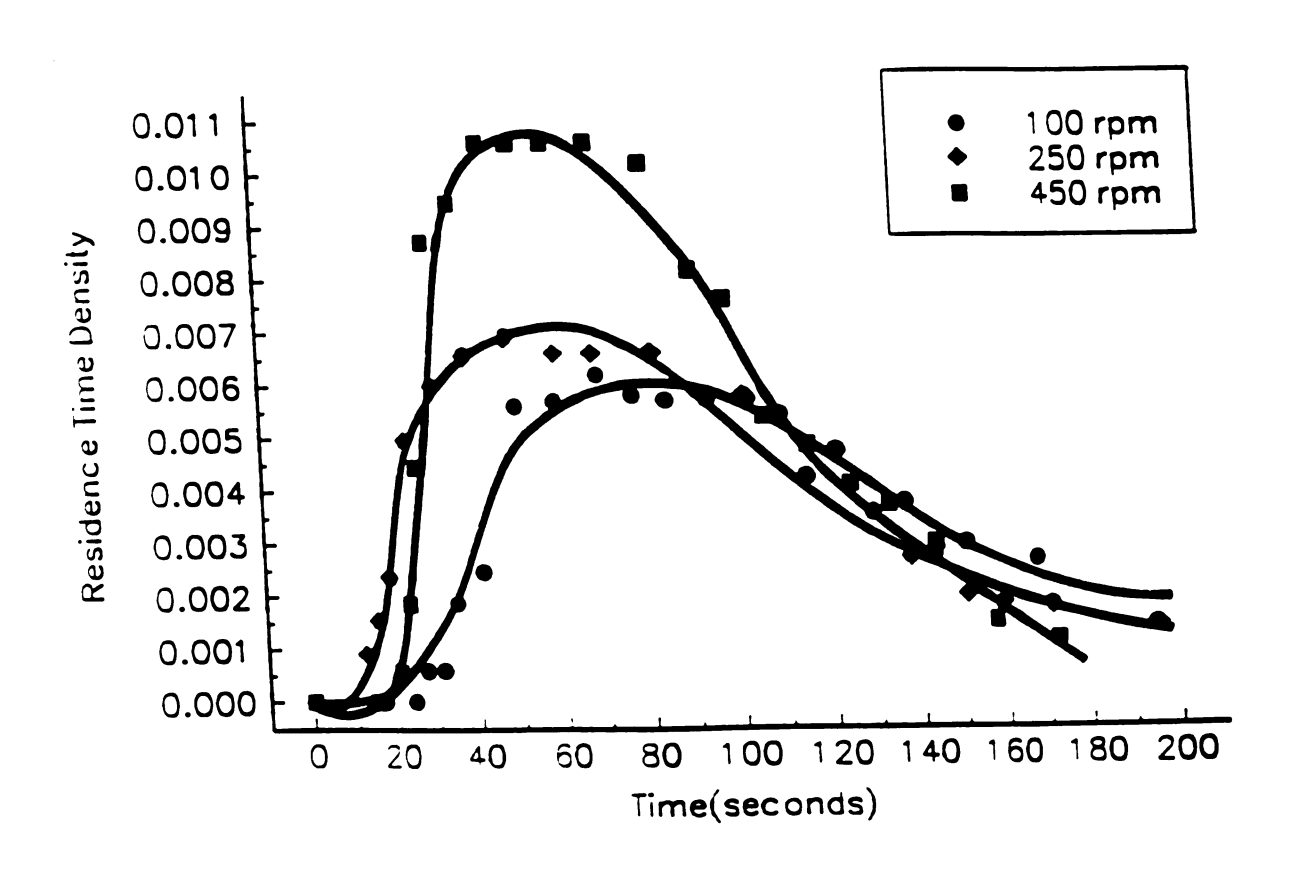


Figure 4-15 Effect of increasing extruder screw rotation rate on the residence time distribution for LLDPE for 34 cm³/min throughput rate

increases with the strain rate as shown in Figure 5. The shear thinning nature of the melts reduces the pressure increase caused by the higher shear rates associated with the greater screw rotation rate. The decrease in the extensional viscosity is relatively smaller so that the level of pressure driven axial flow is reduced.

The same general trends of changes in residence time distributions with different operating conditions were observed by Nichols (31) for PVC and CPE with the same extruder screw configuration. The spreads in residence time distribution in the paddle zones decreased with increasing throughput rates and screw rotation rates. These melts are also both shear thinning. No extensional rheology data is available for these melts to compare to their extruder flow behavior.

4.5 Results on Mixing of Reacting Melts

4.a Levels of Grafting

The LLDPE is significantly more reactive than the LDPE. The large number of short branch sites provides for a higher concentration and better access to tertiary carbons which are more reactive than secondary carbons. The LLDPE could not be reacted under the same conditions as the LDPE because significant crosslinking occurred, resulting in an increase in the extruder load due to the viscosity increase along with greater difficulty maintaining the temperature. To reduce the level of crosslinking, 0.8 % by weight of an antioxidant 2,6 di-tert-butyl-p-cresol (BHT) was added with the LLDPE and maleic anhydride in the main feed port to supplement the stabilizer already included.

The levels of reaction for LDPE and LLDPE processed at different extruder operating conditions are shown in Tables 4-2 and 4-3. The same calibration used to convert the FTIR data to the level of grafting was also used to determine the extents of grafting for the LLDPE system. The polyethylenes responded similarly to changes in extruder operating conditions. The levels of maleation increased with decreasing

Table 4-2 Maleation Levels of LDPE

FEED RT\ RPM	100 rpm	250 rpm	450 rpm	
34 cc/min	2.9%	3.0%	2.1%	
44 cc/min		1.0%	1.2%	
59 cc/min		0.3%	0.2%	

± 0.2%

Table 4-3 Maleation Levels of LLDPE

	100 rpm	250 rpm
34 cc/min	3.5%	2.7 %
44 cc/min		2.3%

 $\pm 0.2\%$

throughput rates. These increases correspond to increases in both the mean and the spread of the residence time distributions. Increases in the screw rotation rates lead to decreases in the extent of grafting. These decreases in reaction level correspond to decreases in the mean and the spread of the residence time distribution.

In order for the desired graft reaction to occur, the polymer and maleate must be

well mixed before the peroxide dissociation occurs and macroradicals are formed. Therefore, the peroxide is added in the extruder only after the polymer and maleate have already been blended together. The cross-linking and grafting are parallel, competing reactions. Cross-linking occurs when two macroradicals combine and hence is second order with respect to the macroradical concentration. Maleation occurs when a macroradical grafts to an anhydride in a mechanism which is first order with respect to the macroradical concentration. Since the undesired cross-linking reaction is of higher order, locally high concentrations of dissociating peroxide should be avoided. The axial dispersion associated with some broadening of the residence time distribution contributes to the uniform distribution of peroxide.

4.5b Effect of Cross-linking on Flow

Shear viscosity curves for LLDPE samples with two different levels of maleation (and cross-linking) are presented along with the curve for unreacted LLDPE in Figure 4-16. While the shear viscosity at low strain rates is increased by an order of magnitude upon limited cross-linking of the LLDPE, the increase in shear viscosity is less significant at the higher strain rates which may be more characteristic of flow in an extruder. Before the rheological testing of the reacted specimens, the residual unreacted peroxide and maleic anhydride were removed from the specimens through acetone washing and vacuum oven drying. The 34 cc/min - 250 rpm reacted LLDPE has a level of maleation of 2.7% while the 44 cc/min - 250 rpm LLDPE has a level of reaction of 2.3%. Viscosity measurements for the reacted melts is much more difficult than those

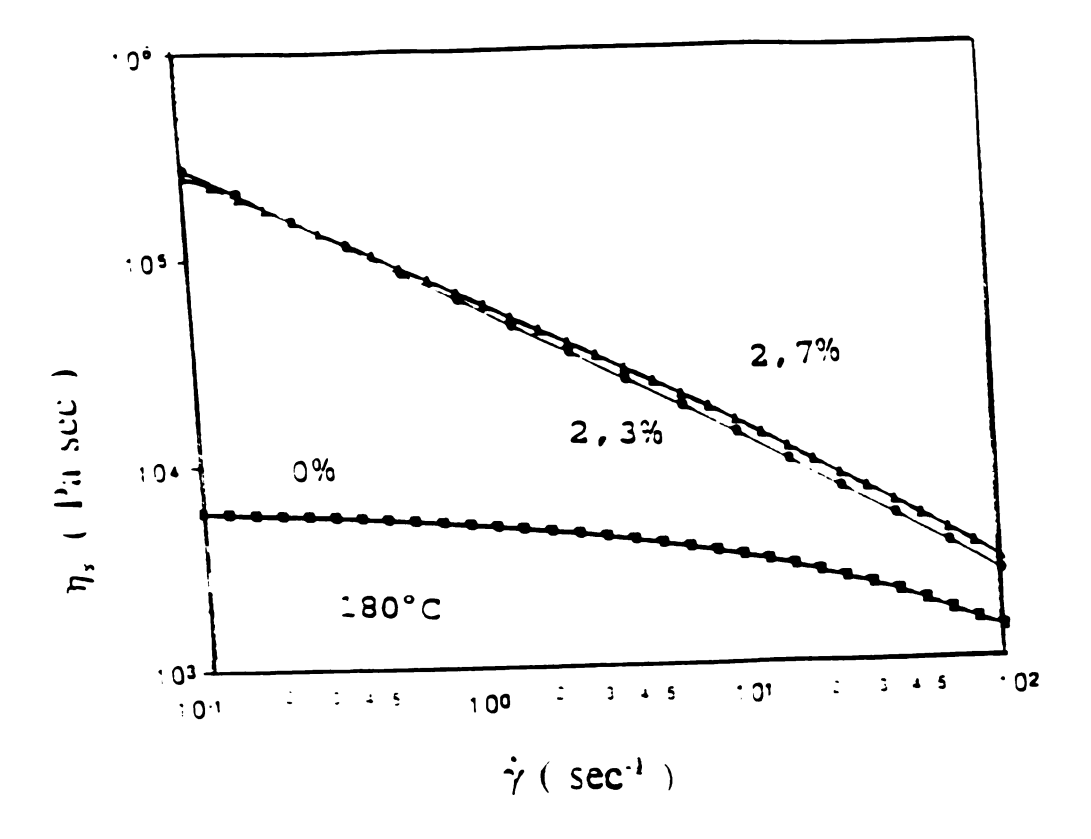


Figure 4-16 Effect of cross-linking on the shear viscosity of LLDPE melt at 180°C (% indicates level of maleation)

of the unreacted polyethylenes. Larger quantities of specimens (~ 2 grams) are required for the rheological tests than for the determination of grafting levels (~ 0.1 grams). The larger quantity specimen is more difficult to separate from the unreacted maleic anhydride than the smaller quantity FTIR specimens.

The presence of grafted and residual ungrafted maleic anhydride can result in some yellowing of the polyethylene. This reduces the sensitivity of the dye color intensity to concentration. Still, residence time distributions were determined for selected runs in the presence of the maleation reaction. A comparison of an FTIR spectrum of the reacted polyethylene with dye added, to the spectrum of a sample without dye but

otherwise processed under the same conditions showed no significant difference. This indicates that the dye does not interfere with the reaction progress.

The effect of increasing throughput rate for the reacting LLDPE melt is shown in Figure 4-17. The higher feed rate results in a reduction in the spread and the mean of the residence time distribution as was the case for the unreacting melt. The means and spreads and the ratios of spread to mean for the measured residence time distributions obtained with reacting LLDPE melt processed under different sets of conditions, are presented in Table 4-4. The effects of changes in operating conditions

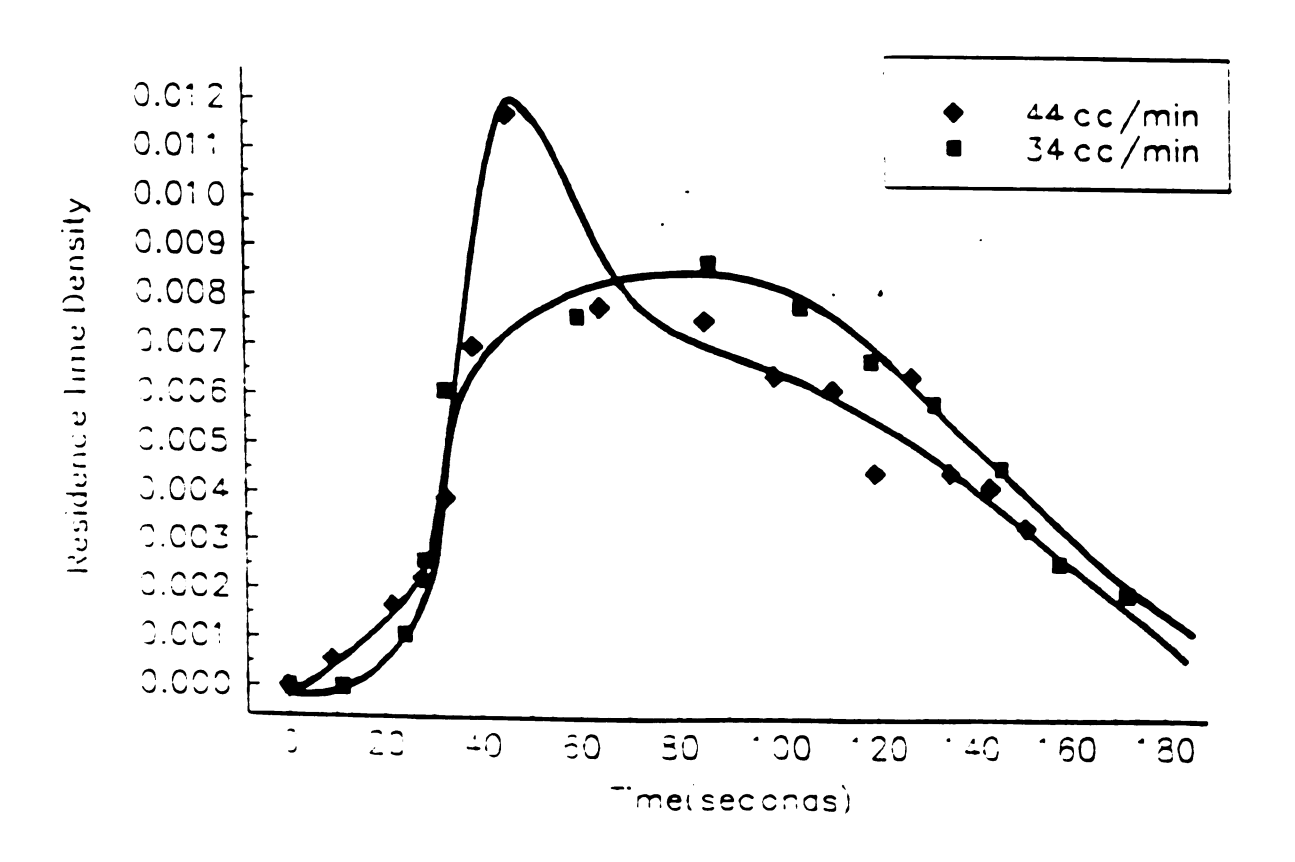


Figure 4-17 Effect of throughput rate on residence time distribution of reacting LLDPE in reaction zone of extruder

are similar to those found for the unreacting melts. The residence time distributions of the reacting LLDPE melt are narrower than those of the unreacted LLDPE melt. This is particularly evident in comparing Table 4-1c with Table 4-4c. However, the effect of the limited cross-linking of LLDPE on the axial mixing of LLDPE is less striking than the difference in mixing observed between LDPE and LLDPE melts.

Table 4-4a Mean Residence Times of LLDPE With Reaction

	100 rpm	250 rpm
34 cc/min	118	94
44 cc/min		89

Time in seconds \pm 5 seconds

Table 4-4b Residence Time Spreads of LLDPE With Reaction

	100 rpm	250 rpm
34 cc/min	57	60
44 cc/min		46

Time in seconds \pm 4 seconds

Table 4-4b Relative Levels of Axial Dispersion for LLDPE With Reaction

	100 rpm	250 rpm
34 cc/min	0.48	0.64
44 cc/min		0.52

4.6 Discussion and Conclusions

The kneading action in the mixing zones of the twin screw extruder leads to a pressure flow in the axial direction. As observed by Eise and coworkers (30), a circumferential pressure profile is set up by the paddle rotation in a co-rotating twin screw extruder. This pressure is proportional to the shear viscosity of the melt at the strain rates generated by the paddle rotation. The stagger of the paddles in the mixing zones creates pressure gradients in the axial direction as well as a non-uniform geometry for axial flow. Thus, a pressure driven axial flow with extensional strain components is produced. The relevant viscosity for this flow is closer to the apparent extensional viscosity obtained from the zero length die experiments described in section 4.2b than it is to the shear viscosity.

The pressure driven axial flow occurs in the reverse as well as the forward direction. The amount of reverse flow is determined in part by the axial stagger of the paddles. This reverse flow or back mixing broadens the residence time distribution. The six kneading discs or paddles are configured in a four at 60° forwarding and 2 at 90° neutral arrangement. This provides a net forwarding action. This observation accounts for the differences observed in the flow of the polyethylene melts. The LDPE has narrower residence time distributions indicative of reduced levels of backmixing. The LDPE and LLDPE have similar shear viscosities so that the pressures generated due to circumferential strain are also of similar magnitudes. The relatively higher extensional viscosity of the LDPE reduces the level of the pressure driven flow. This reduction in both forwarding and reversing axial flow due to reduced extensional strain accounts for

the observed narrower residence time distribution. Since the net action of the extensional strain from the paddle region is a slight forwarding action due to the screw configuration, the small increase in mean residence time should be expected with an increase in extensional viscosity. This was found to be the case as indicated by the slightly higher levels of holdup measured for the LDPE.

During the maleation, the polyethylene melts are also cross-linked to some extent, leading to an increase in their shear viscosity. Viscosity measurements after removal of excess maleic anhydride show an order of magnitude increase at low shear rates but much less increase in viscosity at higher shear rates. During the reaction, the increase in shear viscosity due to cross-linking may be offset by the plasticizing effect of the maleic anhydride in the melt. Still, the reaction resulted in some slight narrowing of the residence time distribution of LLDPE. The effects of both the cross-linking reaction and the presence of maleic anhydride melt on the extensional viscosity of the melts needs to be determined in order to define the effects of rheology on the flow of the reacting melts.

The residence time distribution of the reacting polymer system determines the final product. A longer mean residence time provides for higher levels of reaction for the maleation and cross-linking reactions where time is a limiting factor. The dispersing of the peroxide into the viscous blend of polyethylene and maleic anhydride melt is a critical step in the reaction process. Furthermore, the selectivity of the maleation reaction can be improved by avoiding locally high concentrations of peroxide. This is achieved by greater axial dispersion associated with somewhat broader residence time distributions. The desired residence time distributions can be obtained through altering

the operating conditions in conjunction with the flow geometry.

The rheology of the polymer melt may have a large effect on the residence time distribution. The effect of melt rheology on the residence time distribution depends upon the extruder screw configuration. In paddle arrangements providing for significant reversing action such as those in this work, the residence time distribution will be narrower for melts with greater ratios of extensional to shear viscosity. With open barrel valves and strongly forwarding paddle configurations, the melts with greater ratios of extensional to shear viscosity will have significantly longer mean residence times in addition to narrower residence time distributions.

KINETICS OF MICELLE GROWTH AND CLUSTERING IN DIBLOCK COPOLYMER/HOMOPOLYMER BLEND

5.1 Introduction

Polymer blends provide a means to obtain a desired combination of material properties which may not be achieved as readily with a single polymer. Toughened thermoplastics are common examples. In such blends, some elastomer is added to a relatively brittle polymer in order to improve its toughness. The level of toughening depends upon the morphology of the blend. When polystyrene is toughened with polybutadiene rubber, the dispersed rubber particle sizes must be greater than 1 μm in diameter in order to achieve toughening (59). This critical rubber particle size depends upon the constituents of the blend. Poly (vinyl chloride) may be toughened by rubber particle sizes below 0.1 μm in diameter (60). Control of the morphology of the blend is required in ensure that the desired material properties are obtained.

Melt mixing of two polymers will generally produce a weak and brittle blend as the result of poor interfacial adhesion between the phases (61). The adhesion between incompatible blend phases is a critical factor in

determining the final material properties. The deformation modulus of such blends may follow the linear mixing rule but the ultimate properties will not. Frequently, the properties of the blend can be improved with the addition of a block copolymer as a compatibilizer.

Polymers A and B are two homopolymer components of an incompatible blend. The morphology of the blend can be tailored through the addition of some AB diblock copolymer. The copolymer in such systems acts as a surfactant, reducing the interfacial tension between the two homopolymers. An improved understanding of the morphology in such blends can be obtained through the investigation of the morphology of a slightly simpler system, an AB diblock copolymer dispersed in an A polymer matrix. The A and B polymer block segments tend to phase separate when combined in sufficient concentrations. With the AB diblock as the minor component of the blend, the B blocks segregate to form the cores of micellar structures with the attached A blocks forming surrounding coronae. The size, shape, and spatial distribution of these micelles depends upon the thermal and mechanical history of the blend. Upon annealing at a temperature above the glass transition temperature of each blend component, the morphology as processed can change with time into a more stable one. The work presented here is a description of this evolution in morphology for a high molecular weight A/AB polymer blend.

Considerable theoretical and experimental work has been reported on the morphologies of AB/A polymer blends at equilibrium. Leibler and coworkers (62) have presented a model for micellar formation at thermodynamic equilibrium in a low

molecular weight homopolymer matrix. Their model is based upon a balance between enthalpic and entropic effects. The growth of the micelles results in a decrease in surface area at the A-B interphase which is enthalpically favorable. The micelle growth also results in stretching of the diblock chains and compaction of the micelle corona which is entropically unfavorable. The equilibrium morphology is defined by a balance between these two effects which minimizes the free energy of the system. Kinning and coworkers (63) have experimentally observed the morphology of solvent cast blends of styrenebutadiene diblock copolymer and polystyrene; the molecular weights of the polystyrenes were below the critical molecular weight for entanglement. They note an increase in micelle core radii and a decrease in corona thickness with increasing molecular weight of the matrix homopolymer below the entanglement molecular weight. The effect of temperature on the equilibrium morphology in such systems has been reported by Rigby and Roe (64). As the temperature is increased, the micelle cores swell due to greater dissolution of low molecular weight matrix homopolymer into them. These observations confirm the trends predicted by the theory of Leibler et al. (62) for such systems.

In addition to temperature and molecular weight, the method of blend formation also has a strong effect on blend morphology. Nichols and Jayaraman (65) compared the morphology of AB/A blend formed by extrusion to that of the same blend formed by solvent casting. The extruded blend contained well dispersed 20 nm diameter discs of the AB copolymer while the solvent cast blend contained some onion skinned structures of AB copolymer which spanned up to several microns. Interestingly, these two distinctly different morphologies evolved towards the same morphology upon annealing at an

elevated temperature.

The rate of changes in morphology accompanying annealing depends upon the molecular weights of components in the system. The transition to an equilibrium morphology of AB micelles in a low molecular weight solvent A should occur relatively quickly. For blends with a high molecular weight matrix, the time scale for this transition may be much longer. Halperin and Alexander (66) have examined the mechanisms for relaxation of micelle structure in a low molecular weight homopolymer system. They propose that the rate determining step for morphological evolution in such a system is the addition or extraction of individual AB macromolecules in a micelle. Balazs et al. (67) have analyzed the formation of micelles by polymeric and non-polymeric constituents in low molecular weight solvents. Their numerical simulation predicts that simple scaling relationships derived for low molecular weight micelle constituents are not applicable for associating diblock copolymer molecules. Because of the limited mobility in high molecular weight polymeric systems, the morphology may never attain that of true equilibrium. Semenov (68) has predicted that micelle formation and agglomeration for high molecular weight systems may never achieve a true equilibrium morphology but may instead be limited by activation energy barriers.

The object of this work is to study the changes in morphology upon annealing of a high molecular weight A/AB polymer blend. A blend consisting of 5% by weight styrene-butadiene diblock copolymer dispersed in a high molecular weight polystyrene homopolymer matrix is produced by melt compounding. The kinetics of the morphological evolution of the blend are obtained by comparing the size and spatial

distribution of the micelles of the blend after annealing over progressive time increments.

The results seem to support theoretical assertions of Semenov (68) on dynamics of block copolymer micelles in a high molecular weight polymer matrix.

5.2 Experimental

5.2a Materials

A blend consisting of 95% polystyrene and 5% styrene-butadiene diblock copolymer is examined. The polystyrene is Dow Styron 666APR, with a M_w of 179,000 and a polydispersity index of 1.7. The AB component in the blend is Finaprene 315, a tapered diblock styrene-butadiene copolymer with M_w=136,000 and M_n=120,000. Seventy percent by weight of the Finaprene is styrene and the remaining 30% is butadiene. The styrene block makes up 50% of the copolymer with the rest of the styrene of the copolymer found in the taper. The Finaprene contains a stabilizer and an antioxidant to reduce the likelihood for the temperature sensitive butadiene to degrade or cross-link.

5.2b Blend Preparation

The blend was compounded in a Baker-Perkins (APV) co-rotating, fully intermeshing twin screw extruder. Pre-dried polystyrene and styrene-butadiene copolymer pellets were each weighed out, shaken together, and fed to the extruder as a mixture consisting of 5% copolymer. The extruder barrel length is 13 times its diameter of 30 mm. The screw configuration is described in 3.2c. The extrusion was performed with the barrel temperature of each melt zone maintained at 170°C and a screw rotation rate

of 250 rpm. The highest feed rate consistent with the extruder torque capacity was used. This provided for a mean residence time under two minutes. The blend was extruded through a twin 3 mm diameter circular strand die and into a water bath. The strands were then pelletized and the extrusion procedure was repeated. Finally, the blend was extruded a third time and quenched in the water bath where the strands were collected. The blend was compounded three times to ensure the two components were well mixed. Stabilizer was used to ensure that no noticeable degradation of the material occurred during this process.

The extruded specimens were annealed at 180°C or 200°C under a blanket of nitrogen at a pressure of 1 psig. After the selected annealing period of from 5 minutes up to 2 hours, the sections were removed and quickly (within 3 seconds) quenched by submersion in a cold water bath.

5.2c Characterization of Morphology

The specimens were prepared for transmission electron microscopy (TEM) under the supervision of Dr John Heckman of the Center for Electron Optics. The procedure is similar to that described by Kato (69). The blend morphology was viewed from two separate planes: one normal to and one parallel to the extrudate strand axis. The microtome knife assembly is illustrated in Figure 5-1. Trapezoidal block faces with 0.5 mm sides were carved onto the extrudate strands using a sharp razor blade. Sections 90 nm thick were microtomed from the block face. The surface tension of the water in the boat stretched the thin sections and relieved the compaction caused by the diamond knife

specimen with trapezoidal block face

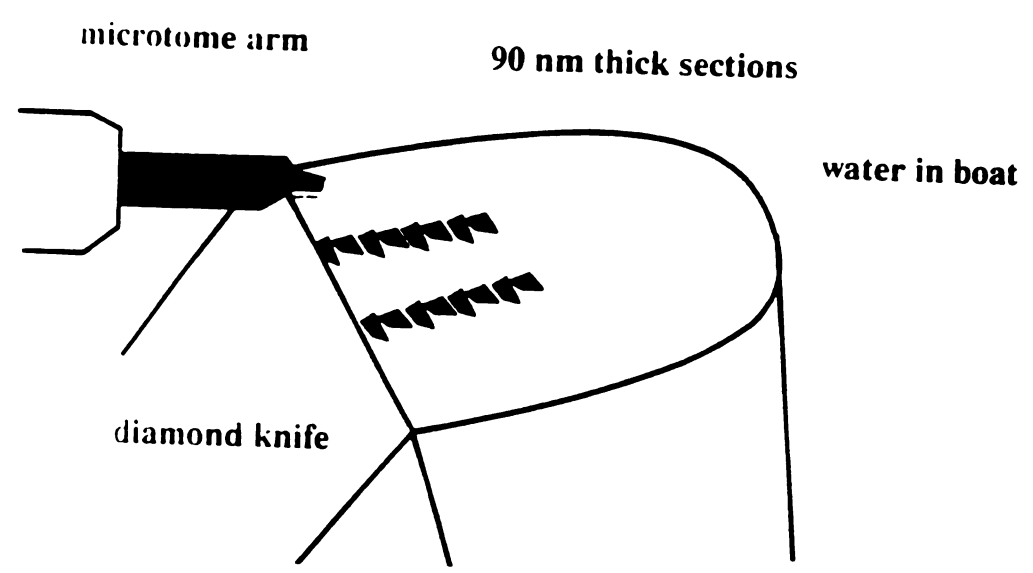


Figure 5-1 Ultra-mircrotome procedure for sectioning of TEM specimens

blade. After a one second exposure to xylene vapor to further relax the sections, they were collected onto 300 mesh copper grids. The sectioned specimens were then exposed overnight to OsO₄ vapor. OsO₄ reacts with the unsaturated double bonds of the butadiene thereby attaching Osmium. Since the ionizing radiation of the electron beam can cause the polymer to decompose and form volatile products, the copper grids were coated with a 1 nm thick carbon film before placing them in the electron microscope. This provides for improved stability of the specimens under the electron beam.

Micrographs were taken either on a Hitachi HU 800 or a JEOL 100 cx electron microscope. The contrast in the micrograph is provided by differences in the scattering of the electron beam provided by the sample. The scattering power is directly related to the atomic number of the atoms in the electron path. Since the atomic number of Osmium is 76 and the atomic number of Carbon is only 6, the Osmium stained regions

appear as dark areas on the micrographs. Negatives of the micrographs were placed upon an overhead projector and projected onto a wall where the major and minor axis lengths of the micelle cores were measured with calipers. The edges of the micelle cores are not distinctly clear in the micrographs. For this reason, the distances measured from the micrographs were precise only to the nearest 0.5 nm, regardless of the magnification used. The distance of each micelle from its core edge to the edge of its nearest neighbor was also measured. At least two micrographs, each with 30 or more micelles evident, were examined for each set of annealing conditions. A minimum of 120 total micelle cores were measured for each reported case. The sectioning method results in a truncation of the micelles. A correction derived given by Equation 5-1 (70) was employed to determine the correct average radii for each set of conditions. The random error due to the sample

$$\frac{R_{measured}}{R_{corrected}} = \frac{1 + \frac{R_{corrected}}{2t_s}}{1 + \frac{2R_{corrected}}{t_s}}$$
(5-1)

size in the determination of the average micelle volume, V_m , from N micelle measurements is estimated to be $\sigma(V_m)/(N)^{\frac{1}{2}}$ (71). This potential error ranges from 9 to 12% in this work.

5.3 Results

5.3a Micelle Growth

Representative micrographs of the extruded blend are shown in Figure 5-2a and 5-2b. The morphology as seen in the plane normal to the strand axis is illustrated in

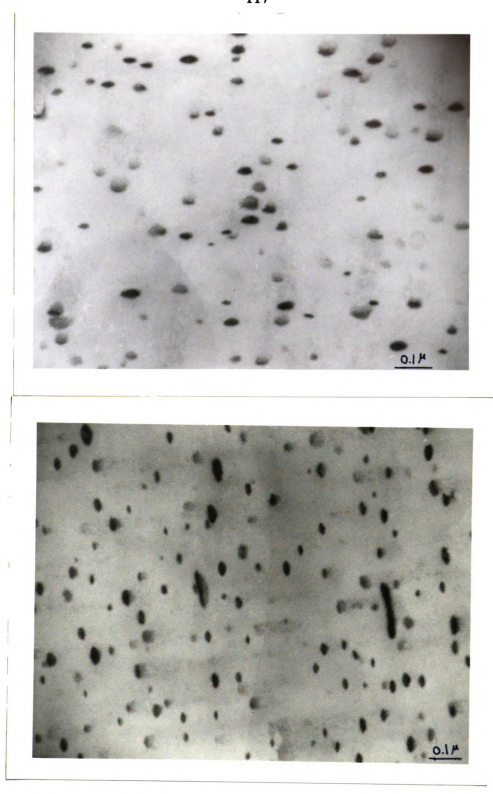


Figure 5-2 Oriented blend morphology before annealing as viewed from plane (Top) normal to strand axis (Bottom) containing strand axis

Figure 5-2a while Figure 5-2b shows the morphology in the plane containing the extrudate strand axis. The aspect ratio, defined as the average ratio of the major to minor axis length of the micelle core, is 2.3 as viewed from the plane normal to the extrudate strand axis. About 10% of the cores in the plane containing the strand axis are significantly elongated with an aspect ratio of 10 or more. The axes of these cylinders are aligned with the axes of the extrudate strands. Thomas (71) observed similar orientation of morphology in injection molded species of a rubber modified thermoplastic. The average micelle core radius is 12.8 nm. This is the radius of a sphere with a projected area equal to that of the ellipsoidal micelle cores. The morphology of a blend of the same copolymer and a higher molecular weight polystyrene with a broader molecular weight distribution was investigated previously (72). The average size of the micelles formed in the lower molecular weight polystyrene are approximately half as large as those in the higher molecular weight matrix. A summary of individual micelle measurements taken from the plane normal to the extrudate strand axes before and after annealing is given in Table 5-1.

Upon annealing at either 180°C or 200°C, the fraction of highly elongated ellipsoids or cylinders in the axial plane disappears. This transformation occurs quickly. No cylinders are evident in the axial plane after the blend is annealed for 5 minutes at 180°C as shown in Figure 5-3. The time scale for other changes in morphology described below is much longer. The average aspect ratio, a/b, of the micelles does not change significantly at 180°C. The micelle cores become noticeably more spherical after annealing at 200°C. The average aspect

Table 5-1 Summary of Micelle Core Measurements

Annealing Conditions	Number		verage ius (nm) corr.	Avg a/b	ф
Unannealed	140	10.6	12.8±0.4	2.2	.019
180°C For 20 minutes	88	11.8	14.7±0.6	2.0	.015
180°C For 1 hour	82	11.9	14.7±0.6	2.4	.029
200°C For 20 minutes	145	12.3	15.2±0.4	2.1	.013
200°C For 1 hour	160	16.1	21.2±0.6	2.0	.034
200°C For 2 hours	120	18.9	26.5±0.9	1.6	.025



Figure 5-3 Morphology of blend after annealing 5 minutes at 180°C as viewed in plane of extrudate strand axis

annealing at this higher temperature.

The ultimate morphology obtained after annealing is strongly dependent upon the annealing temperature. The increases in average micelle core radii at 180°C and 200°C are shown in Figure 5-4. A marginal 15% increase in core radius was noted after heating

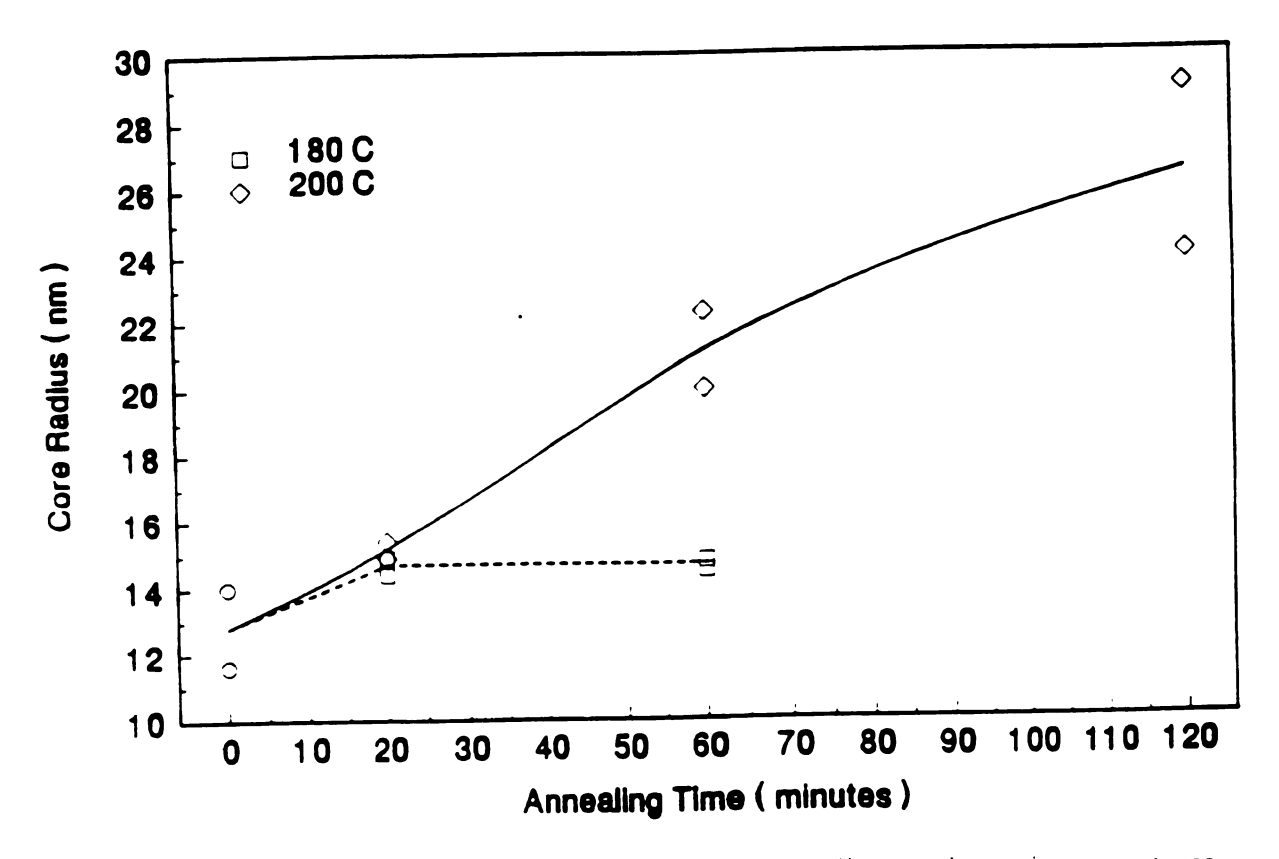


Figure 5-4 Growth of miceile cores upon annealing at elevated temperatures

the blend for 1 hour at 180°C. In Figure 5-5, the distributions of micelle radii are compared before and after annealing at 180°C for one hour. Little difference is evident

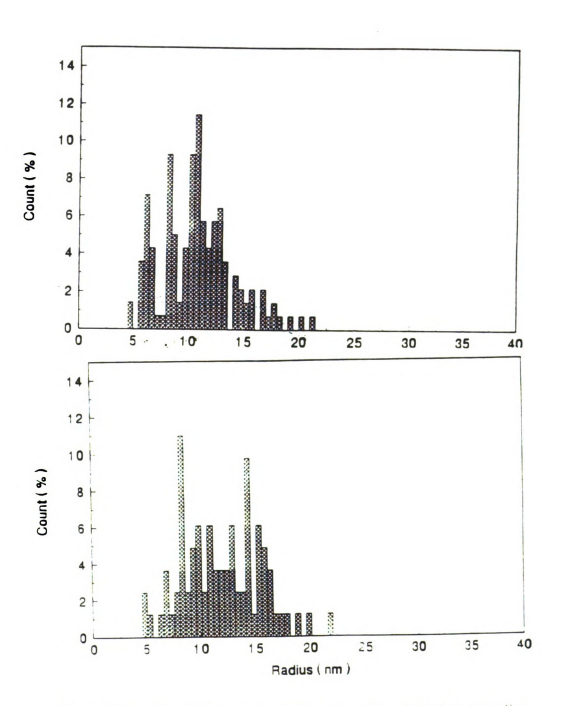


Figure 5-5 Distributions of micelle core radii A) before annealing B) after annealing at 180°C for 1 hour

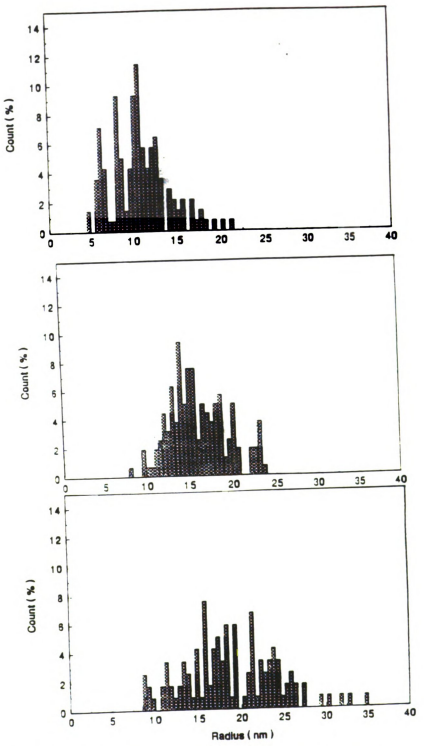


Figure 5-6 Distributions of micelle core radii A) before annealing and after annealing at 200°C for B) 1 hour C) 2 hours

in the distributions. When annealed at 200°C, the micelle cores increased over 60% in radius in 1 hour and increased over 100% in 2 hours. The distributions of micelle radii are shown before and after annealing for 1 and for 2 hours at 200°C in Figure 5-6. The micelle cores with radii below 10 nm disappear upon annealing for 1 hour. After 2 hours of annealing, micelles with radii between 25 and 35 nm have appeared which broadens the distribution of sizes.

5.3b Micelle Clustering

The micelles in the blend are well separated when extruded. In order to quantify the rate of clustering, the edge to edge distance between each micelle and its nearest neighbor was measured from the micrographs of the blend. The samples annealed at 180°C for up to an hour exhibit little evidence of clustering as seen in Figure 5-7a. The distribution of nearest neighbor distances for the specimen annealed for one hour is compared to that of the unannealed specimen in Figure 5-2. Upon annealing at 200°C for a sufficient time, the micelles agglomerate into clusters as seen in micrograph of Figure 5-7b. Distributions of nearest micelle neighbor distances are shown in Figure 5-8 for the extruded blend before and after annealing for up to 2 hours at 200°C. A large increase in the count of closely spaced micelles occurs upon annealing. The rate of clustering at 200°C is illustrated in Figure 5-9 where the median nearest neighbor distances are plotted versus the square root of time. The median distance is proportional to the square root of time. This suggests that a diffusion process is the rate limiting step for the clustering phenomenon.

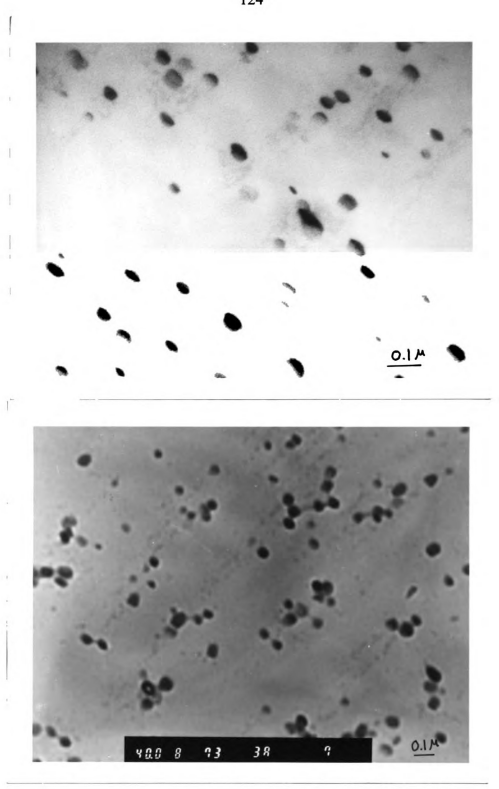


Figure 5-7 Morphology of blend after annealing for (Top Picture) 1 hour at 180°C (Bottom Picture) 2 hours at 200°C

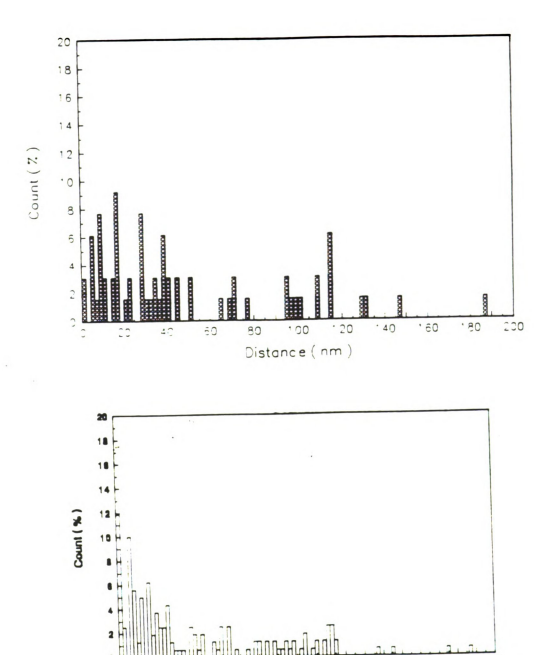


Figure 5-8 Median nearest neighbor distribution of micelle cores
An neture annealing B) after annealing 2 hours at 200°C

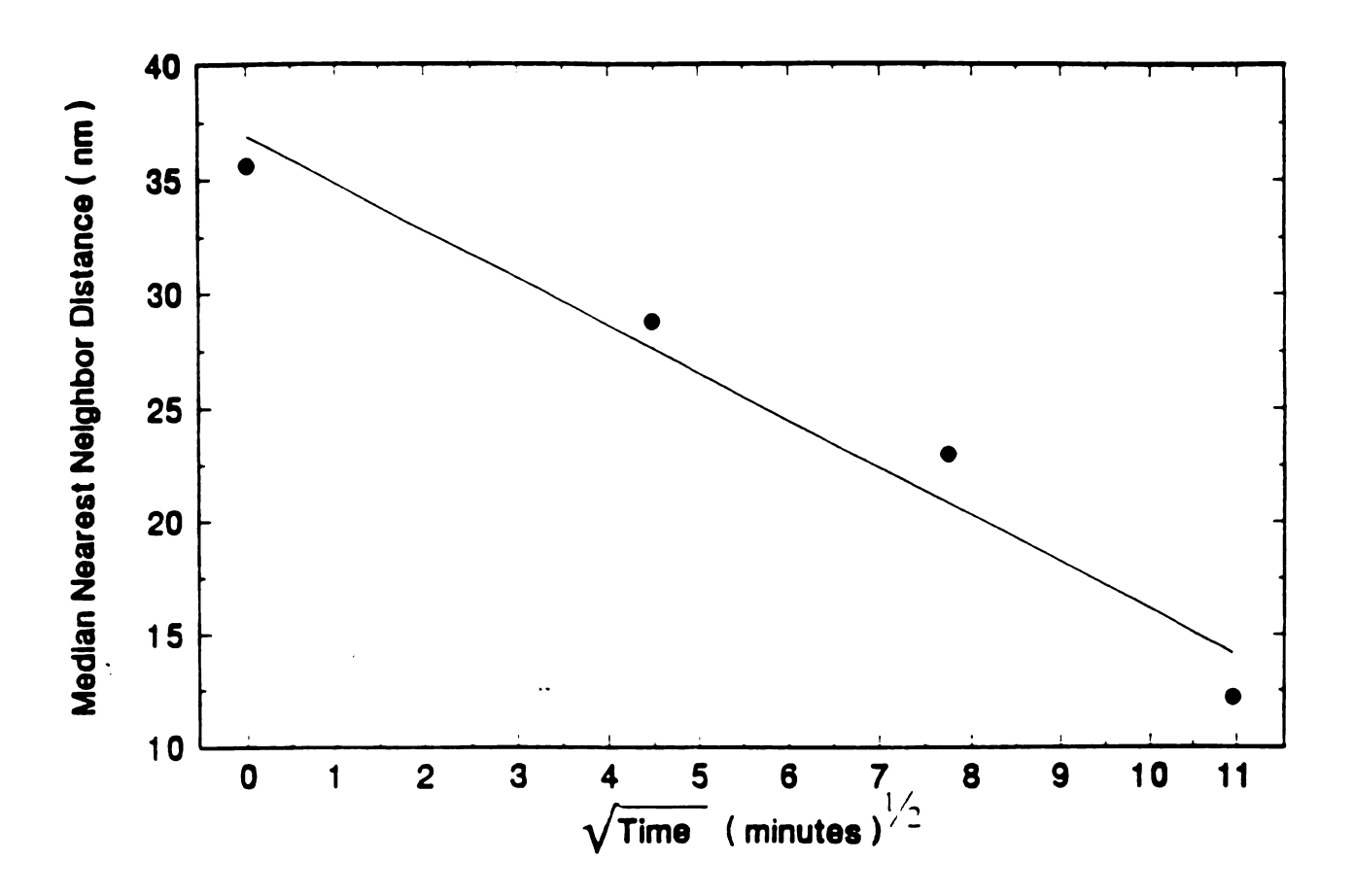


Figure 5-9 Average nearest neighbor distance plotted *versus* the square root of the annealing time: Linear curve suggests diffusional mechanism

5.4 Discussion

The micelle growth must be attributed to either one of or a combination of two distinct mechanisms. The first is the diffusion of individual polymer chains through the coronae and into the micelles. The diffusing macromolecule may be a styrene-butadiene diblock copolymer chain from a smaller micelle which has dissolved into the matrix polymer, a matrix polystyrene chain, or a tapered polystyrene block segment from the micelle corona. The mechanism for an individual copolymer chain to diffuse into a micelle has been described by Anianson and Wall (73). The second method for micelle core growth is for two smaller micelles to contact and fuse into a larger micelle. For this fusion process to occur, the repulsion of the coronae cilia from adjacent micelles as discussed by Leibler and Pincus (74) must be overcome. These two mechanisms have been numerically modelled in a low molecular weight matrix system by Balzas *et al.* (67). For their low molecular weight simulation, they predict that the Anianson-Wall mechanism will predominate over the fusion mechanism.

As seen in the distributions of micelle radii, the micelles with a diameter below 15 nm disappear and larger micelles with diameters greater than 25 nm appear after annealing at 200°C. If the growth in average micelle radius were completely due to the fusion of smaller micelles, the volume of material in the micelle cores should remain constant. The densities of polystyrene and polybutadiene above their glass transition

$$V_{PB} = 1.1138 + 8.24 \times 10^{-4} T \left(\frac{cm^3}{g} \right)$$
 5-2

temperature is given by Equations 5-2

$$V_{PS} = 0.9217 + 5.412x10^{-4}T + 1.687x10^{-7}T^2 \left(\frac{cm^3}{g}\right)$$
 (3)

and 5-3 as a function of temperature where T is in degrees Centigrade (63). The volume fraction of polybutadiene in the blend is 0.0184 at either 180°C or 200°C. The measured volume fraction of micelle cores, Φ , is shown in Table 5-1. These values were determined from two separate micrographs of each blend. The precision levels tabulated reflect the variation in measurements between the two micrographs. A large error is associated with this measurement because small variations in micelle positions at the edge of each micrograph can have a large influence on the fraction of micrographs area occupied by micelle cores. In spite of this error, an increase in the volume fraction of micelle cores with annealing time is indicated. Before annealing, the volume fraction of micelle cores is 0.019, approximately the same as the volume fraction of polybutadiene in the blend. The micelle growth results in a larger total volume in the cores than can be accounted for by butadiene alone. The incompatibility of polystyrene and polybutadiene has been shown to decrease with increasing Temperature in a low molecular weight system (75). Micelle cores became swollen with low molecular weight matrix polymer until the micelles eventually dissolved completely. Evidence of micelle core swelling at elevated temperatures due to the dissolution of a high molecular weight matrix polymer has been obtained by Nichols (31). After annealing the styrene-butadiene / polystyrene blend for an hour at 200°C followed by an hour at 130°C, pockets of polystyrene appeared in the micelle cores. These pockets resulted from polystyrene from either the matrix or copolymer block which had dissolved into the matrix at 200°C precipitating from the butadiene at 130°C.

The micelle growth depended heavily upon the annealing temperature. In the 180°C annealed specimens, the micelle cores grew from 13 to about 15 nm in radius in 20 minutes and remained the same size after an additional 40 minutes of annealing. In the 200°C annealed specimens, the micelles grew slightly faster in the first 20 minutes of annealing and continued to grow through an annealing time of 2 hours where they exceeded 25 nm in average diameter. The relatively limited mobility of polymer chains at the lower annealing temperature can account for the slower rate of growth over the first 20 minutes. The continued growth of micelles seen after the first 20 minutes is because the pseudo equilibrium morphology at 180°C is different than that at 200°C. The obvious experimental procedure to examine this issue would be to characterize the morphology after even longer annealing times or higher temperatures. This may not be feasible since the degradation of polymer chains which can accompany the more rigorous annealing conditions may also affect the blend morphology.

The kinetics of coarsening of two-phase immiscible metals systems has been modelled based upon the theory of Ostwald ripening (76). Grains of a second face grow from nucleation points from a supersaturated solution. This theory, although derived for metals, has also been applied successfully to a blend of polypropylene and ethylene-propylene rubber (77). The theory predicts that the volume of dispersed particles increases linearly with time and that the distribution of particle sizes remains self-similar

(78). Neither of these predictions is consistent with the data presented in this work. The relative complexity of the micellar structure with its surrounding coronae

The tremendous stresses applied to compound the blend result in an oriented morphology. Upon annealing, this extruder generated orientation disappear. The time scale for this transformation is shorter than the time scales for micelle core growth and clustering. The hinderences on these two phenomena caused by the coronae do not occur for the rearrangement of diblock molecules within a micelle.

Interactions between micelles may be either repulsive or attractive. This is governed in part by the coronae of the micelles. The effect of the coronae on micellar interactions depends upon the molecular weight of the matrix polymer. In low molecular weight solvent systems, matrix polymer swells the micelle coronae thereby causing the diblock chains to become extended. Repulsion between the coronae of adjacent micelles in these systems arises from entropy considerations (74). In high molecular weight systems such as those in this work, the matrix polymer does not swell the micelle corona (63). In fact, the molecular weight of the homopolymer must be at least an order of magnitude less than the corresponding block of the copolymer in order for the two to be miscible (79). In these high molecular weight systems, the A block cilia are therefore compacted against the micelle core rather than extended. The mixing of the coronae of adjacent micelles may be more favored than mixing of the coronae and the surrounding homopolymer matrix. For such a system, Semenov (67,80) has predicted a strong attractive force between the micelles at equilibrium. However, the true equilibrium morphology may never be reached because of the limited mobility in the high molecular

weight polymer matrix. The observable morphology of the blend may be determined by potential energy barriers rather than equilibrium free energy.

An examination of the kinetics of clustering may provide needed insight into this phenomenon. The diffusion rate determined from the slope of the line plotted in Figure 10 is $1.3 \times 10^{-21} \text{m}^2/\text{sec}$. The diffusivity for Brownian motions of spheres is given by equation 5-4 for comparison.

$$D = \frac{kT}{6\pi\eta R} \tag{5-4}$$

With the viscosity, η , of the Styron 666APR melt at 200°C equal to 400 Pa-s (31), the Brownian diffusion coefficient for well separated spherical particles the size of the micelle cores is about 4×10^{-17} m²/sec. This value is four orders of magnitude greater than the measured diffusion rate. The effect of the corona on the mobility of the micelle may be at least partially responsible for this tremendous discrepancy. The cilia may intermingle and entangle to some limited degree with the matrix homopolymer, thereby inhibiting micellar diffusion. The diffusion may be hindered by strong energy barriers to the diffusion of block copolymer chains in the high molecular weight polymer matrix discussed by Semenov (67). Similar experiments on micellar clustering with a range of block copolymer molecular weights are required to further elucidate the dynamics of clustering.

5.5 Conclusions

The morphology of blends comprised of a high molecular weight polystyrene matrix and a styrene-butadiene diblock copolymer depends on both the mechanical and thermal history. The orientation of the blend morphology created during the compounding procedure disappears quickly with annealing. Over a longer time scale, the micelles grow in volume and become more spherical. This coarsening is due to dissolution of the matrix or cilia polystyrene into the micelle core because of the increased miscibility of polystyrene and polybutadiene at higher temperatures. When annealed at 200°C, the micelles group into cluster formations. The decrease of median nearest neighbor distance time suggests a diffusional mechanism. The slow rate of micelle clustering indicates strongly hindered diffusion in the high molecular weight system.

CHAPTER VI

CONCLUSIONS

6.1 Functionalization of Polymer Melts

6.1a Effect of Shear and Extensional Strain

The model flow reactor experiments demonstrated the significance of the extensional and shear strain rates in the functionalization of polymer melts. The functionalization reaction examined was the peroxide catalyzed grafting of dibutyl maleate onto polypropylene. Extensional strain was found to be a critical feature of the flow field for the reaction which requires the mixing of a stream of peroxide solution with a viscous polymer melt. Up to a four fold increase in the level of maleation was observed in the continuous flow reactor with the addition of extensional strain. This is attributed primarily to the greater efficiency of extensional flows for dispersing peroxide into the melt. Additionally, some increase in the reaction level within the continuous flow reactor as compared to the batch reactor can be attributed to axial dispersion which contributes to the mixing. Contrastingly, shear alone was found to have a limited influence on the reaction progress. Significant increases in the shear rates produced in the batch, Couette flow reactor led to only minor increases in the level of reaction.

6.1b Effects of Extruder Flow Field

Melt functionalization reactions are typically carried out in commercial polymer melt processing devices such as extruders. The effects of changing operating conditions (throughput rate, screw geometry, and screw rotation rate) on the flow of polypropylene and dibutyl maleate in a co-rotating, fully intermeshing twin screw extruder were examined.

The extruder flow geometry must be accounted for in the characterization of extruder flow. The barrel valve setting is a powerful control factor for the extruder flow. This relatively small change in the screw configuration caused large changes in the residence time distribution of the melt. Closing the barrel valve results in longer mean residence times and broader residence time distributions. Each of these changes results in higher levels of reaction.

A range of operating conditions was examined which provided various levels of extruder hold-up volume. For a constant screw configuration, the hold-up volume correlated with the ratio of throughput rate to screw rotation rate. The mean residence time decreases with increasing screw rotation rate. The spread of the residence time distribution depends strongly on the throughput rate. As the throughput rate increases, the distribution becomes narrower and more peaked. The effects of the screw rotation rate on the flow depended upon the operating conditions. With the extruder nearly flooded, an increase in the screw rotation rate led to a small decrease in the spread of the residence time distribution along with a decrease in the mean residence time. When the extruder was relatively starved, the residence time distribution broadened when the

screw rotation rate was increased. This indicates an increase in the level of axial mixing.

The levels of grafting were correlated with parameters determined from the residence time distributions obtained in the absence of reaction. The hold-up volume is a poor predictor of the level of reaction. The mean residence time is only somewhat better. The predicted level of peroxide decomposition is determined from a combination of the peroxide dissociation kinetics and the entire residence time distribution. The level of maleation was found to correlate strongly with this parameter. Therefore, the residence time distribution is sufficient to describe the complex extruder flow in the context of a melt functionalization reaction.

6.1c Effect of Melt Rheology

The strong correlation between the residence time distribution of peroxide in the extruder and the level of reaction is important because it establishes the measurement of the residence time distribution as a means to adequately characterize the extruder flow. Flows of two distinct low density polyethylene melts were investigated by the comparison of their residence time distributions. Across the entire range of extruder operating conditions (and resulting extruder flow fields), the branched polyethylene, LDPE, has narrower residence time distributions than the linear, LLDPE melt. This narrower residence time distribution is indicative of reduced levels of back mixing. The LDPE and LLDPE have similar shear viscosities so that the pressures generated in the mixing zones due to circumferential strain are also of similar magnitudes. The relatively higher extensional viscosity of the LDPE reduces the level of the pressure driven flow. This

reduction in both forwarding and reversing axial flow in the mixing zones accounts for the observed narrower residence time distribution. The paddles constituting the mixing zones are configured to produce a moderate forwarding flow. Since the axial flow in these regions has significant components of extensional strain, a small increase in mean residence time is seen with an increase in extensional viscosity.

The degradation and cross-linking reactions which occur respectively in the polypropylene and polyethylene systems result in significant changes in the shear viscosities of the melts, particularly at low strain rates. The degradation of polypropylene results in a broader, less peaked residence time distribution in a single screw extruder (37). In this work however, the limited number of measured residence time distributions of the reacting melts were not significantly different from the nonreacting melts. This discrepancy may be due to the different geometry.

The effect of melt rheology on the residence time distribution depends upon the extruder screw configuration. In paddle arrangements providing for significant reversing action such as those in this work, the residence time distribution will be narrower for melts with greater ratios of extensional to shear viscosity. With open barrel valves and strongly forwarding paddle configurations, the melts with greater ratios of extensional to shear viscosity will have significantly longer mean residence times in addition to narrower residence time distributions.

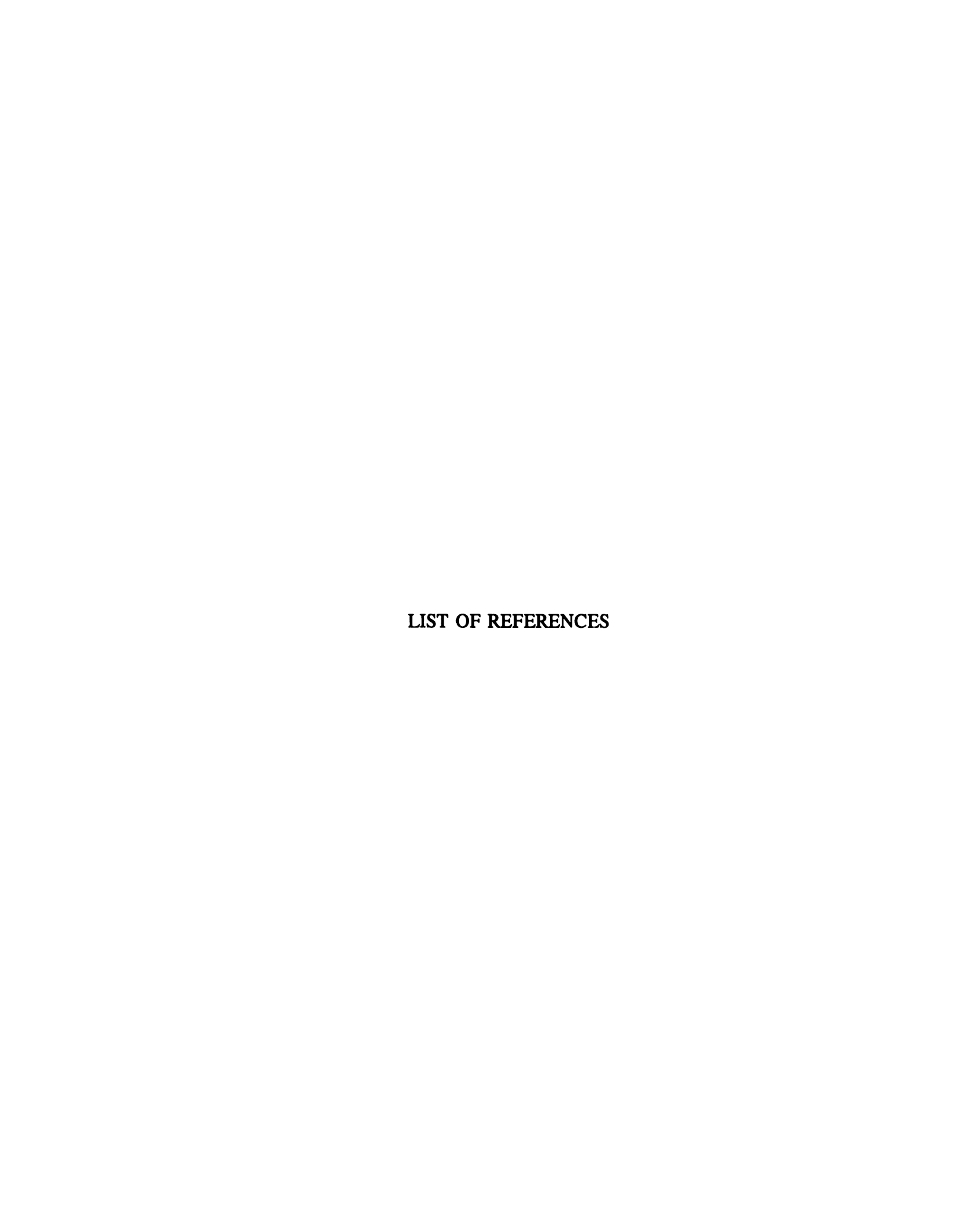
6.1d Effect of Extruder Flow on Reaction

A longer mean residence time provides for higher levels of reaction for the maleation and cross-linking reactions where time is a limiting factor. A broader residence time distribution indicates better axial mixing which increases the selectivity of the maleation reaction. The greater backmixing indicated by the broader distribution allows for more of the unreacted maleic anhydride to come into contact and react with polyethylene macroradicals. The desired residence time distributions can be obtained through altering the operating conditions in conjunction with the flow geometry.

6.2 Micelle Kinetics in Polymer Blend

The kinetics of micelle growth and clustering were examined for a blend of polystyrene and styrene-butadiene diblock copolymer. The copolymer is 70% styrene by weight. When a blend consisting of 5% of the copolymer is melt compounded in an extruder at 170°C, the butadiene blocks form the cores of micelles. The attached polystyrene blocks form the coronae surrounding these cores. Upon extrusion, the cores are shaped as small discs with an average sphere equivalent radius of 10 nm. When the blend was annealed at elevated temperatures (180°C or 200°C), the micelle cores became more spherical and also increased in size. The shape change occurred rapidly; The micelles appeared much more spherical when annealed for only 5 minutes at 180°C. The growth in size proceeded at a slower pace. The final micelle growth measured after long annealing times (1 - 2 hours) depended strongly upon the annealing temperature. The specimens annealed at 200°C exhibited clustering as evidenced by the distributions

of measured median nearest micelle neighbor distances. The rate of clustering is much slower than would be predicted by Brownian motion. This indicates that the diffusion is strongly hindered.



- 1. Ottino, J. and R. Chella, Polym. Eng. Sci. 23, 357 (1983).
- 2. Nauman, E., Chem. Eng. Commun. 8, 53 (1981).
- 3. Hogt, A., Compalloy Proc., Princeton, NJ, 189 (1990).
- 4. Tadmor, Z. and B. David, Intern. Polym. Proc. 3, 38 (1988).
- 5. Su, R., G. Chang and M. Lee, Antec '89, 531 (1989).
- 6. Ide, F. and A. Hasegawa, J. Appl. Polym. Sci. 18, 963 (1974).
- 7. Ganzeveld, K., Janssen, L., Polym. Eng. Sci. 32, 467 (1992).
- 8. Lazàr, M., Rado, R., Rychly, J., Adv. Polym. Sci.: Polym. Phys. Ed. 95, (1990).
- 9. Borsig, E., A. Fiedleroua, L. Rychla, M. Lazar and G. Haudel, J. Appl. Polym. Sci. 37, 467 (1989).
- 10. Gaylord, N, M. Mahendra, R. Mehta, J. Appl. Polym. Sci. 33, 2549 (1987).
- 11. Gaylord, N., M. Mishra, J. Polym. Sci.: Polym. Lett. Ed 21, 23 (1983).
- 12. Aglietto, M. R. Bertani, G. Ruggeri and A. Segre, Macromolecules 23, 1928 (1990).
- 13. Greco, R. G. Maglio, P. Musto, J. Appl. Polym. Sci. 33, 2513 (1987).
- 14. Shiah, C. and I. Chen, Antec '89, 1398 (1989).
- 15. Pearson, J. Mechanics of Polymer Processing, Elsevier Appl. Sci. Pub. LTD, New York (1985).
- 16. Suwanda, D. and S. Balke, Antec '90, 1908, (1990).
- 17. Elmens, P. and H. Meijer, Polym. Eng. Sci. 30, 893 (1990).
- 18. White, J. Twin Screw Extrusion, Hanser Pub., New York (1991).
- 19. Rauwendaal, C., Antec '81 1013, (1981).
- 20. Sakai, T., N. Hashimoto, and N. Kobayoshi, Antec '87, 1087 (1987).

- 21. Booy, M. Polym. Eng. Sci. 18, 973 (1978).
- 22. Kalyon, D. and H. Sangani, Polym. Eng. Sci. 29, 1018 (1989).
- 23. Sydlowski, W. and J. White, J. Non-Newt Fluid Mech. 28, 29 (1988).
- 24. Xiaozheng, Z., W. Rong and W. Naiyi, Antech '90, 153 (1990).
- 25. Wang, Y., J. White and W. Szydlowski, Intern. Polym. Proc. 4, 262 (1989).
- 26. McCullough, T., R. Rakos and D. Sebastian, Antec '90, 147, (1990).
- 27. Bigio, D. and M. Wigginton, Antec '90 1905, (1990).
- 28. Gotsis, A., Z. Ji and D. Kalyon, Antec '90 139(1990).
- 29. Bigio, D., K. Cassidy, M.Dellapa and W. Baim, Intern. Polym. Proc. 7, 111 (1992).
- 30. Eise, K., J. Curry and J. Nangeroni, Polym. Eng. Sci. 23, 642 (1983).
- 31. Nichols, K., A Study of Mixing, Morphology, and Rheology for Melt Mixing of AB/A Polymer Blends, PhD Thesis, Michigan State University (1990).
- 32. Grenci, J., J. Biesenberger, D. Todd, Proc. Int. Polym. Proc. Soc., p. 121, Hamilton, Ont., April (1991).
- 33. Hannachi, A. and Mitsoulis, Intern. Polym. Proc. 5, 244 (1982).
- 34. Grace, H., Chem. Eng. Commun. 14, 225 (1982).
- 35. Wu, S., Polym. Eng. Sci. 27, 335 (1987).
- White, J. "Maleination of Thermoplastics in Internal Mixers", Presentation at Polym. Proc. Soc. Meeting, Knoxville, TN (1992).
- 37. Tzoganakis, C., J. Vlachopoulos and A. Hamielec, Intern. Polym. Proc. 3, 141 (1988).
- 38. Cimmino, S., L. D'orazio, R. Greco, G. Maglio, M. Malinconico, C. Mancarella, E. Martuscelli, R. Palumbo, and G. Ragosta, Polym. Eng. Sci. 24, 48(1984).
- 39. Kowalski, R., Compalloy '89, 347(1989).

- 40. Sakai, T, ANTEC '88, 1853(1988).
- 41. Hogt, A., ANTEC '88, 1478(1988).
- 42. de Vito, G. et al., J. Polym. Sci. Polym. Chem. Ed. 22, 1335(1984).
- 43. Peacock, A. Polym. Commun 25,169 (1984).
- 44. FIDAP Package, Fluid Dynamics International Inc., Evanston, Ill, U.S.A (1992).
- 45. Doremus, P. and J. Piau, J. Non Newt Fluid Mech 14, 79 (1983).
- 46. Todd, D., Polym. Eng. Sci., 15, 437, (1975).
- 47. Janssen, L., <u>Twin Screw Extrusion</u>, Elseviers Scient. Publ. Co., New York (1978).
- 48. Janssen, L., R. Hollander, M. Spoor and J. Smith, AIChE 25, 345 (1979).
- 49. Pinto, G. and Z. Tadmor, Polym. Eng. Sci. 10, 279 (1970).
- 50. Todd, D. and Baumann, Polym. Eng. Sci. 18, 321 (1978).
- 51. Koenig, J., Spectroscopy of Polymers, ACS, Washington D.C., (1992).
- 52. Wu, C. and A. Su, Polym. Eng. Sci. 31, 1629 (1991).
- 53. Dreiblatt, A. and K. Eise, <u>Mixing in Polymer Processing</u>, C. Rauwendaal, ed., ch. 5, Marcel Dekker, Inc., New York (1992).
- 54. Munstedt, H. and H. Laun, Rheologica Acta 20, 211 (1981).
- 55. Tremblay, B. J. Non Newt. Fl. Mech., 43, 1, (1992).
- 56. Cogswell, F., Polym. Eng. Sci. 12, 64, (1972).
- 57. Shroff, R., L. Cancio, and M. Shida, J. Rheology, 21 429, (1977).
- 58. Gaylord, N. and R. Mehta, J. Polym. Sci.: Polym. Chem., 26 1189, (1988).
- 59. Donald, A. and E. Kramer, J. Mater. Sci. 17, 1765, (1982).
- 60. Bucknall, C. (ed.) <u>Toughened Plastics</u>, Applied Science Publishers, New York, (1977).

- 61. Bonner, J. and P. Hope, <u>Polymer Blends and Alloys</u>, Ch. 3, M. Folkes and P. Hope, ed., Chapman & Hall Inc., New York (1993).
- 62. Leibler, L., H. Orland and J. Wheeler, J. Chem. Phys, 79, 3550, (1983).
- 63. Kinning, D., E. Thomas and L. Fetters, J. Chem. Phys., 90, 5806, (1989).
- 64. Rigby, D. and R. Roe, Macromol. 19, 721, (1986).
- 65. K. Nichols and K. Jayaraman, Proc. Xth Int. Cong. on Rheol., Sydney, Australia, 148, August (1988).
- 66. Halperin, A. and S. Alexander, Macromol. 22, 2403, (1989).
- 67. Balazs, A., M. Gempe, and J. Brady, J. Chem. Phys., 92, 2036, (1990).
- 68. Semenov, A., Macromol. 25, 4967, (1992).
- 69. Kato, K., Polym. Eng. Sci. 7 38, (1967).
- 69. Berney, C. B., R. E. Cohen and F. S. Bates, Polymer, 23, 1222, (1986).
- 70. Gebizlioglu, O. S., A. S. Argon and R. E. Cohen, Polymer, 26, 519, (1985).
- 71. Thomas, D. A., J. Polym. Sci: Polm. Symp. **60**, 189-200 (1977).
- 72. Polance, R., K. Nichols and K. Jayaraman, submitted to Polymer, March (1994).
- 73. Anianson, E. and S. Waal, J. Phys. Chem. 78, 1024 (1972).
- 74. Leibler L. and P. Pincus, Macromol. 17 2922, (1984).
- 75. Roe, R., M. Fishkis, J. C. Chang, Macromol. 14 1091 (1981).
- 76. Ostwald, Z. Phys. Chem, 37 385, (1901).
- 77. Mirabella, F., Polym. Mater. Sci. Eng., 67 372, (1992).
- 78. Voorhees, P., J. Stat. Phys., 38 231, (1985).
- 79. Eastmond, G. C. and D. G. Phillips, Polymer 20 1501, (1979).
- 80. Semenov, A., Macromol. 22 2849, (1989).

